doi: 10.13133/2280-6148/17480 *Journal of Mediterranean Earth Sciences 13 (2021), 31-76*

J M E S **Journal of Mediterranean Earth Sciences**

Storm signature in the Messinian and Pleistocene record of drift-and swash-aligned Mediterranean gravel beaches. Role of precession-driven intensification of the Mediterranean cyclogenesis

Francesco Massari *

Dipartimento di Geoscienze, Università di Padova, Padova, Italy.
** Corresponding author: francesco.massari@unipd.it*

ABSTRACT - The stratal organization and general architecture of the lower Messinian and middle-upper Pleistocene progradational gravel beach lithosomes built out on respectively South-Alpine and Apenninic palaeo-shorelines support the view that the predominant signature is that left by processes linked to storm impact and immediate storm-decay recovery. The reconstructed wave spectrum probably had in most cases a bimodal shape during storm events, with waves of local origin associated with a component of moderate swell, probably linked to the influence of an inferred dominant long-fetch southerly wind. During the waxing stage of storms, powerful erosion occurs of the upper-beachface by high-steepness waves and surf zone processes. A strong offshore-directed return flow (undertow) during the storm peak could quickly reach a supercritical state and be potentially subject to hydraulic jumps at the beachface-shoreface transition The effects, mostly conspicuous in Apenninic lithosomes, include: i) scours paved/infilled by coarse gravel, recording the impact of hydraulic jumps, whose upstream migration generated sandy backset laminasets; ii) low-amplitude wavy to lenticular structures that are inferred to result from the migration and aggradation of antidunes; iii) local chute-and-pool structures. Concurrently, strong runup led to building-up of a storm berm and overwashing. During the waning stage of the storm long-period waves led to the fast recovery of upper-beachface gravels and renewed overtopping and overwashing, together with strong oscillatory motion at the sea bed leading to the generation or accretion of wave megaripples in the upper shoreface and toe of the beachface. The studied Pleistocene and Lower Messinian lithosomes show significant differences in general architecture. Due to the oblique approach of storm waves, the former palaeo-beaches, located on Apenninic palaeo-coasts, can be defined as drift-aligned systems during high-energy events, with the development of very dynamic intermediate states characterized by a prominent bar/rip topography, an energetic undertow, and large cross-shore and alongshore transport gradients. Conversely, the near-perpendicular wave approach on the Messinian shorelines, located on the landlocked embayment at the northern end of the Palaeo-Adriatic Sea, resulted in an almost swash-aligned configuration, with remarkably scarce to absent effectiveness of longshore drift and virtual lack of three-dimensional inshore topography. During the early Messinian times, as well as during the middle and late Pleistocene, the deposition was strongly influenced by precession-driven climate fluctuations. During precession minima, characterized by maximum seasonality, a greater influence of Atlantic-born depressions in the Mediterranean during winter aphelion could have increased the activity of cyclonic storms and the river discharge. It is believed that the storm signature, although inferred to represent and intrinsic feature of the stratigraphic record of gravel beaches, was emphasized in the studied lithosomes due to this climatic context.

Keywords: gravel beach lithosomes; storm impact; supercritical flow; drift- and swash-aligned systems; preservation potential; precession cycles.

Submitted: 26 May 2020-Accepted: 23 September 2021

1. INTRODUCTION

The macroscale development of coastal morphology and its changes in time are a complex function of many inter-related and mutually interacting factors, including the textural nature and volume of sediment available in the littoral zone in relation to the beach location with respect to sediment sources, facies preservation potential, gradient of the sea floor, wave climate and how it influences the degree of storminess, tidal range, open- or short-fetch character of the coastal belt, and rate of sea level variation and shoreline migration (Orford, 1987; Bitencourt

and Dillenburg, 2020, with references). These factors specifically influence the reflective vs dissipative beach profiles, the gradient and elevation of the beachface, and the stratigraphic organization of the deposits, therefore resulting in different facies associations.

The literature centred on several aspects of gravel beach morphodynamics is very large (e.g., Carter and Orford, 1993; Jennings and Shulmeister, 2002; Austin and Masselink, 2006; Ivamy and Kench, 2006; Austin and Buscombe, 2008; Almeida et al., 2017, among many others). Specifically, the response of coarse-clastic beaches to storms has been inspected with reference to several facets: the adjustments of nearshore topography and shoreline variation (e.g., Bramato et al., 2012; Harley et al., 2014); the geomorphic and sedimentary changes generated by different kinds of storms (Roberts et al., 2013); the role of swash zone hydrodynamics in terms of coarse sediment transport (Mason and Coates, 2001; Elfrink and Baldock, 2002; Masselink and Puleo, 2006; Bertoni et al., 2010; Masselink and van Heteren, 2014; Almeida et al., 2017), and in terms of beach recovery (Ivamy and Kench, 2006; Bergillos et al., 2016). Attempts at modelling the coarse-clastic beach response to high-energy events have been done on the basis of different approaches (e.g., McCall et al., 2014, 2015; Almeida et al., 2017).

Reconciling modern littoral processes with ancient stratigraphy is frequently difficult because of the largely different timescales considered and the incompleteness of the stratigraphic record. This aim was pursued with variable success by the investigations on ancient examples of gravel beach progradational units (e.g., Clifton, 1981; Leckie and Walker, 1982; Maejima, 1983; Dupré, 1984; Bourgeois and Leithold, 1984; Leithold and Bourgeois, 1984; De Celles, 1987; Massari and Parea, 1988 a,b; Hart and Plint, 1989, 1995; Postma and Nemec, 1990; Maejima et al., 2001; Neal et al., 2002; Clifton, 2003). Compared to most studies on present-day beaches, focused on the more accessible intertidal and supratidal regions, the investigations on the ancient record, particularly when high-quality outcrop data sets are available, offer a favourable opportunity for extensive insight into the facies associations; this is particularly important for the deposits of upper shoreface and lower-beachface, hardly accessible in present-day beaches due the logistical challenge of making *in situ* measurements during highly energetic events. One of the significant results of this study on ancient record is to document the incidence of supercritical flows in the toe area during storm events and their role in generating distinctive types of sedimentary structures. The paper aims moreover at stressing the different response of drift- and swash-aligned beach states to the impact of storm events. As stressed by Aagaard et al. (2013), in the former states, characterized by development of a nearshore bar/rip morphology, strong morphodynamic feedbacks between hydrodynamic processes and morphology create large cross-shore and alongshore transport gradients, ensuring high morphological variability, dynamic beach states and high sediment transport rates. Conversely, the swash-aligned beach state dominated by cross-shore motions results in remarkably less dynamic systems, characterized by poor morphological variability and considerably reduced alongshore transport gradients.

The palaeo-climatic context in which the studied lower Messinian and middle-upper Pleistocene beach lithosomes were generated was one of precession-paced climate variations with minima of precession characterized by maximum seasonality. As stressed by Sabino et al. (2020) and Toucanne et al. (2015), minimum insolation at autumn/winter aphelion during the minima of precession was accompanied by significant increase in the intensity of the Mediterranean storm track, due to the extension of North Atlantic depressions toward the Mediterranean area. In the interpretation of the stratal organization and general architecture of the studied beach deposits, the role of this particular climatic setting is inferred to have been of importance in enhancing the storm imprint.

2. GEOLOGIC AND STRATIGRAPHIC SETTING

The progradational gravel beach sequences that are the subject of this study are high-frequency cycles of early Messinian and middle to late Pleistocene age (Figs. 1, 2) represented in the stratigraphic record by upward-coarsening tongues that contain a distinctive vertical facies succession from a transgressive lag to inner shelf intensely bioturbated mudstones, to shoreface and foreshore beach deposits. They form part of the sedimentary successions of the foreland basins of the eastern Southern Alps (Venetian-Friulian Basin) (Massari, 1975, 2017; Massari et al., 1986; Massari and Parea, 1988a; Stefani et al., 2007; Mancin et al., 2016), and respectively Apennines (Brückner, 1980; Neboit, 1981-1982; Ciaranfi et al., 1983; Ricci Lucchi, 1986; Massari and Parea, 1988a; Amorosi et al., 1998; Cantalamessa and Di Celma, 2004; Artoni, 2013; Santoro et al., 2013; Ghielmi et al., 2013; Di Celma et al., 2016; Ghielmi et al., 2019). For the sake of brevity, the Pleistocene beach deposits of the Apenninic palaeo-coasts are indicated in the following text as Apenninic lithosomes; likewise, the Messinian ones are referred to as South-Alpine lithosomes.

The Venetian-Friulian basin-fill is a SSE-ward thinning-out sediment wedge with a maximum thickness of about 3500 m near the eastern South-Alpine front, laid down with upward coarsening trend mostly during the middle to late Miocene (Serravallian–Messinian), concomitantly with the most intense shortening phase leading to SSE-ward thrust propagation (Massari et al., 1986; Castellarin and Cantelli, 2000; Stefani et al., 2007; Mancin et al., 2016). During the Messinian the peripheral bulge shifted to the present-day coastal area and created a morphological threshold; thus, the foreland basin in this stage was a true perched basin. As noted by Mancin et al. (2009) and Toscani et al. (2016), a rapid exhumation of hinterland

Fig. 1 - A) Index map showing the location of studied beach lithosomes in the Venetian-Friulian and Apenninic foreland-basin fills. For the location of the studied lithosomes a reference is made in the text to the cartography of the Italian Geographic Military Institute (IGM); B) Schematic Early Messinian palaeogeography. SVL: Schio-Vicenza Line.

units, estimated at around 4 km, started at about 10 Ma according to thermal modelling of apatite fission track data (Zattin et al., 2003) and sediment petrographic data (Stefani et al., 2007), and had a strong impact on the Venetian-Friulian basin in terms of coarse clastic input. The latter was moreover enhanced during the Messinian due to the concomitance of chain exhumation with high-frequency climate variability. Huge volumes of coarse clastics were supplied at this time by fan delta systems along the South-Alpine margins close to the front of the thrust belt (Massari et al., 1986; Massari and Mellere, 1993; Ghielmi et al., 2013).

The palaeogeographical setting which can be reconstructed in the early Messinian times for the Venetian-Friulian foreland basin was a roughly rectangular landlocked embayment bounded at eastern and western sides by the reliefs linked respectively to the external Dinaric thrust-fold belt and to the activity

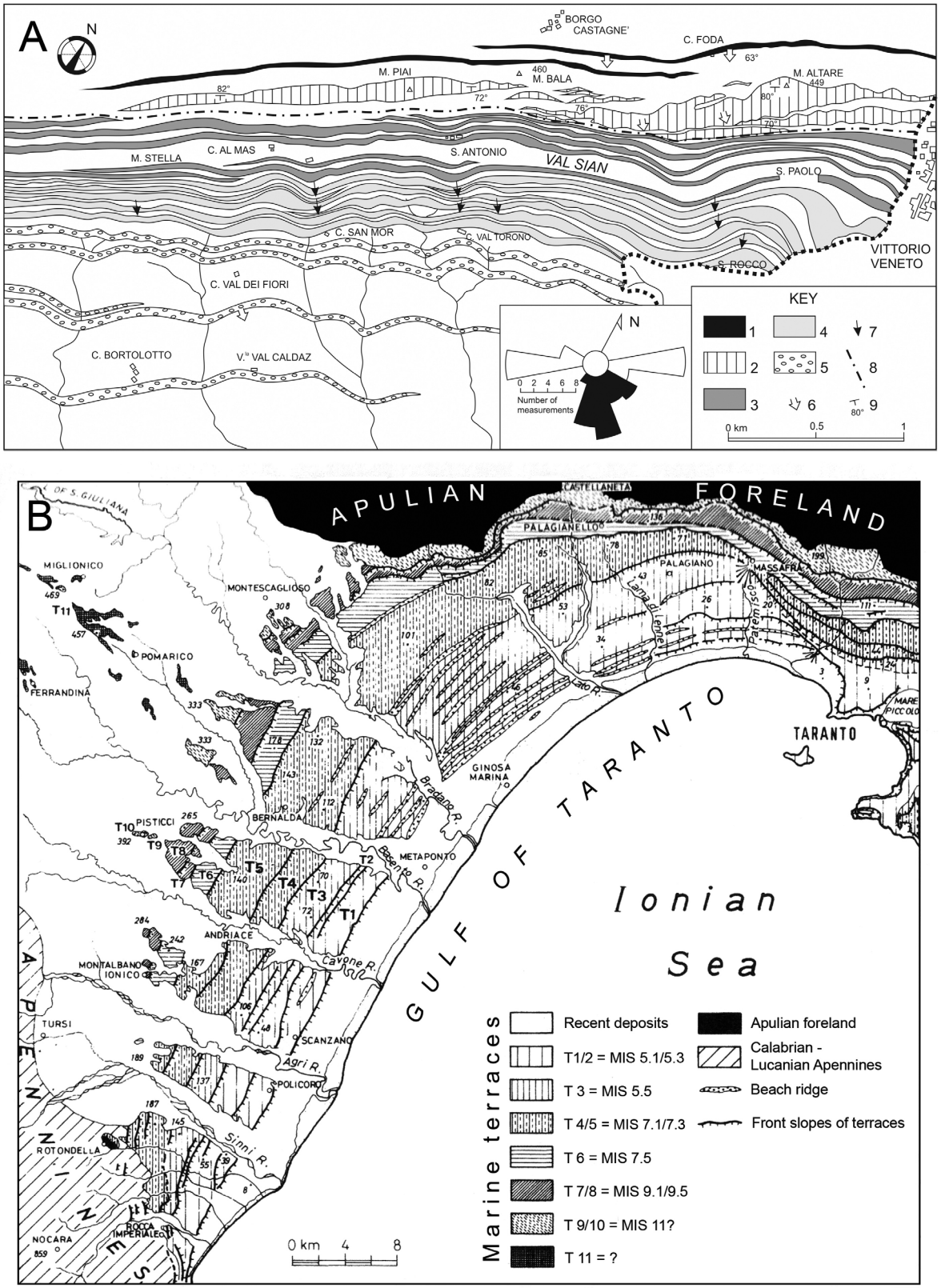

Fig. 2 - A) Geological map of the upward-shallowing Tortonian-Messinian succession in the Vittorio Veneto area (eastern Southern Alps). Slope mudstones with channelized gravel bodies (1 and 2) are unconformably overlain by delta-front sandy cycles (3) and progradational gravel beach lithosomes (4); these in turn grade upwards into channelized gravels of alluvial fan fringe (5) alternating with flood-plain and lacustrine mudstones. 6: generalized sediment transport direction; 7: dip direction of clinostratification in progradational beach lithosomes; 8: angular unconformity; 9: attitude of beds. Rose diagram in inset summarizes dip directions of clinostratification of beach lithosomes (26 measurements) and direction of crest of gravel megaripples in lower beachface gravels (14 measurements). From Massari and Parea, 1988a; B) Pleistocene marine terraces in the hinterland of the Gulf of Taranto. The map is after Brückner (1980), slightly modified; the dates are mainly after Santoro et al. (2013).

of the Schio-Vicenza Fault (Fig. 1), and at the southern side by a peripheral bulge. During this stage the basin was still connected to the Mediterranean and a belt of gravel beach lithosomes formed near the chain front, at the top of a progradational succession of prodelta to delta front deposits (Fig. 2A). The prodelta mudstones preceding the delta front sand-prone succession contain a foraminiferal assemblage indicative of dysoxic conditions, including *Rectuvigerina tenuistriata gaudryinoides*, *R. t. siphogenerinoides*, *Uvigerina striatissima*, *U. peregrina*, *U. rutila*, *Hopkinsina bononiensis*, *Orthomorphina bassanii* and *Bolivina ferasinii* (Massari et al., 1976). This association is regarded as biostratigraphically meaningful and already indicative of an early Messinian age (e.g. Sturani and Sampò, 1973). The following delta front deposits contain foraminifers indicative of hypohaline setting such as *Ammonia beccarii*, *Elphidium* sp., *Florilus boueanus*, and grade conformably into an interval about 160 m thick consisting of five beach lithosomes which are part of the subject of this work. The littoral deposits formed by the progradation of an ENE-WSW-oriented palaeoshoreline facing a presumably low-gradient shelf and are organized into stacked facies sequences, with gravel clinobeds mostly made up of limestone and dolostone detritus supplied by the active erosion of the uplifting Mesozoic units of the eastern Southern Alps (Stefani, 1987). Gravel was delivered to the sea by means of a network of distributary channels representing the terminal reaches of the ancestors of the rivers crossing the present-day eastern South-Alpine hinterland. The fine-grained deposits of the lithosomes contain a specialized faunal assemblage including *Ostrea* shells and Potamididae, and local backshore and brackish marsh deposits bear lignite horizons. This interval grades conformably to a thick continental succession of alternating alluvial fan to braided-stream gravels and lacustrine mudstones containing terrestrial and lacustrine molluscs dated to the Pontian (= Late Miocene) by Wenz (1942). This succession is bounded at the top by a deep erosional unconformity, in turn overlain by Pliocene marine outer shelf silty marls attributed to the lower Piacenzian or upper Tabianian (Massari et al., 1976). The continental deposits are indicative of an important fresh-water influx into the basin and are inferred to have been laid down during the Messinian Salinity Crisis (MSC). In absence of soundly constraining biostratigraphic data, the marine beach lithosomes may be indirectly dated to the early Messinian on the basis of their interposition between lowermost Messinin deposits and a continental succession correlatable with the MSC; they are inferred to fall within the interval 7-6 Ma.

The Apenninic progradational gravel beach lithosomes represent the uppermost shallowing-up part of the post-orogenic succession of the Apenninic foredeep; they have been studied in two main areas, the Adriatic side of central Italy (Marche region), where they result from the building out of NNW- to NW-oriented palaeoshorelines, and the hinterland of the Gulf of Taranto in southern Italy, where the NNE-trend of the Pleistocene palaeocoast matched the direction of the present-day shoreline (Fig. 1). Most of the studied examples of the latter area crop out in the Bradanic Trough (Basilicata region), a NW-SE trending elongate foreland basin showing a flight of SE-ward stepping marine terraces between the Apenninic front and the Apulian foreland (Fig. 2B); these consist of coarse-grained beach deposits laid down under a vigorous wave climate and in the presence of a continuous and copious supply of sediment provided by riverine input and active longshore drift (Massari and Parea, 1988a, b). The palaeo-beaches were fed by the ancestors of the present-day Apenninic rivers, represented by short, high-gradient bedload streams backed by steep hinterlands and today characterized, particularly in southern Italy, by flash floods providing an abundant but discontinuous supply of gravel to the beaches. The Pleistocene coasts of the Bradano Trough faced a steep-gradient inner shelf of the palaeo-Ionian Sea (Massari and Parea, 1990; Massari, 1997), allowing the waves to hit the shore without significant attenuation. The overall architecture of the terrace succession was controlled by the interference between the uplift due to isostatic adjustment and concurrent sea-level fluctuations driven by the glacio-eustasy. As the rate of Pleistocene eustatic sea-level changes always outpaced the rate of uplift, the high-frequency lithosomes are assumed to be controlled by glacio-eustasy, and their development is considered to be primarily controlled by the orbitally driven cycles in the Milankovitch frequency band. Dating of marine terraces of this area is mainly based on Santoro et al. (2013), whereas the age of the beach lithosomes of the Adriatic side of central Italy is based on Artoni (2013) (see also Ragaini et al., 2006; Ghielmi et al., 2019).

The terrace construction by coastal outbuilding occurred mainly during the substages of the interglacial periods, in times of highstand, stillstand, and the early falling stages of relative sea level, and resulted in the formation of offlapping gravel lithosomes with distinct clinoforms (Massari and Parea, 1988 a,b; Massari, 1997). The lithosome architecture reflects the base-level control: specifically, "climbing" progradation responded to relative sea level rise in the presence of adequately high sediment supply producing an abnormal expansion of the facies associations (e.g., Davis and Clifton, 1987), whereas progradation in the context of a downward shift of the base level created lithosomes with internal unconformity surfaces. Moreover, variations in thickness and geometry of beach clinoforms can be commonly recognized in the direction of progradation: the inner parts of the lithosomes, constructed during the early stages of progradation, lie disconformably on older deposits, show lower and gently dipping clinoforms, and may be significantly thinner and lacking some subunits relative to the outer, seaward-developed parts, which are increasingly complete in their subunits and characterized by progressively higher and steeper clinoforms as the progradation advances into deeper water on the shelf.

In the presence of comparable other conditions, thicker lithosomes with higher clinoforms are also linked to particular locations, such as near river mouths, in areas inferred to have been exposed to the full energy of waves, or where a particular shelf morphology is present. Erosional and non-depositional discontinuities are present in the studied successions, reflecting changes in the wave/storm climate or minor fluctuations in the relative sea level (Hampson and Storms, 2003, with references).

The studied beaches can be classified as pure gravel beaches according to the field-based classification scheme of Jennings and Shulmeister (2002). The beachfaces were gravel-dominated even at sites with relatively abundant sand supply, since there is evidence that energetic waves dispersed much of the sand to shoreface or backshore sinks. Clasts range in size from granules to cobbles, usually well rounded. In the case of standstill prograding geometries, assuming that no significant compaction occurred following deposition, the palaeowater depth can be approximately inferred from the height of the lower beachface clinoforms, and was inferred to range from 1.8 to 5.5 m.

3. METHODS

A field survey was carried out in the study areas (Fig. 1) aimed at performing a sedimentological analysis of South-Alpine and Apenninic gravel beach units. A total of 20 gravel beach lithosomes (5 in the eastern South-Alpine area and 15 in the Apenninic area) were investigated in several exposures using measured sections combined with field sketches covering the entire outcrop extent. Cliff-face photomontages allow the stratigraphic organization and facies architecture to be defined and intra-lithosome key surfaces to be identified and traced laterally. This procedure was accompanied by an investigation of sedimentary structures, palaeocurrent data, and gravel fabric and texture in order to reconstruct the genetic processes involved in the building out of the lithosomes.

4. PRESENT-DAY WAVE CLIMATE

The Mediterranean wave climate is influenced by the reduced scale and complex geometry of the basin and sub-basins, characterized by the presence of islands, protruding peninsulas, embayments, and jagged coastlines, with complex and pronounced orography gradients, which lead to large spatial and temporal variability in the surface wind field over the basin and in coastal areas, as well as complex air-sea interface dynamics (Cavaleri and Bertotti, 2004). Microtidal conditions exist along much of the coasts.

Wave conditions are typically low or moderate, but extreme events can be very destructive. Due to its mid-latitude location, the Mediterranean basin, landlocked between Africa and Europe and hence between two contrasting climates, is subject, despite its relatively limited dimensions, to extratropical severe storms, mainly forming and growing via baroclinic instability (Casas-Prat and Sierra, 2013, with references). Strong heating of the lower layers of the atmosphere and of the Mediterranean surface leads to the generation of intense low-pressure systems (cyclogenesis) with characteristics very similar to tropical cyclones (hence the name assigned to these systems: Medicanes, namely Mediterranean hurricanes), and with important implications for the local wave and current fields. Although not particularly intense in terms of minimum central pressure, the associated wind speeds can be quite strong (Cavaleri et al., 2018). Nowadays, the Mediterranean borderlands are under the influence of the autumn/winter (i.e., October/March) Mediterranean storm track, with the Gulf of Genoa and the Aegean Sea representing two of the most active cyclogenetic regions (Toucanne et al., 2015).

Although the longer-term "memory" typical of the oceanic sites is lacking, and relatively short fetch in the landlocked Mediterranean Sea results in a dominant wind sea, present-day beaches during storm events commonly experience wave conditions characterized by a combination of locally generated wind waves and moderate swell (Inghilesi et al., 2012; Casas-Prat and Sierra, 2013; Ruju et al., 2019). The wave spectrum does not display the complexity of the energy distribution among the various frequencies and directions of wave systems typical of the ocean: a 2D spectrum predominates, namely wind sea and swell. Moreover, due to the limited dimensions of the basin, the spatial and temporal gradients are stronger than in the ocean, commonly implying rapidly changing conditions (Cavaleri et al., 2018).

The Adriatic Sea, a "small" semi-enclosed sub-basin of the Mediterranean, is unique in its shape, a rectangular elongated basin flanked by mountain ranges, with semi-diurnal microtidal regime (Duo et al., 2018). The major winds hitting the Adriatic coasts are Bora and Sirocco. Bora is a cold, intense wind from the northeast, with a maximum fetch of 200 km, blowing in jets from localised gaps along the coastal mountain ridges, and it is characterized by rapid growth and decay. This wind is subject to strong bursts with consequent severe wind seas (Cavaleri et al., 2018); related storms in the northern Adriatic are more common in winter, associated with short fetches, unstable conditions, and steep waves. Sirocco is a generally warm wind approaching from the southeast, originating in the Arabian and Sahara deserts and arising from a warm, dry, tropical airmass that is pulled northward by low-pressure cells across the Mediterranean Sea. It blows along the main axis of the Adriatic, channelled between the Apennines and Dinaric Alps, and is characterized by long, moderate-intensity fetches of up to 700 km, causing long waves. Therefore, a swell component is particularly important for waves traveling along the main basin axis (Lionello et al., 2003). Storms generated by Sirocco generally impact the northern Adriatic coast almost perpendicularly to the

shoreline, with fully developed sea states, and long and regular waves, and they are associated with high storm surges (Cavaleri et al., 2018).

Bartholomä et al. (1998) observed that the most important wind effect on the coasts of the Ionian Sea is the strengthening of the swell, which, in general, approaches from the southeast. A fully developed sea from this direction is able to produce breakers up to 5 m in height. The swell elevates the waterline along the beach by up to 2 m, leading to the inundation of large parts of the backshore.

5. THE FACIES ASSOCIATIONS OF THE ANCIENT BEACHES

This study is exclusively focused on the offlapping part of the lithosomes, including facies associations pertaining to the successive sedimentary belts involved in the progradation process, from the offshore transition zone through the shoreface and beachface to the backshore.

Following the suggestion of Bourgeois and Leithold (1984), a geomorphological terminology has been chosen in the description of the anatomy of beach lithosomes; indeed, a dynamic-zone terminology may be misleading, as the individual zones are subject to significant changes in position and width in response to the hydrodynamic conditions. In the nomenclature adopted here both the seaward-inclined subaerial and underwater beach surfaces are included under the term *beachface*, which therefore refers to the whole seaward dipping profile of the beach, from the highest berm to the landward boundary of the shoreface. Accordingly, the *upper beachface* indicates the normally emerged, gently sloping part of the beach, and the *lower beachface* refers to the steeper underwater slope of the beach. A bipartition into upper and lower beachface deposits can also be recognized in the architecture of the fossil counterparts (Fig. 3), highlighted by different dip angles of clinoforms, textural and fabric features of gravels, and stratification types. The deposits extending immediately landward of the crest of the highest berm are regarded as representative of the *backshore* zone.

A number of facies associations (FAs) can be identified. They correspond to the subunits which can be identified in the beach lithosomes, in turn reflecting the successive geomorphological zones typical of the littoral setting.

5.1. FACIES ASSOCIATION 1 (FA1)

5.1.1. Description

This facies association is characterized by sheet-like layers 3.5 to 53 cm thick, predominantly composed of medium to fine sand, alternating with bioturbated mudstone interbeds (Fig. 4A). The former show high lateral persistence, a sharp base, sometimes normal grading highlighted by well-rounded small pebbles, granules, or coarse sand grading to fine sand, and internal hummocky/swaley cross stratification commonly associated with, or replaced by, planar-parallel lamination. Rows of granules, as well as alignments of clay chips, locally emphasize the lamination. Wave ripples or combined-flow ripples may be present at the top, but commonly the sedimentary structures in the upper parts of the beds are blurred to a variable extent by bioturbation. Thin-shelled oyster shells, bored pebbles, and local concentrations of plant remains may be sparsely present. Burrows, represented by the *Skolithos* ichnofacies, include *Ophiomorpha*, *Thalassinoides*, *Bichordites*, *Cylindrichnus*?, endogenic meniscus-filled echinoid repichnia, and local escape burrows. Liquefaction and fluidization structures are present in places, the latter emphasized by the upward active injection of sand with the generation of water-escape flame structures.

5.1.2. Interpretation

Sheet sands have been repeatedly described in the literature of shelf to nearshore deposits (e.g., Zhang et al., 2016, with references) as storm layers laid down in the so-called "offshore transition zone" situated in the palaeo-bathymetric range between the fair-weather wave base and storm wave base, where the sand/mud rhythm results from an alternation of storm and fair-weather conditions. In this zone, episodic storm-generated combined flows typically result in graded, waning-flow beds characterized by hummocky cross-stratification (Dott and Bourgeois, 1982; Walker and Plint, 1992). Swift et al. (1983) postulated that hummocky cross-bedding in modern continental shelves is the product of combined-flow storm currents, in which intensified oscillatory motion is superimposed on wind-driven along-coast geostrophic currents.

The bioturbated fine-grained division records the re-settling of a normal population of infaunal benthic organisms after the high-energy event. Liquefaction and fluidization structures may be triggered by different processes, including pore pressure changes induced by the cyclic stresses of storm waves, or loading that occurs when sand is rapidly deposited on top of water-saturated muds, leading to fluid expulsion (Oliveira et al., 2009), or earthquake shocks.

5.2. FACIES ASSOCIATION 2 (FA2)

5.2.1. Description

Almost completely consisting of sands, this FA is typically present beneath the gravelly clinoform-stratified units and can be subdivided into two parts. As highlighted below, the best expression of this FA is in the Apenninic palaeo-shoreline deposits.

5.2.1.1. The lower part

The dominant pattern of this part (Fig. 4B) is represented by large-scale, gently convex-up and concave-up laminasets of fine to medium sand, ranging from 13 to 40 m in wavelength and 1.2 to 2.7 m in thickness, outlining the geometry of large-scale bedforms, commonly bounded by gently curved, extensive erosional surfaces draped in places by concentrations of clay chips or thin mudstone

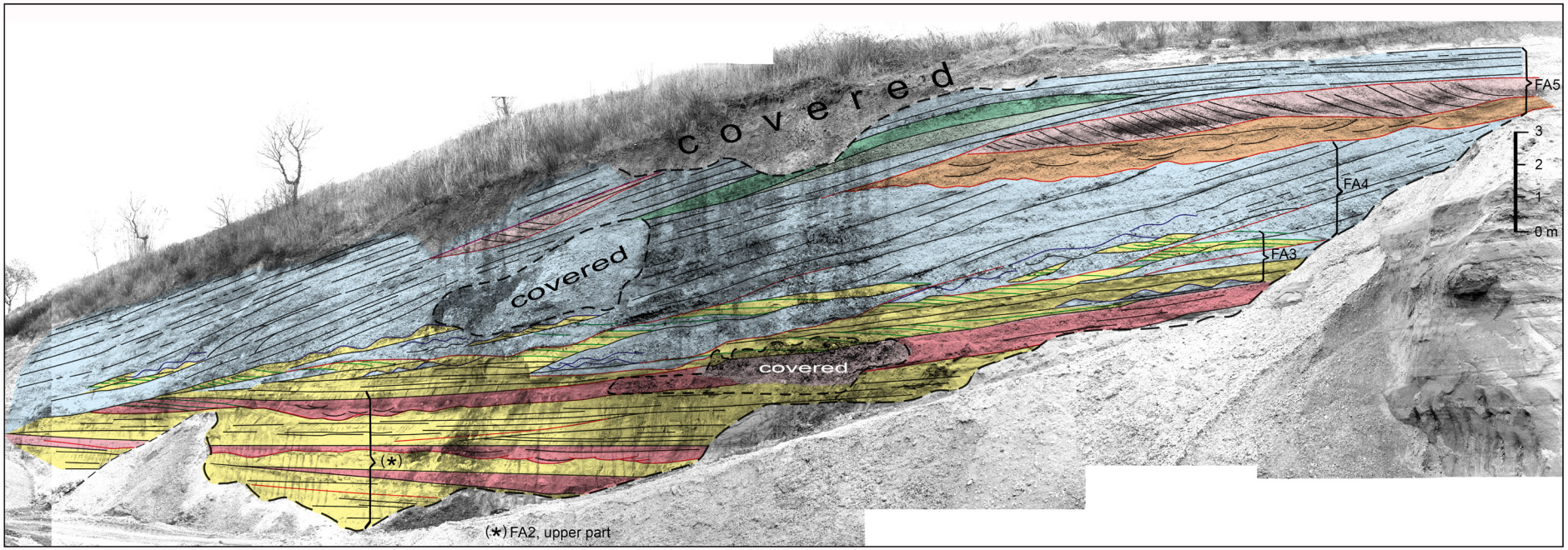

Fig. 3 - View of an Apenninic progradational middle Pleistocene gravel beach lithosome in a dip-oriented section (land to right). The line drawing documents details of the facies architecture and stratal surfaces. In the clinoform-stratified wedge (light blue), the gentle inclination of the upper part (upper beachface) and steeper dip of the lower part (lower beachface) can be appreciated. The intervals corresponding to the identified facies associations (FA) are indicated. See next figures for the facies interpretation of the variously coloured parts. Abandoned quarry near Villa Gigli, WSW of Porto Recanati, SE of Ancona (1:25,000 topographic map "Recanati").

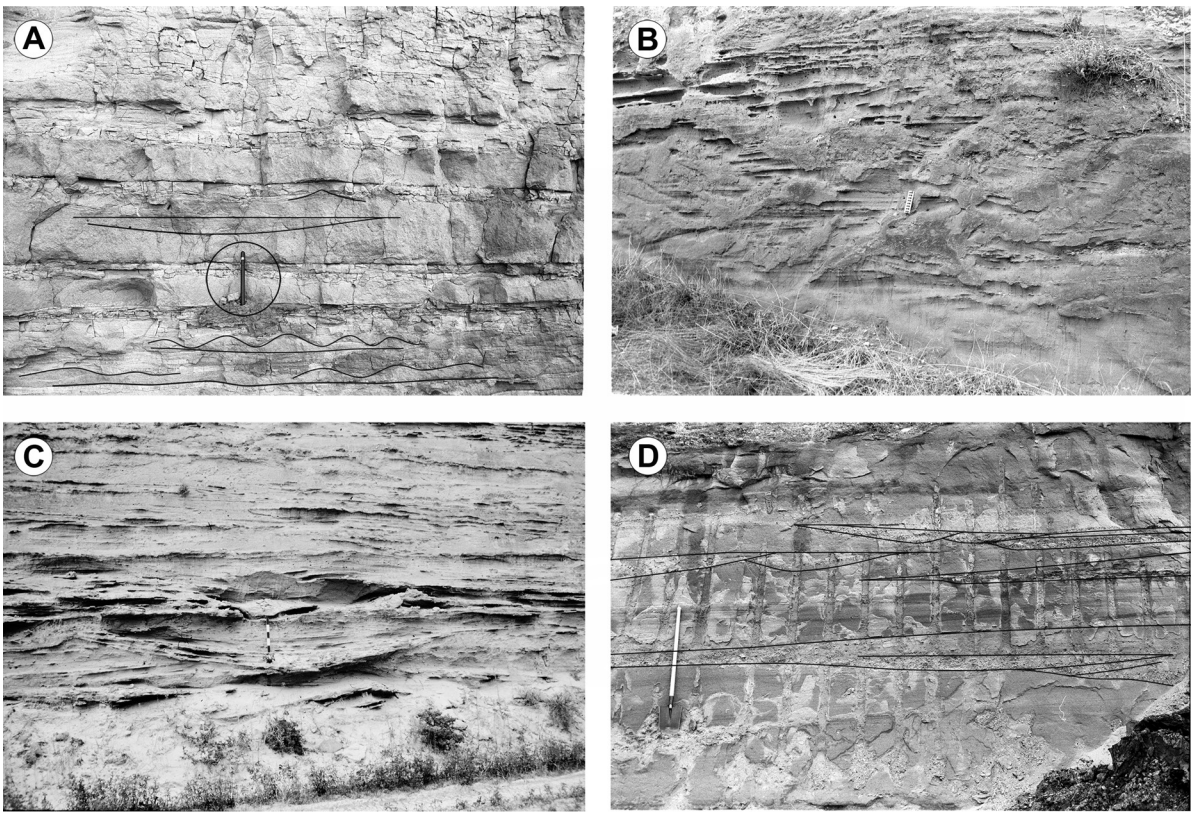

Fig. 4 - Details of FA1 and FA2 facies associations. A) Storm layers (FA1). Encircled pen 13 cm long for scale; B) Low-amplitude convex-up and concave-up sand laminasets with large wavelengths bounded at the base by gently curved erosional surfaces (FA2, lower part). Scale bar 16 cm long. Both photos: Middle Pleistocene complex, road S. Benedetto del Tronto - Acquaviva (1:25,000 topographic map "San Benedetto del Tronto", central Italy); C) Swaley cross-stratification (FA2, lower part). Scale bar 50 cm long. MIS 5.1-5.3 terrace, near Masseria S. Salvatore, about 1200 m SE of Serra Marina (1:50,000 topographic sheet "Ginosa", southern Italy); D) Details of the upper part of FA2 in a nearly strike-oriented section. Scour-based lenses are interpreted as the record of rip channel fills. Their basal surfaces are floored by a mix of granules and small pebbles and show (upper lenses) a pattern of coalescence of broad shallow scours suggesting channel migration. Shovel 1.2 m high for scale. Middle Pleistocene, abandoned quarry near Villa Gigli, WSW of Porto Recanati, SE of Ancona (1:25,000 topographic map "Recanati", central Italy).

layers. The internal lamination of the sets is generally conformable with the profile of the bedforms and shows relationships with the basal erosional surfaces ranging from conformable to onlapping or downlapping at low angles (<15°). These large-scale bedforms predominantly show a trend of migration toward the clinoform-stratified gravel unit. The gently curved basal scour surfaces of the laminasets or some internal laminae may be floored by well-rounded small pebbles and/or granules, present as scattered clasts or small clusters or segregated into thin discrete alignments or discontinuous rows 1-2 clasts thick. Amalgamated hummocky/swaley cross-stratified sets may be locally associated (Fig. 4C), with hummocks/swales spaced a few metres to up to 5 m apart. Other components are sparse plant remains, including well-rounded pebble- to cobble-sized wood fragments, and rare mollusc remains (mostly pectinids and ostreids). Burrows include sparse *Thalassinoides* and rare exhumed *Cylindrichnus.* Fluid-escape structures are locally present.

5.2.1.2. The upper part

The upper part of FA2 is dominated by the amalgamated stacks of discrete laminasets of fine to medium sand bounded by low-angle erosion surfaces, consisting of sub-horizontal or low-angle planar laminae, or low-amplitude curved laminae, typically encasing coarser-grained flat lenses with erosional bases and planar tops (Figs. 3, 4D, 5), and including in places sand and/or mixed gravel/sand wave megaripples. A trough cross-bedded interval commonly follows upwards, marking the transition to FA3.

The erosion surfaces bounding the amalgamated stacks of laminasets range from sub-horizontal or slightly inclined to gently curved, locally floored by rows of granules or small pebbles. Burrows include *Bichordites*, common tubes, and escape burrows.

The encased flat lenses show maximum thickness (up to 60 cm) near the toe of the clinoform-stratified unit and a trend thinning and fining outwards; they mostly consist of sand, but sometimes show a trend outward-fining from gravel close to the toe of the clinoform unit into sand (e.g., the lens in a higher position in figure 3). They can be traced in sections nearly parallel to the palaeo-flow for up to 27 m and in sections normal to

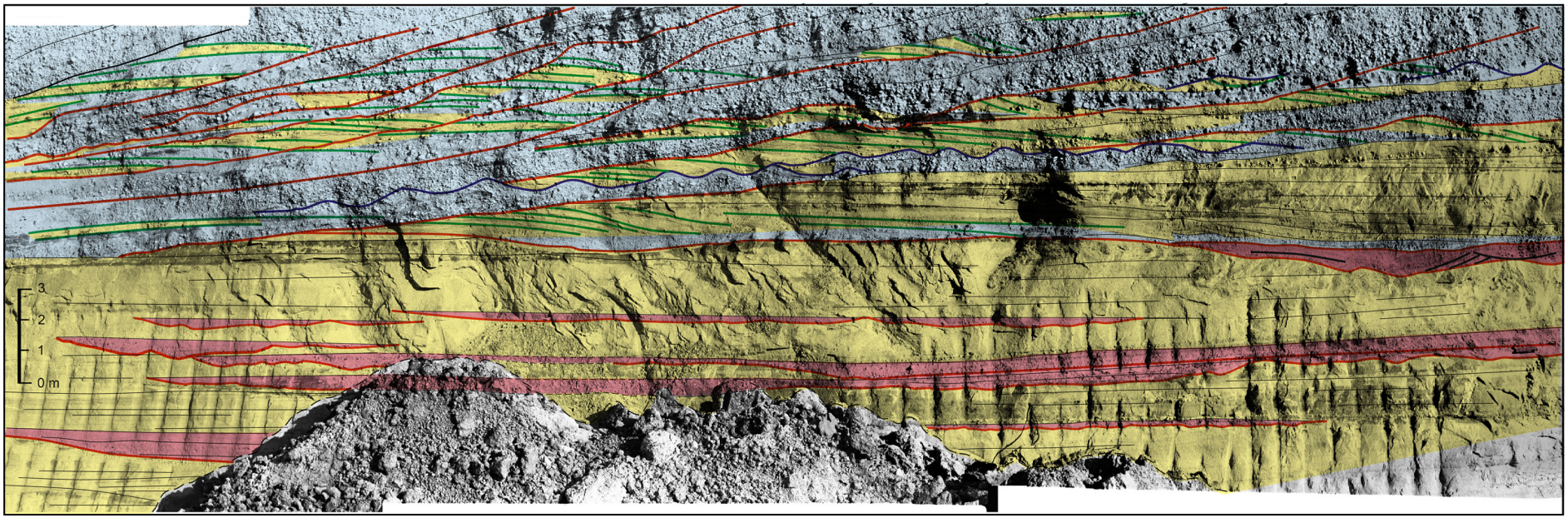

Fig. 5 - Detail of the lower part of the lithosome of figure 2 (nearly dip-oriented section, land to right), showing the upper part of FA2 and FA3 facies associations. The line drawing documents details of the facies architecture and stratal surfaces. The lower part shows flat lenses (pink) with an erosional base and planar top, regarded as infills of rip channels, embedded in mostly sub-horizontal, planar-parallel laminated sand (yellow). The sand laminaset at the base of the clinoform-stratified part shows low-angle upstream-dipping laminae (left) grading laterally into planar-subhorizontal laminae. In the upper part of the photo, sets of upstream-dipping laminae of sandy and in places gravelly composition climb the lower slope of clinoforms (flow to left). In association: gravel megaripples. Yellow: sand; light blue: gravel; pink: rip channel fills; green lines: backset bedding; blue lines: megaripple profiles; red lines: erosion surfaces. Middle Pleistocene, abandoned quarry near Villa Gigli, WSW of Porto Recanati, SE of Ancona (1:25,000 topographic map "Recanati").

it for 4 to 12 m; the basal surfaces may show a pattern suggesting the coalescence of broad shallow scours (Fig. 4D) and are commonly floored by a mix of granules and small pebbles; this pavement passes generally upwards with normal grading into sand. Some lenses appear to be localized in the shallow depressions of large-scale sandy bedforms. The internal structure of the lenses consists of planar-parallel laminae or, sometimes, low-angle, upstream-dipping cross-laminae. Sets or cosets of trough cross-laminated sand are present as local constituents of the lenses (Figs. 3, 5); they are bounded at the base by scour surfaces and show palaeoflow directed in general obliquely away from the prograding unit.

Locally associated sandy and/or mixed gravel/sand wave megaripples are either symmetrical or, more commonly, asymmetrical with some laminae dipping toward the clinoform unit, and show wavelengths ranging from 15 cm to 1 m (on average 48 cm). They locally display typical internal features, such as intricately interwoven bidirectional cross-lamination (De Raaf et al., 1977), and commonly bear drapes or internal rows of highly spherical small pebbles and/or granules.

A trough cross-bedded interval some metres thick commonly marks the transition to FA3 and is represented by sets and cosets of medium to coarse sand with sparse granules and small pebbles. Individual cross-bedded sets are on average 25 cm thick and are distinguished from each other by variations in grain size. Interspersed within the cross-bed sets are local bundles of planar-horizontal laminae, locally accompanied by rows of small pebbles, or, rarely, thin mud drapes. Occasionally, the set bounding surfaces or internal laminae of the sets bear veneers of finely macerated coalified organic debris. Palaeocurrent directions inferred from the cross-bedding are either unimodal, and sub-parallel or slightly oblique with respect to the strike of the clinoform-stratified bodies, or bimodal with opposite dips of the foreset laminae. Burrows are restricted to rare *Planolites* and *Ophiomorpha*, and low intensity of bioturbation suggests unstable, mobile substrates. The trough cross-bedded interval may be completely lacking in some lithosomes and in this case the contact between FA2 and FA3 is marked by a distinct break in particle size, suggesting the presence of an erosional discontinuity.

All the elements of FA2 described above are typically represented in the Apenninic lithosomes. Conversely, in the South-Alpine domain only a few of them are preponderant, namely amalgamated hummocky/swaley cross-stratified sets and sandy megaripples; trough cross-beds generated by outward-directed flows are sparsely present, whereas trough cross-bedding oriented sub-parallel to the inferred shoreline has only rarely been observed.

5.2.2. Interpretation

FA2 is interpreted to represent the sand-prone shoreface setting in front of the gravel beaches.

The *lower part* of FA2 is regarded as the record of lower shoreface macroforms such as sandy nearshore bars and the associated interbar troughs. Similar large-scale structures have been reported from the shoreface deposits of coarse-textured littoral successions by Leithold and Bourgeois (1984), Massari and Parea (1988a), and Hart and Plint (1995), among others. The stratal organization suggests predominant onshore bar migration under the influence of late-storm to storm-decay waves. The thin mud layers may be laid down when the environmental energy decreases to low values, allowing the settling from the suspension of fines put in suspension during storms and/or introduced by river floods. The related cohesive fine-grained deposits cannot be easily removed by subsequent high-energy events, except as rip-up clasts.

The *upper part* of the zone is inferred to represent the record of bar/rip morphology in an upper shoreface setting. The laminated sands are inferred to be laid down by storm-intensified flows on the crests and slopes of migrating longshore bars, combining a unidirectional component due to storm-induced near-bed flows and an oscillatory component linked to high wave-induced orbital velocities. The flat, scour-based normally graded and laterally discontinuous lenses showing a texture coarser-grained than the adjacent shoreface deposits are regarded as the infills of rip channels, locally showing evidence of localization in the interbar troughs (e.g., Davidson-Arnott and Greenwood, 1976; Leithold and Bourgeois, 1984; Massari and Parea, 1988a; Hart and Plint, 1995, 2003). Rip currents are offshore-directed flows representing an important cross-shore cause of sediment transport far beyond the surf zone during storms (Masselink and van Heteren, 2014, with references). An offshore-directed pressure gradient is created along the shoreline as a response to the net landward movement of water as waves shoal. This imbalance is relieved by offshore directed rip currents through breaks in shore-parallel longshore bars or gaps between oblique bars. The coalescence of broad shallow scours shown by basal erosional surfaces (Fig. 4D) may be produced when rip channels oblique with respect to the shoreline migrate in the direction of the longshore current together with the associated low-amplitude sand bars during high-energy events (Hunter et al., 1979; Clifton, 1981). Lateral migration may result in a width of the erosional depressions larger than that of the original rip channels. Similar structures are reported in gravel-bearing shoreface deposits by Dupré (1984), Leithold and Bourgeois (1984), and Katsura et al. (1984). The oblique dip direction of the associated trough cross-bedded units with respect to the dip of the clinoforms of the prograding bodies suggests a localization of rip channels in nearshore interbar troughs oblique to the shoreline, as part of a skewed bar/interbar system; the erosional basal relationships of the trough cross-bedded units suggest that they formed by the three-dimensional dune migration that occurs when rip flow weakens, partly reworking the higher-energy laminated deposits laid down at the storm-peak stage.

The trough cross-bedded interval commonly occurring

in the upper part of the FA2 is attributed to the longshore drift of three-dimensional dunes in the more onshore area of the upper shoreface. Dunes probably migrated parallel to or at a low angle with respect to the reconstructed shoreline orientation, suggesting a significant control of longshore currents. The local absence of this interval in some lithosomes, generally accompanied by a grain-size discontinuity, may indicate erosion of the upper part of the shoreface succession during the progradation of the clinoform-stratified wedge, possibly in concomitance with lowering of base level.

As noted above, the characteristic elements of FA2 are all represented in the Apenninic palaeo-shoreline deposits, where they are suggestive of a storm-induced nearshore bar/rip morphology, with a surf zone expanded offshore during storms; the palaeoflows suggest that bars and rip channels oriented obliquely to the shore may have been a common feature. Wright et al. (1979) pointed out that large-scale inshore rhythmic topography is consistently absent from reflective beaches, but cellular circulation and rip currents may be present during storms. It may be inferred that during high-energy events the Apenninic palaeo-beaches could change from more or less reflective to an intermediate state (in the sense of Wright and Short, 1984). Conversely, in the South-Alpine domain, only a few of the elements of FA2 are preponderant, namely amalgamated hummocky/swaley cross-stratified sets and sandy megaripples, while others are scarcely represented. Specifically, seaward-directed trough cross-beds sparsely occurring in South-Alpine units are interpreted to record episodic deposition from seaward-directed unidirectional flows, either linked to river floods near the mouth of effluent delta distributary channels or to the sporadic activity of storm-induced rip currents. Associated with rare evidence of longshore directed trough cross-bedding, these features suggest that the change to an intermediate state during storms was an unusual event in this area.

5.3. FACIES ASSOCIATION 3 (FA3)

5.3.1. Description

This facies association refers to the complex structures and stratal organization of the toe of the clinoform-stratified units. The toeset beds typically show a primary dip decreasing outwards from about 4° to about 1° and a taper downdip with an asymptotic progressive downlapping pattern (Figs. 3, 5, 8). FA3 shows partly different characteristics in the two groups of beach lithosomes. The most typical depositional theme in the Apenninic units is represented by sharp-based couplets made up of pebble to cobble gravel layers capped by sandy lenticular sets of cross-laminae dipping upstream at moderate to high angles (Figs. 3, 5, 7). By comparison, the South-Alpine lithosomes are dominated by low-amplitude, sandy and gravelly wavy/lenticular structures (Fig. 9), with cross-laminae usually dipping upstream at low angles. Additional constituents of the FA3 in both groups of lithosomes are represented by wave megaripples.

The FA3 gravels are primarily an ill-sorted mixture of components ranging from cobbles, sometimes outsized, to sand, and they are the coarsest occurring in the beach lithosomes. Clast-supported gravel beds with interstitial sand infilling the pore throats of the clasts are about 76 %; layers with clasts supported by a sand matrix are 24%. Gravel beds commonly display size and shape bimodality, with sparse spherical to subspherical large pebbles or cobbles in a matrix consisting of a population of small pebbles/granules with variable shapes (Figs. 7 A,D; see also 9A and 10D). Alternatively, only the finer-grained clast population may be present in unimodal-sized layers (e.g., Fig. 7D, upper part). Sometimes the layer tops show a drape one-clast-thick of spherical clasts. High-sphericity pebble/cobble gravels increase in abundance in the outer part of the toeset zone. Observations on 93 beds of FA3 show that in the coarse dimensional mode the spheres are 87%, the rods are 7%, and the blades are 6%, while the discs are missing.

Azimuthal roses of clast long-axis fabric are obtained in South-Alpine units (Fig. 6), where measurements were feasible due to the common exposure of stratal surfaces. The fabric ranges from moderately to weakly preferred or nearly isotropic, as shown by the infills of deep scours (Fig. 7 C,D); unimodal roses show upcurrent dipping clast long axes, commonly with steep imbrication angles. In general, the clast fabric is remarkably less preferred than in the FA4 beds (see below). Directions of imbrication tend locally to deviate either rightwards or leftwards with respect to the dip direction of the clinoforms of the prograding body. Gravels in toeset beds of the Apenninic units (only visual observations) commonly show a disorderly fabric; upslope-, or rarely downslope-dipping imbrication were locally observed.

As noted above, the "leitmotif" of the Apenninic lithosomes is represented by sharp-based gravel to sand couplets consisting of pebble to cobble gravel layers capped by lenticular sets of upstream-dipping, usually sandy cross-laminae (e.g., Fig. 7). The gravel beds show thicknesses usually ranging from one-clast to 30 cm and end generally updip either by pinch out or by truncation at the contact with the FA4 gravel clinobeds (Fig. 8); a physical continuity between FA4 and FA3 beds is present only in a minority of cases. An inspection of the relationships between FA4 and FA3 layers highlights that the toeset beds are less numerous than FA4 beds, the latter commonly showing a downlap relationship to the former.

The FA3 gravels at the base of backset laminasets are mainly represented by a single layer, and sometimes by a bundle of two or three layers. The basal surfaces of gravel layers are usually gently erosional, but in places appear as bowl-shaped asymmetrical scours up to 70 cm deep, with a steeper margin facing away from the clinoform unit, generally coinciding with the slope break at its foot. These deep scours are either completely infilled with structureless or crudely graded gravel showing chaotic fabric (Fig. 7 C,D) or floored by a relatively thin gravel

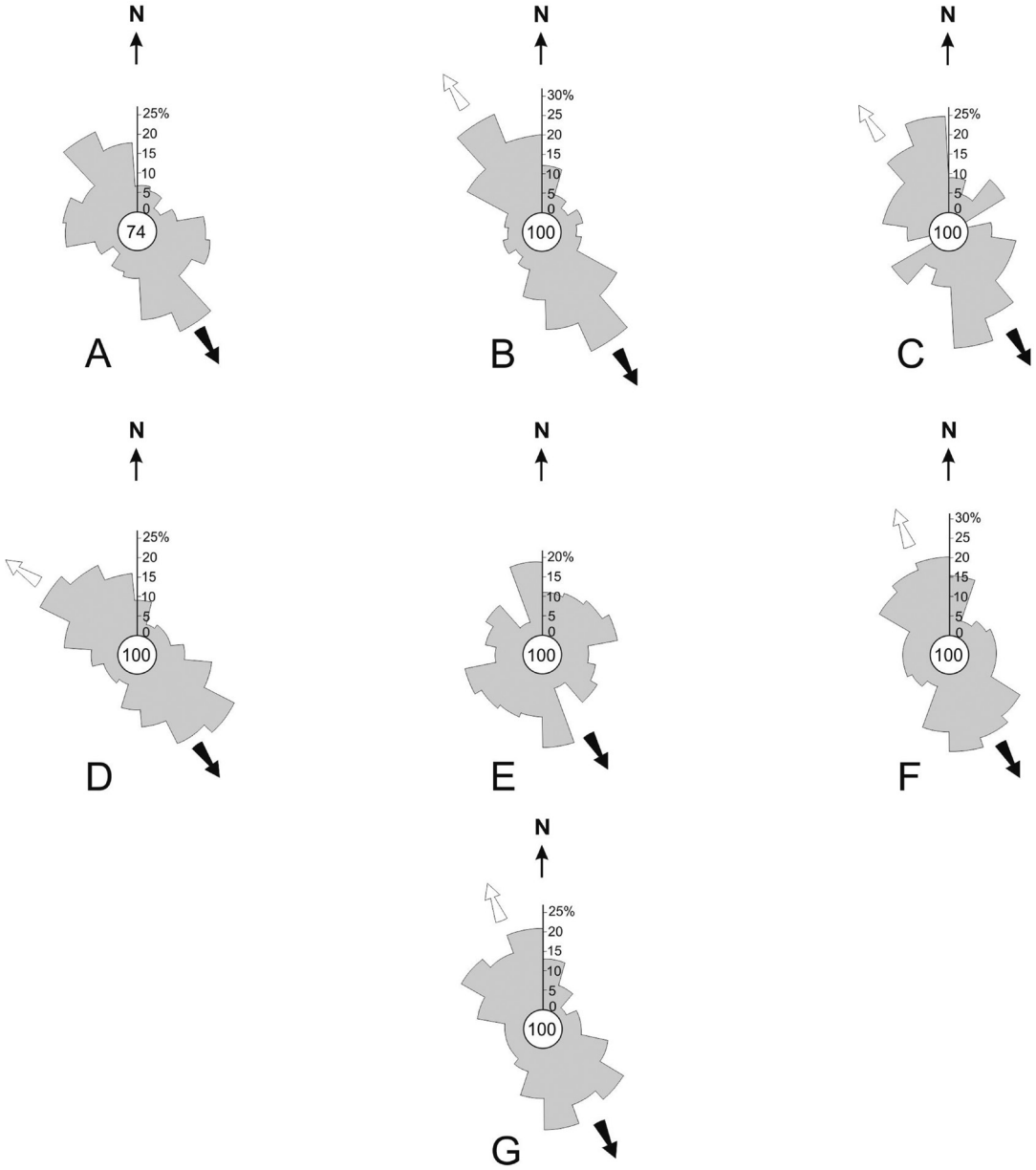

Fig. 6 - Rose diagrams illustrating the fabrics of FA3 gravels in a South-Alpine beach lithosome. Measures of the long-axis orientation of rods showing an a-axis to b-axis ratio over a minimum of 1.70 were made on the upper surfaces of layers occurring in succession upwards. A solid arrow shows the direction of progradation; an open arrow indicates the approximate dip of imbrication, as inferred from field evidence. For each sample, some annotations on the textural characteristics are added. A) sample 580: bimodal clast texture with subspherical large pebbles and rare cobbles in a matrix of small pebbles; B) sample 582: ill-sorted bimodal texture with large pebbles and rare cobbles with variable shapes, in a matrix of small pebbles and sand; C) sample 584: poorly sorted, clast-supported pebbles with variable shapes; D) sample 586: poorly sorted, bimodal clast texture with large pebbles and rare cobbles in a matrix of small pebbles; E) sample 589: bimodal clast texture with large subspherical pebbles in a matrix of small pebbles; F) sample 590: poorly sorted with pebbles of variable sizes; G) sample 591: poorly sorted, clast sizes ranging from large pebbles to granules. South-eastern side of Monte Stella (about 4 km SW of the town of Vittorio Veneto; 1:25,000 topographic map "Vittorio Veneto").

layer (Fig. 8); in the former case the set of backset-laminated sand lies on the planar upper surface of the gravel infill, and in the latter case on the gravel-paved scour (Fig. 8).

The sets of backset cross-laminae which form the upper units of the couplets (Figs. 3, 5, 7) are in general composed of fine to medium sand, although some sets include laminae consisting of coarse sand, granules and/or small pebbles (e.g., Fig. 5); the coarser-grained backset laminae commonly show an updip decrease in abundance and grain size of component particles, sometimes from gravel to sand. Rarely, backset-bedded sets are entirely made up of gravel. Clasts occurring within the laminasets locally show imbrication indicating flow opposite to the dip of the laminae, a characteristic of backset bedding. The substrate of the backset laminasets is in most cases

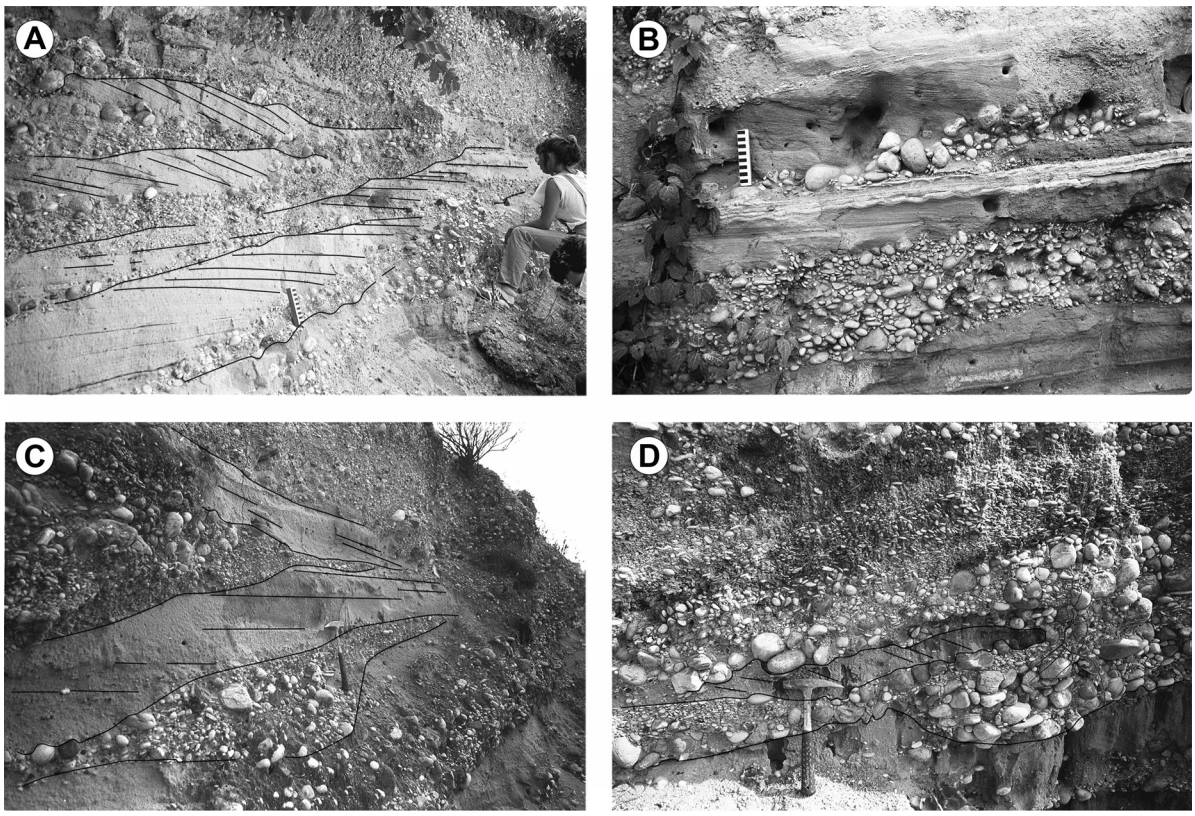

Fig. 7 - Details of toeset beds (FA3 facies association) in nearly dip-oriented sections of Apenninic beach lithosomes (land to right; flow to left). A) Couplets consisting of gravel layers overlain by sandy lenticular sets of upstream-dipping cross-laminae. Scale bar 16 cm long. Middle Pleistocene, abandoned quarry near Villa Gigli, WSW of Porto Recanati, SE of Ancona (1:25,000 topographic map "Recanati", Marche region); B) Scour-based gravel layers overlain by sets of backset-laminated sand, in turn capped by wave ripples. Note the high sphericity of larger pebbles. Scale bar 16 cm long. Middle Pleistocene, near the village of Pedaso, SE of the town of Ancona (1:50,000 topographic sheet 315 "Fermo", Marche region); C) and D) Deep troughs infilled with ill-sorted gravel with a chaotic fabric, overlain by sets of backset-laminated sand. Note the gravel bimodality, with large spherical clasts in a matrix of small pebbles, particularly in the lower layers of figure 7D, and the unimodal layer consisting of landward-imbricated small pebbles in the upper part of figure 7D. Hammer for scale. Same locality as figure 7A.

gravelly; uncommonly it is sandy. A distinction should be made between the gravel layers at the base of the gravel/sand couplets, generally showing sharp contact with the sandy backset laminasets, and the gravel backset laminae locally interstratified with sandy backset laminae.

The sets are 15-45 cm thick; an exceptional thickness of 82 cm was shown by a sandy set with scattered granules and pebbles. Bioturbation is absent. The sets can be followed for up to 18 m in dip-oriented sections, and gradually wedge out both downdip and updip; in the updip direction the sets generally "climb", to some extent, the lower slope of the clinoform-stratified units. The downslope end of the sets generally overtakes that of underlying gravel layers; less commonly it coincides approximately with it or is located slightly upslope. In dip-oriented sections the sets show in most cases a gently lenticular geometry. Their basal surfaces are generally adjusted to the top of the underlying gravel layers without evidence of erosion, and they range from sub-planar (Fig. 7 A,B) to concave-up where the sets backfill gravel-paved bowl-shaped scours (Fig. 8); the basal contacts may be erosional where the sets, especially the coarser-grained ones, overlie a sandy substrate. The top surfaces of the sets are slightly convex-upward and usually somewhat irregular, being more or less sharply truncated at the contact with the overlying gravel beds (Fig. 7A); in the absence of top-truncation they rarely show a regular and symmetrical, gently convex-up profile (see Fig. 10A, lower left). Locally, the top surfaces are moulded into megaripple profiles (Fig. 3). In dip-oriented sections the internal backset laminae dip at angles of 10° to 28° with respect to the basal surfaces of the sets. They are either planar, concave with basal tangential contact, or slightly convex. Convex laminae commonly thicken upstreamward when progressively abutting against the basal surface of the set (Fig. 7A). In the outer reach of the toeset zone, backset laminae may pass into planar-parallel, horizontal laminae (Fig. 5). Intrasets of small--scale ripple cross-laminae occasionally occur between the backset cross-laminae. Sometimes bundles of backset laminae with a slightly different orientation are separated from one another by reactivation surfaces, or, rarely, by a thin mud drape. In strike-oriented sections the sets appear as very flat planoconvex lenses 3 to 6 m long, with

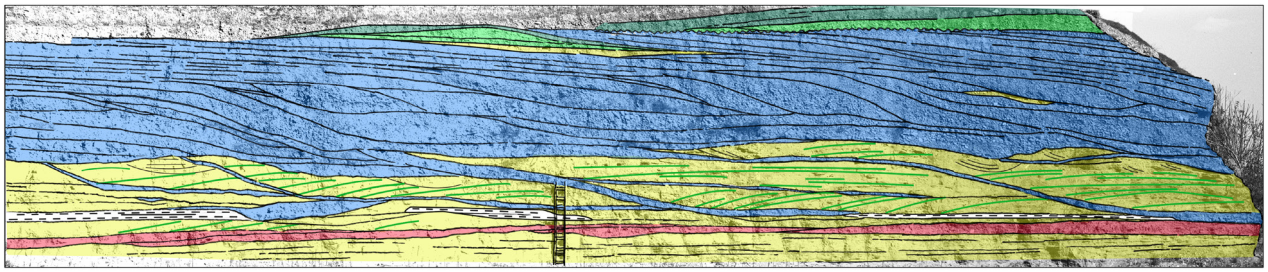

Fig. 8 - View of an Apenninic beach lithosome with a gentle dip of clinoforms in a nearly dip-oriented section (land to left). The line drawing documents the facies architecture and stratal surfaces. In the toeset area, concave-upward, asymmetrical, deep scour surfaces with steep seaward-facing margins are paved by gravel and backfilled by upcurrent dipping sand laminae. Lower-beachface gravel beds forming the bulk of the clinoform-stratified unit are commonly lenticular with erosional bases, locally sigmoidal with a developed asymptotic tail; they mostly show updip and downdip wedging out. Upper-beachface gravels in the upper part of the unit show regular thin bedding and storm berms at the top. Yellow: sand; light blue: gravel clinobeds of the prograding body; red: inferred infill of rip channel; hatched lines: mud layer; light green: planoconvex low-relief gravel ridges at the core of storm berms; dark green: layers involved in the accretion of storm berms; green lines: backset bedding. The rung ladder is 2.4 m high. MIS 5.1 terrace, quarried near the village of Scanzano Jonico, close to the km 422.100 of the State Road "Ionica" (1:50,000 topographic sheet "Policoro").

planar bases and very gently convex-up tops, and internal lamination following the upper profile.

An additional component of FA3 is represented by low-amplitude, wavy to lenticular bedforms, generally symmetrical, ranging in composition from fine sand to pebble gravel (Fig. 9). As noted above, these structures form the bulk of the toeset deposits in the South-Alpine units (Fig. 9), while they are minor components of the Apenninic units. Sandy bedforms (Fig. 9 A,B) are 1.6 to 3.6 m in wavelength and in general consist of fine to coarse sand, with laminae highlighted by slight variations in grain size, locally by rows of granules or small pebbles (Fig. 9A). The basal surfaces are generally planar or slightly wavy, and the top is broadly convex-up or wavy; internal laminae are either in phase with a convex-up top surface or dip upstream at angles of less than 10° (Figs. 9A) with slight upcurrent convergence or divergence. Groups of laminae may be separated by reactivation surfaces. Gravelly bedforms (Fig. 9C) appear as low-amplitude wavy bedforms with wavelengths ranging from 0.5 to 2 m, and locally rough internal lamination either conformable to the wavy pattern or showing low-angle upstream-dipping laminae in the gentle troughs of the structure.

Some Apenninic lithosomes thicker than average show a characteristic spectrum of structures (Fig. 10) which, although uncommon, are considered important for the interpretation of the nature of involved flows in the toeset area. Figure 10A shows an array of gravel lenses arranged lateral to one another with a wavy upper surface, overlain by sandy lenticular sets of backset laminae localized in the troughs between the crests of the gravel bedforms. The toeset of the same beach lithosome shows low-amplitude swales and hummocks in coarse granule- and pebble-bearing sandstones (Fig. 10 B-D); laminae in the swales taper toward the trough margins and are first concordant with the basal surfaces, then decrease in concavity upwards (Fig. 10 B,C). They show a significantly coarser grain size on the upstream sides of the troughs (Fig. 10C).

Toeset deposits of some Apenninic lithosomes show an intimate interstratification of backset laminasets with trough cross-laminated sets of medium to coarse sand, the latter tending to predominate in the upper part of the composite units (Fig. 11). The lack of bioturbation in both structures indicates that the rate of production of physical structures exceeded that of bioturbation. The angles measured between the average orientation of trough axes and the dip azimuth of the backset laminae range from approximately 90° to 120° (Fig. 12).

Wave megaripples, mostly made up of gravel, locally sand or mixed gravel/sand, are another component of FA3 (Figs. 3, 5, 13). They show wavelength ranging from 25 to 110 cm and wavelength/height ratio from 5.5 to 7.5. When overlain by sand, the profiles of gravel megaripples are well recognizable in cross-section; when overlain by gravels, their identification, not straightforward, may be based on subtle differences in fabric, grain size, or morphometric features. Sometimes the top surface of sets of backset sand laminae is moulded into megaripple profiles. Like the associated toeset layers, the gravelly bedforms commonly show a size and shape bimodal texture, with a variable proportion of high-sphericity pebbles of intermediate to large size contained in a matrix of minute pebbles and granules of variable shapes (e.g., Figs. 9A, 13). Locally spherical clasts are present as predominant constituents of the megaripples or as a veneer one-clast thick draping the surface or one side of the bedforms.

Symmetrical profiles are common; local asymmetry is highlighted by the steeper sides of the bedforms facing away from the clinoform-stratified unit and a few internal laminae dipping in the same direction. An opposite asymmetry is less common. The crests of the megaripples are peaked or rounded and locally are planed off; in this case the original presence of wave-produced bedforms can sometimes be inferred from the clast fabric. Where a preferred clast orientation is present, the fabric is bipolar,

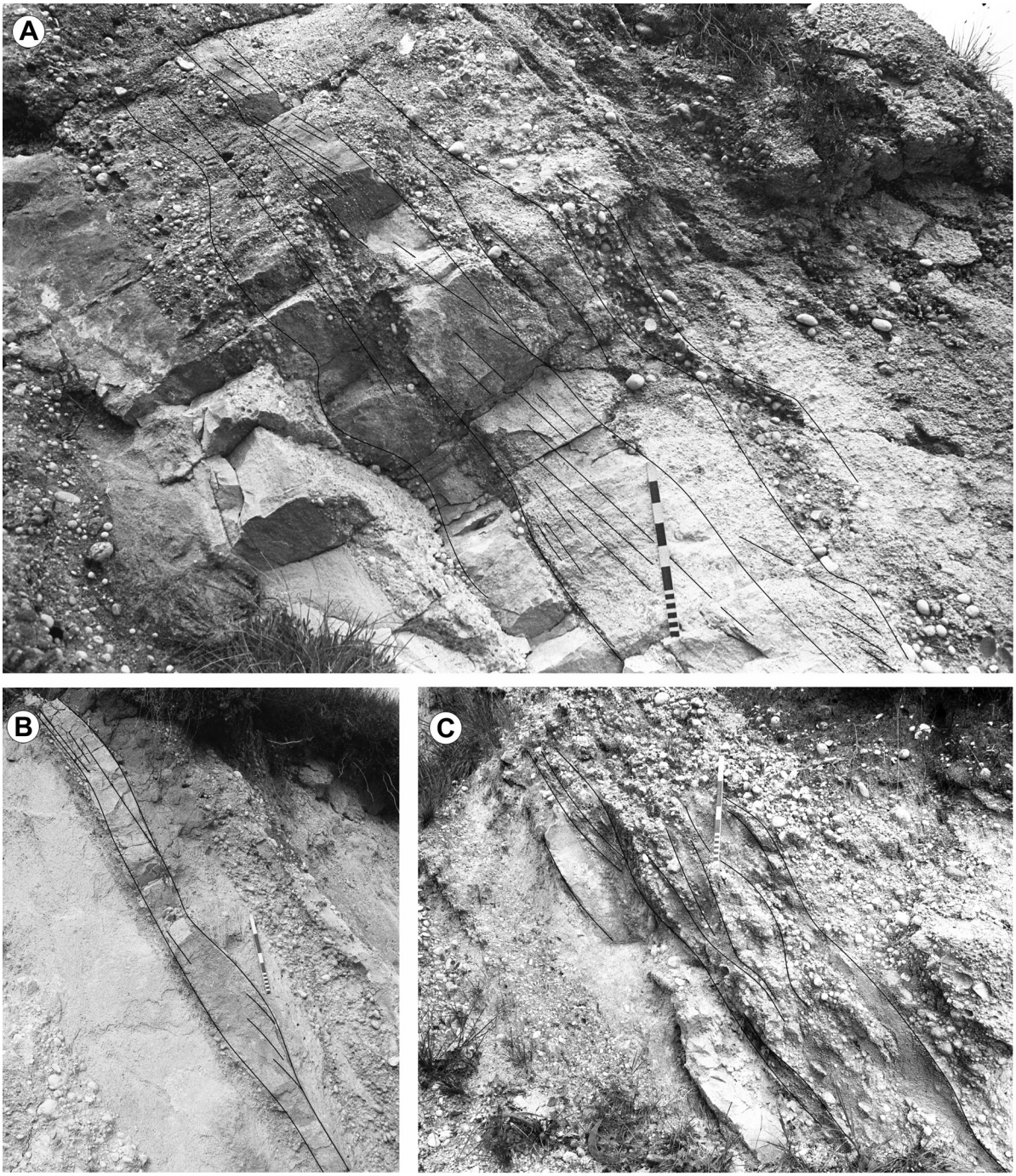

Fig. 9 - Details of toeset deposits (FA3 facies association) from nearly dip-oriented sections of tectonically tilted South-Alpine beach lithosomes (land to upper left; flow to lower right). A) Beneath the scale bar: granule-bearing sandy bed showing low-angle upstream-dipping cross-laminae. Below and above it: gravel megaripples containing spherical pebbles of intermediate to large size in a matrix of small pebbles and granules. Scale bar 40 cm long. Track between C.se Val Torond and S. Antonio, about 2.5 km SW of the town of Vittorio Veneto; B) Sandy bedform (centre of the photo) with low-angle, upstream-dipping lamination and gently wavy upper surface. Scale bar 40 cm long; C) Low-amplitude gravel and sand wavy bedforms (middle of the photo) overlain by gravels showing size and shape bimodality, with abundant spherical pebbles of intermediate to large size in a matrix of small pebbles and granules of variable shapes. Scale bar 40 cm long. Photos B and C: south-eastern side of Monte Stella, about 4 km SW of the town of Vittorio Veneto (reference map for all photos: 1:25,000 topographic map "Vittorio Veneto").

with co-existing opposite clast imbrications; this feature is commonly associated with high-angle to sub-vertical orientations of clast long-axes. Sometimes the bipolarly imbricated adjoining groups of clasts, when seen in cross section, show chevron-like patterns similar to those shown by adjacent groups of laminae in sandy wave ripples.

Mud drapes are locally present in the toesets, sometimes draping the megaripples and preserving their profiles

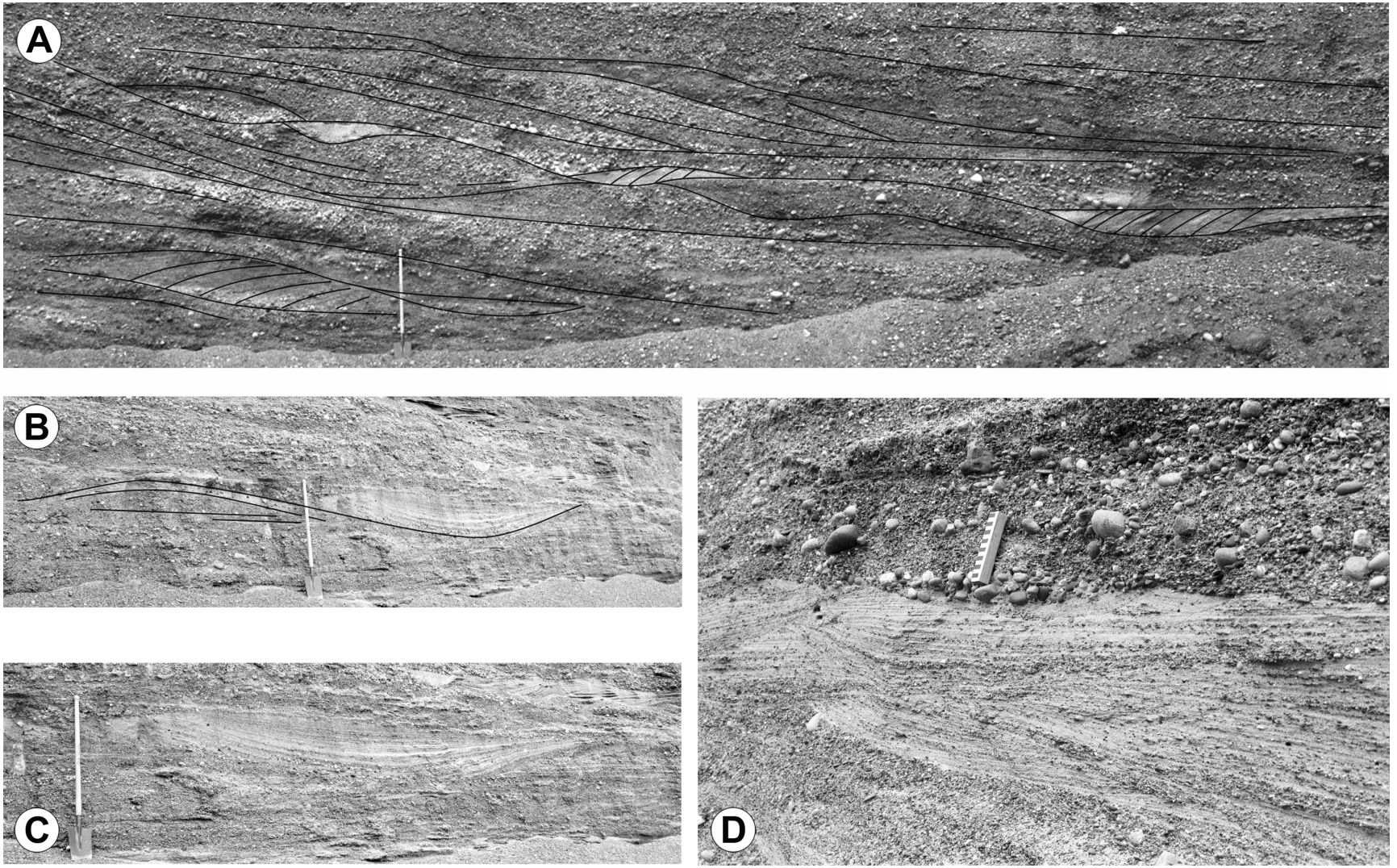

Fig. 10 - Toeset structures of a thick Apenninic beach lithosome (nearly dip-oriented section; land to left, flow to right). A) At the centre of the photo: a series of laterally adjacent gravel lenses with wavy upper surface, overlain by lenticular sandy backset laminasets localized in the troughs between the crests of gravel bedforms; in the lower left: backset-laminated pebbly sand bounded at the top by a gently convex-up profile; B) Hummock and swale interpreted as chute-and-pool bedforms (lateral to the shovel) in granule- and pebble-bearing sandstone and fine-grained gravel; C) Detail of the swale showing that laterally tapering laminae are significantly coarser-grained on the upstream side (left) of the trough. Photos A-C: shovel 1.2 m high for scale; D) Inferred chute-and-pool structures in granule-bearing sand overlain by a gravel layer showing size and shape bimodality, with spherical pebbles of intermediate to large size in a matrix of small pebbles and granules. Scale bar 16 cm long. All photos: MIS 5.5 terrace, SARIM quarries, country Lama di Pozzo, NW of Ginosa Marina (1:50,000 topographic sheet "Ginosa").

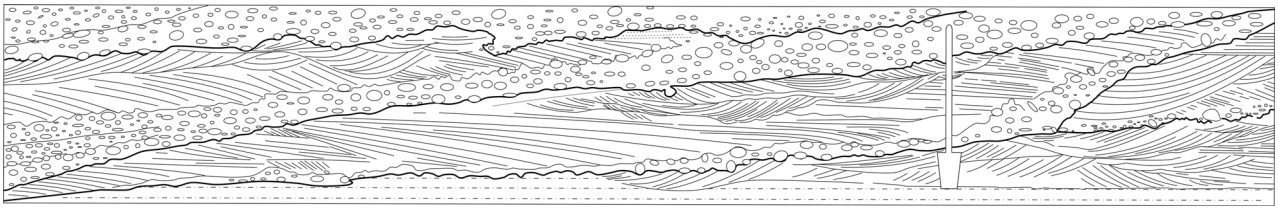

Fig. 11 - Nearly dip-oriented section of the lower part of an Apenninic beach lithosome (land to right) showing details of toeset deposits. Gravel layers bounded at the base by scour surfaces are overlain by sandy composite units consisting of backset-laminasets interstratified with trough cross-laminated sets. The latter is predominant in the upper parts of the composite structure and oriented on average perpendicular to the dip of the clinoforms of the prograding body. MIS 5.1 terrace quarried immediately south of the village of Scanzano Jonico (1:50,000 topographic sheet "Policoro"). Shovel 120 cm high for scale.

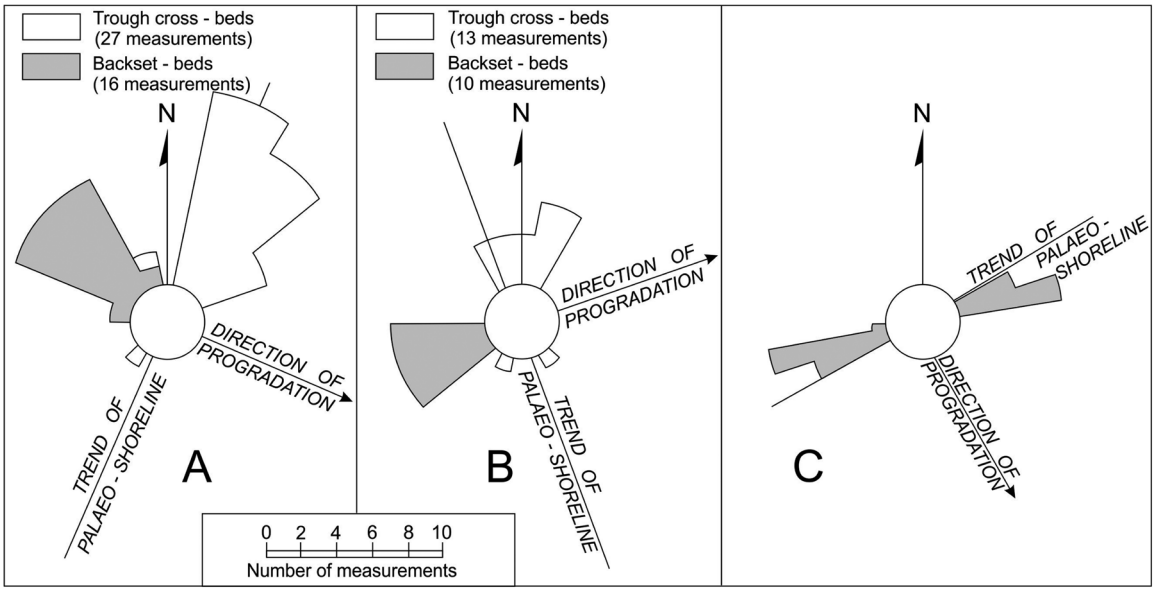

Fig. 12 - A) and B) Azimuthal roses showing dip directions of backset laminasets and axes of trough cross-beds relative to the inferred trend of the palaeo-shoreline and the direction of progradation in the Apenninic beach lithosomes of Scanzano Jonico (MIS 5.1 terrace, A), and Villa Gigli near Porto Recanati (middle Pleistocene, B); C) Directions of megaripple crests relative to the trend of the palaeo-shoreline in South-Alpine beach lithosomes of the Vittorio Veneto area (14 measures).

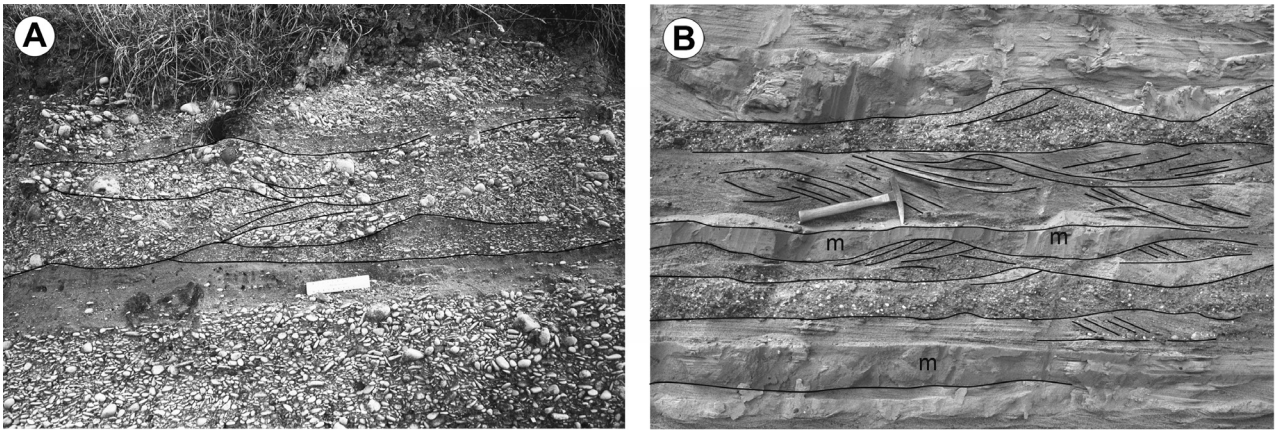

Fig. 13 - Examples of megaripples preserved in the toeset of Apenninic beach lithosomes. A) Gravel wave megaripples with pebble clusters variably oriented. Ruler 12 cm long for scale. Nearly dip-oriented section; land to right. Middle Pleistocene, abandoned quarry near Villa Gigli, WSW of Porto Recanati, SE of Ancona (1:25,000 topographic map "Recanati"); B) Sand/gravel wave megaripples with profiles preserved by muddy cap (m), or locally truncated by the emplacement of gravel layers. Nearly dip-oriented section (land to right). MIS 9.5 or 11 terrace, quarry IME Falcone, Road from the S.S. 407 Basentana to the village of Pomarico (1:50,000 topographic sheet "Ferrandina").

from erosion (Fig. 13B); commonly, they are partly truncated or reduced to rip-up clasts.

Both FA2 and FA3 locally show the following in association: sparse bored pebbles, plant debris, bivalves (oyster shells, thick- or thin-shelled, sometimes attached to pebbles, and rare pectinids), local *Ophiomorpha*. Enigmatic structures appear on stratification surfaces as rings with a diameter of 7 to 16 cm, consisting of small pebbles in a sand matrix; in vertical cross section they appear as U-shaped structures. Soft-sediment deformation structures, ranging from gravel pockets sinking into sand, to pillar-like diapiric flame structures, with evidence of the upward active injection of sand or gravel, commonly accompanied by convolute lamination, were locally observed.

5.3.2. Interpretation

In order to interpret the context in which the stratal organization and sedimentary structures of FA3 are generated, it is helpful to anticipate some considerations concerning the inferred hydrodynamic processes active during high-energy events. Masselink and Puleo (2006) pointed out that in the presence of high and steep storm waves, the upper part of the beach is severely depleted and flattened out, being subjected to severe erosion and the offshore discharge of sediments by surf zone processes, i.e., breaking waves and return flow. Particularly exposed to erosion are the ordinary berms, which are essentially recovery deposits constructed by the onshore advection of gravel under fair-weather conditions.

It is suggested that during the waxing stage of storms of variable magnitude the material eroded from the upper part of the beach is discharged offshore and mostly stored on the lower beachface slope as FA4 beds. On the other hand, FA3 layers are interpreted to be laid down at the toe of the beachface only during the peak stage of higher-magnitude storms, by flows inferred to bypass the slope of the lower beachface. This may explain the fact that FA3 beds in the studied lithosomes are less numerous than FA4 beds, the latter commonly downlapping on the former. The resulting architecture is believed to represent the record of events of different energy and recurrence intervals, as suggested by Dupré (1984).

The clast long-axis fabric of toeset gravels (Fig. 6), measured in South-Alpine deposits, ranges from nearly isotropic to weakly or moderately preferred, with a-axis sub-parallel to flow in the latter case and dipping upstream. This supports the assumption that high-concentration flows are involved, partly dominated by dispersive pressure due to grain collisions.

The structures of FA3 deposits indicate that during the peak of severe storms, the offshore-directed flows could quickly reach a supercritical state. Low-amplitude wavy-bedded to lenticular structures, sandy and gravelly in composition, locally accompanied by low-angle, generally upstream-dipping cross-lamination (Figs. 9, 10A), are inferred to result from the growth of antidunes under stationary or upstream migrating waves (e.g., Alexander et al., 2001; Duller et al., 2008; Cartigny et al., 2014). Similar structures are reported by Bourgeois and Leithold (1984) in the Pleistocene marine terraces of SW Oregon. Lack of erosion of the bedform crests of both gravel and sand structures is thought to reflect high rates of sediment load fallout and therefore a high rate of aggradation during rapid flow deceleration associated with antidune activity.

There is moreover evidence that flows can undergo hydraulic jumps at the beachface-shoreface transition, which corresponds to a distinct slope break (Di Celma et al., 2020). Evidence is provided by local bowl-shaped scours filled or paved by gravel (Figs. 7 C,D, 8), suggesting strong erosion under the impact of a hydraulic jump, with the associated backset-bedded laminasets (Figs. 5, 7, 8) indicating the upstream migration of hydraulic jump (Fig. 14). The flow expansion due to the transition from supercritical to subcritical flow, with rapid dissipation of flow speed at the hydraulic jump, is accompanied by instantaneous loss in competence and transport capacity and enhanced mixing by internal recirculation vortices (Cartigny et al., 2014). As a result, a steep-sided scour is carved by the high turbulence accompanying the process and immediately filled by coarse-grained material forming a structureless and massive deposit (hydraulic jump facies) (Figs. 7 C,D, 14) (Gorrell and Shaw, 1991; Russell and Arnott, 2003; Postma et al., 2014; Massari, 2017). Similar high-angle, steep-walled, gravel-filled scours, interpreted as the product of a nearly instantaneous cut-and-fill process, are ilustrated by Dupré (1984), Bourgeois and Leithold (1984), Hart and Plint (1995), and Sanders (1997). The features reported by the authors show the characteristics of rapidly infilled scours formed under hydraulic jumps. The associated sets of backset laminae inferred to reflect the upstream shift of hydraulic jumps are remarkably similar in origin to those described by Nielsen et al. (1988), Cartigny et al. (2014), Massari (2017), and Slootman et al. (2018). Vaucher et al. (2018) gave an account of erosional troughs backfilled by upstream-dipping laminae, associated with chute-and-pool structures in the surf–swash transition zone of a modern intertidal setting. In an Apenninic storm-dominated gravel beach lithosome of central Italy, Di Celma et al. (2020) described structures identical to those illustrated in this work. They proposed that accelerated backwash flows travelling down the steeply dipping slope of the beachface experienced an erosional hydraulic jump at the toe of the beachface, with the development of a backset laminaset following the upstream migration of the hydraulic jump. This interpretation mostly fits the reconstruction proposed in this study, with the difference that the involved supercritical flow undergoing hydraulic jump is identified here in a strong offshore-directed return flow (undertow).

As pointed out by Greenwood and Osborne (1990), the undertow is a near-bed offshore-directed flow responding to the wave- and wind-generated onshore mass transport momentum flux and the hydraulic pressure gradient

induced by the set-up of the mean water level. Bed return flow increases with the incident wave height and plays an important role in the erosion of the upper part of the beach and in the transport of large volumes of beach sediments seawards (Svendsen, 1984; Masselink and Black, 1995; Aagaard and Vinther, 2008, with references). Unlike rip currents, which are localized, the undertow affects the nearshore waves everywhere (Svendsen, 1984). In the surf zone, strong storm-generated undertow is known to generate vigorous near-bed sediment transport in the offshore direction (e.g., Dupré, 1984; Greenwood and Osborne, 1990; Conley and Beach, 2003). The undertow may reach a velocity of 0.6m s^{-1} in the shoreface (Héquette et al., 2001), and maximum velocities close to the bed are reached in the surf area (Masselink and Black, 1995) because of the added contribution of onshore mass transport in the upper part of the water column by wave breaking and surf bores/rollers (Svendsen, 1984). The speed of the undertow depends on the negative cross-shore gradient of wave radiation stress and this gradient depends partly on the beach slope; for given wave conditions, the undertow is stronger on steeply sloping beaches with narrow surf zones than on gently sloping beaches (Longuet-Higgins, 1983; Aagaard et al., 2013). On steeper slopes the wave height is less attenuated, resulting in larger height to depth ratios of the broken waves and larger return flow velocities (Masselink and Black, 1995). The largest transport rates occur in the bottom 5 or 10 cm of the water column (Conley and Beach, 2003) where sediment concentrations are the largest. It is believed that the offshore-directed near-bed undertow accelerating under the cross-shore pressure gradient during storm peak conditions can reach the supercritical state on the lower beachface and be subject to hydraulic jumps at the slope break of the beachface-shoreface transition (Fig. 14) and sometimes on the lower beachface itself (see below).

In the studied examples the flow during the upslope migration of hydraulic jump predominantly transports suspended sediment, forming mostly sandy backset laminasets. Local association of gravelly and sandy backset laminae in some sets is interpreted to reflect the accelerations and decelerations of the flow. The sharp contact of gravel layers with the sets of backset

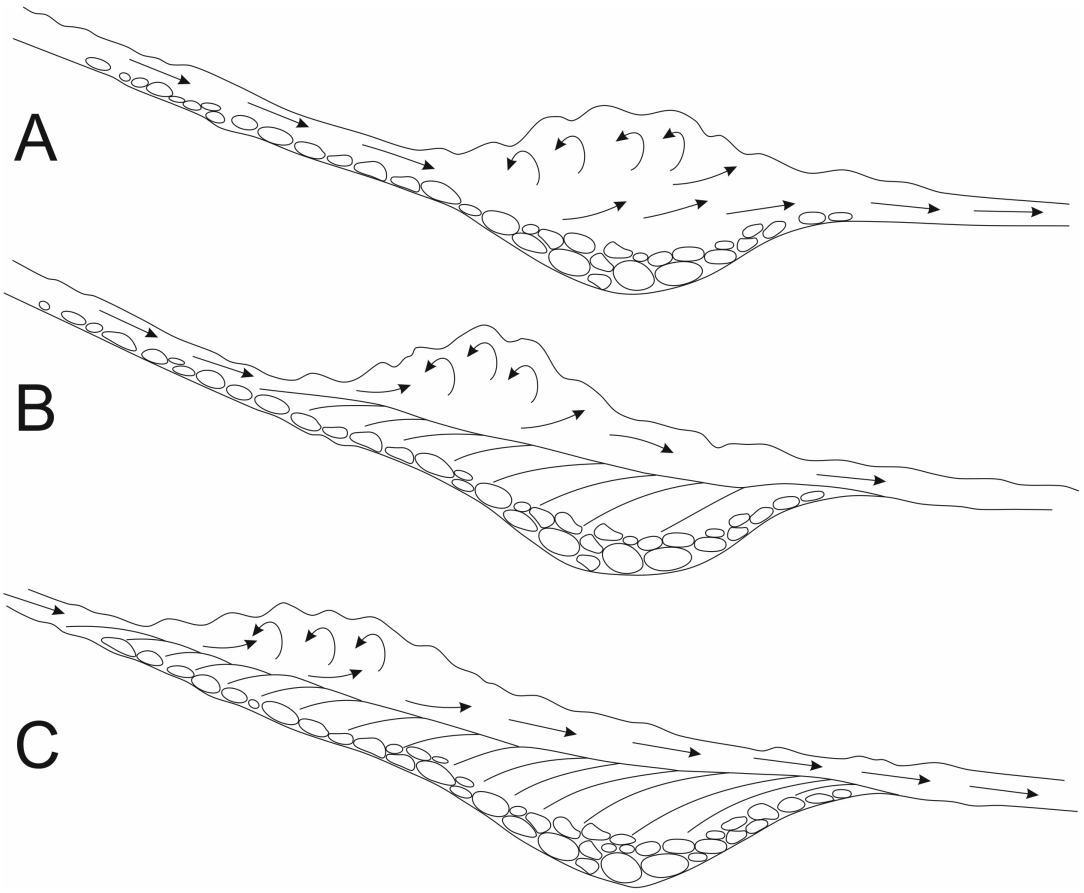

Fig. 14 - Cartoon showing the formation of hydraulic jump and related sedimentary structures at the toe of the beachface. A) A strong offshore-directed return flow (undertow) produced at the storm peak by the breaking of large storm waves and high cross-shore pressure gradients is subject to hydraulic jumps at the beachface-shoreface transition. As a result, a scour is carved by the high turbulence accompanying the process and immediately paved by coarse gravel forming a structureless and massive deposit (hydraulic jump facies); B) and C) The upstream migration of the hydraulic jump generates sandy backset laminasets.

laminae in the gravel/sand couplets suggests a relationship of short-term succession in the deposition of the two terms (Fig. 14), and probably excludes their concomitant emplacement, as claimed by Di Celma et al. (2020). Moreover, the remarkable length of the backset laminasets in the cross-shore direction, the local evidence of pauses in their accretion, as highlighted by reactivation surfaces and intrasets of ripple laminae, as well as the local interstratification with trough cross-laminated sets, indicate that the accretion of the backset laminasets was commonly discontinuous, with successive addition of increments from time to time, probably during the peak and early decay stages of the storm.

The uncommon hummocky- and swaley-shaped structures observed in the toeset of some thick Apenninic lithosomes (Fig. 10 B-D) are interpreted as unstable, hybrid chute-and-pool bedforms with a high aggradation rate (Slootman et al., 2019); the deposition of coarser clast sizes on the upstream facing slope of the swales (Fig. 10C) is considered a diagnostic feature indicating deposition by rapidly decelerating flow immediately downstream of the hydraulic jump by rapid suspension fallout (e.g., Alexander et al., 2001; Cartigny, 2012; Slootman et al., 2019). Another single peculiar structure consisting of a series of antidune gravel waves overlain by sandy sets of backset laminae infilling the troughs between the crests of gravel waves, possibly represents an incipient cyclic step structure (Fig. 10A). Rarely observed moulding of the tops of sets of backset laminae into regular, symmetrical, gently convex-up surfaces (e.g., Fig. 10A, lower left of the photo) is interpreted as the record of an eventual return to supercritical flow after the upstream shift of the hydraulic jump, leading to the development of an antidune bedform (Massari, 2017).

The composite units consisting of an interstratification of backset and trough cross-bedded laminasets locally observed in Apenninic units (e.g. Scanzano Jonico lithosome; Fig. 11) suggest that during storm events a mutual transition could occur in the surf zone between supercritical flows subject to hydraulic jumps and the migration of three-dimensional dunes under the action of longshore drift. The tendency of trough cross-bedded sets to predominate in the upper part of these composite units (Fig. 11) suggests that active longshore flow prevails in the declining stage of the storm, when a wider surf zone and strong longshore pressure gradients can be established (e.g., Aagaard and Vinther, 2008). Similar relationships were described and figured by Maejima et al. (2001).

The variable angles (in the 90°-120° interval) measured between the shoreline trend inferred from the direction of progradation and the azimuthal mode of trough cross-beds in Apenninic lithosomes (Fig. 12 A,B) indicate that the migration of three-dimensional dunes induced by longshore drift ranged from sub-parallel to oblique to the shoreline; this in turn suggests variable orientations of the nearshore bar/trough system. In all the surveyed sites the main palaeo-wind direction probably matched that of the present-day south-easterly Sirocco wind, blowing along the axis of the Adriatic Sea. The predominant mode of the trough cross-bedding (Fig. 12 A,B) indicates a downwind current; this pattern has been documented even in the present-day western Adriatic coasts, where Sirocco episodes generate a downwind current, opposite to the usual fair-weather countercurrent flow (Poulain, 2001), favoured by the interaction of the airflow with the local orography. It is thought that the active longshore drift on the Apenninic palaeo-shorelines was due to the general oblique wave approach to the shorelines. In spite of different orientation of the Bradanic coast facing the Gulf of Taranto with respect to that facing the central Adriatic, active longshore drift, chiefly bound to the action of the winds from S and SE, presently moves the deposits from Capo Spulico NNE-wards, i.e. toward the coast between the rivers Lenne and Patemisco. The longshore drift had the same trend in all the marine terraces of this area (Parea et al., 1980). Therefore both the central-Adriatic and Bradanic palaeo-coasts considered in this study should be regarded as *drift-aligned* systems (Davies, 1980; Orford et al., 1991), characterized by the activation of a bar/trough system during high-energy events, and therefore changing from an inferred more or less reflective behaviour under fair-weather conditions to an intermediate state (in the sense of Wright and Short, 1984) during storm events.

Conversely, the South-Alpine N60E-S60W-trending palaeo-shorelines, located on the landlocked embayment of the northern end of the palaeo-Adriatic (Fig. 1), were probably impacted almost perpendicularly by the waves, as indicated by the orientation of the crests of wave megaripples, which is fairly close to the trend of the shores (Fig. 12C), and paucity of trough cross-bedding linked to longshore drift. Accordingly, these shores can be regarded as almost *swash-aligned* systems (Davies, 1980; Orford et al., 1991). These were facing a probably low-gradient shelf sea, thought to experience significant wave attenuation before reaching the shore.

The shape and size bimodality commonly observed in the gravel layers of FA3, akin to the "outer frame" of Bluck (1967) and characterized by a population of spherical to subspherical cobbles and pebbles of intermediate to large sizes contained in a matrix of minute pebbles with variable shapes and granules (Figs. 7 A,D, 9 A,C, 10D), is thought to result from two distinctive modes of transport. It is suggested that the finer-grained population eroded from the upper beachface during high-energy events is transported downdip as highly concentrated traction carpets subject to the effects of the dispersive pressure, particularly in the case of steeper-clinoform units, whereas the coarser population of most rollable spheres, having greater momentum and settling velocity, moved downslope mostly by rolling and saltation. The mixing of the two populations leads to the deposition in the inner toeset zone of a sediment with the characteristic shape and size bimodality. Unimodal layers consisting only of the small-pebble population (e.g., upper part of

Fig. 7D) were probably deposited by flows dominated by the traction-carpet population. On the other hand, the predominance of larger spherical clasts in the outer part of the toeset zone may be due to their ability to "outrun" the finer-grained constituents, due to their greater momentum, leading to a selective concentration. This is a typical effect of a shape-sorting process.

The thin mud layers locally present in the toeset area may be laid down during the pauses between high-energy events, possibly in the trough located between the beachface and the first bar system.

Wave megaripples, which are another important component of FA3, are vortex ripples characterized by wavelengths linearly proportional to the near-bed wave orbital excursion. Orbital velocities required to mobilize the bottom sediment at the beachface toe and upper shoreface, in order to produce gravel megaripples, are thought to be readily induced by long-period waves, which feel shoaling effects at greater depth than short-period wind waves and can generate strong tractive-oscillatory motion at the sea-bed (Yorath et al., 1979; Wright and Walker, 1981; Bourgeois and Leithold, 1984; Cotter, 1985). Trains of wave megaripples are thought to form either during storms characterized by wave fields including a long-period component, able to effectively interact with the sea-bed, or, more commonly, in the storm-retreating stage, when steeper, short-period waves are generally replaced by longer-period waves impacting the shoreline. It is suggested that under these conditions, the shear stress induced by shoaling waves, resulting in vigorous oscillatory motion with a dominant landward component, can transport and selectively concentrate the spherical, most rollable, and mobile clasts either as predominant constituents of the megaripples or as a veneer one-clast thick draping the surface or one side of the bedforms or the tops of some beds. The common bimodal composition of gravel megaripples, with a variable proportion of intermediate to large spherical pebbles in a matrix of minute pebbles and granules (e. g., Fig. 9A), indicates the moulding into megaripple forms of previously laid down toeset layers having comparable textural features. The variable angles and reversals of imbrication dip locally observable in the cross-sections of megaripples may reflect alternating landward- and seaward-directed shear stress due to asymmetric orbital motion at the sea-bed. The local erosional truncation of the megaripple crests is thought to result from the high bed shear stress linked to the emplacement of gravel layers during subsequent high-energy events.

Pocket structures due to the liquefaction-induced sinking of gravel into loose liquefied sand, and pillar structures involving the rise of water and fluidized particles, are generated by pore pressure changes induced either by the cyclic stress of storm waves or sudden loading due to the rapid deposition of gravel on water-saturated sand or earthquake shocks. Structures appearing as rings of circularly arranged small pebbles in a sand matrix on stratal surfaces and as U-shaped forms in cross section are enigmatic (burrows? cross sections of loading pockets?).

5.4. FACIES ASSOCIATION 4 (FA4)

5.4.1. Description

The Facies Association 4 is represented by the steepest gravel clinobeds of the progradational beach lithosomes, dipping at angles ranging from 7° to 15°. The layer distinction, not always obvious due to crude stratification and a tendency to amalgamation, is based on differences in clast size and fabric.

The units with steeper and higher clinoforms show comparatively more regular, nearly tabular layers in dip-oriented sections (Fig. 15A), except for coarser thicker beds that show a slightly concave-up erosional base. Conversely, the units with a gentler dip of clinoforms are characterized by beds commonly lenticular with more pronounced basal erosion, locally sigmoidal (Fig. 8). Moreover, in these units some layers show a long asymptotic outer tail, on which younger beds downlap with an angular basal contact (Fig. 8).

In dip-oriented sections, most FA4 beds display a distinct wedging out downslope. In some lithosomes of the South-Alpine succession, FA4 beds may grade downdip, near the transition to toeset beds, to low-relief wavy/lenticular structures akin to those typifying the FA3 gravels in these units. FA4 layers show common wedging out updip either depositionally or by truncation at the transition with the FA5 gravels (Figs. 8, 15A). In this transitional zone local evidence of erosion at the expense of FA4 gravels is shown by remnants of them (arrows in figure 15A). Only in a minority of cases (not exceeding 10-15%) is a physical downdip continuity shown between finer-grained FA5 gravel beds and FA4 layers or between the latter and FA3 beds (Fig. 8).

Local major, low-angle truncation surfaces (reactivation surfaces) cross the set of clinobeds, leading to the juxtaposition of groups of strata with different attitudes; they dip at steeper or lower angles with respect to the layers they cut, and are conformably overlain by younger beds. Gravels directly overlying these internal unconformities are usually coarser-grained than average.

Rarely, slumped gravels are present, showing random clast orientations and local contorted folding.

Only a few examples of sufficiently wide sections with an orientation sub-perpendicular to the dip of clinoforms were available in the performed field survey. The best exposure was shown by a quarry located on the left side of the River Agri, near the State Road "Ionica" (southern Italy) (MIS 5.1 terrace). This provides a strike view of a beach lithosome on a front 208 m long. At three different levels of the FA4 succession, thicker and coarser-grained (large pebbles and cobbles), flat-lenticular beds 8-15 m long and up to 70 cm thick with either a planar or very gently concave-up base and a broadly convex-up top appear laterally spaced some 10-15 m apart, alternating with finer-grained beds adjusting to the concavity of the intervening spaces; a thickness compensation pattern is thus generated. Except for these relationships, the

finer-grained gravel layers at other levels of the FA4 succession are laterally persistent, generally showing an approximately tabular geometry.

The FA4 beds range in thickness from 10 to 70 cm (average 30 cm), consist of pebbles and local cobbles, and commonly show a distinct coarsening downdip. The gravels are predominantly clast-supported, with a texture that is commonly openwork, sometimes closed-work, with sand occluding the gravel interstitial voids. Layers with clasts supported by a sand matrix are rare and may grade upwards into clast-supported gravel at the top. Sorting is fairly good to poor, generally worsening downdip. Gravel beds are predominantly ungraded and less commonly inversely or normally graded; inverse grading, generally limited to a finer-grained basal band, is present particularly in layers of lithosomes with higher and steeper clinoforms. FA4 gravel beds in South-Alpine lithosomes show a fairly good correlation between maximum particle size and bed thickness (Fig. 16).

The clast shapes are poorly differentiated; blades and rods tend to predominate, particularly in the middle-upper part of the subunit, which is characterized by mostly unimodal granulometry (Fig. 15 B,C); spherical large pebbles and cobbles appear only in the beds transitional to the toe, generally embedded in a matrix of small pebbles with variable shapes, resulting in the same bimodal texture as that commonly shown by the FA3 gravel beds.

In the South-Alpine units, clast imbrication ranges from well to poorly developed and dips almost systematically upslope (Fig. 15B), with an average angle of 40° with respect to the clinoforms. An upward-steepening of clast imbrication angles within the beds is commonly present (Fig. 15C), sometimes accompanied at the top

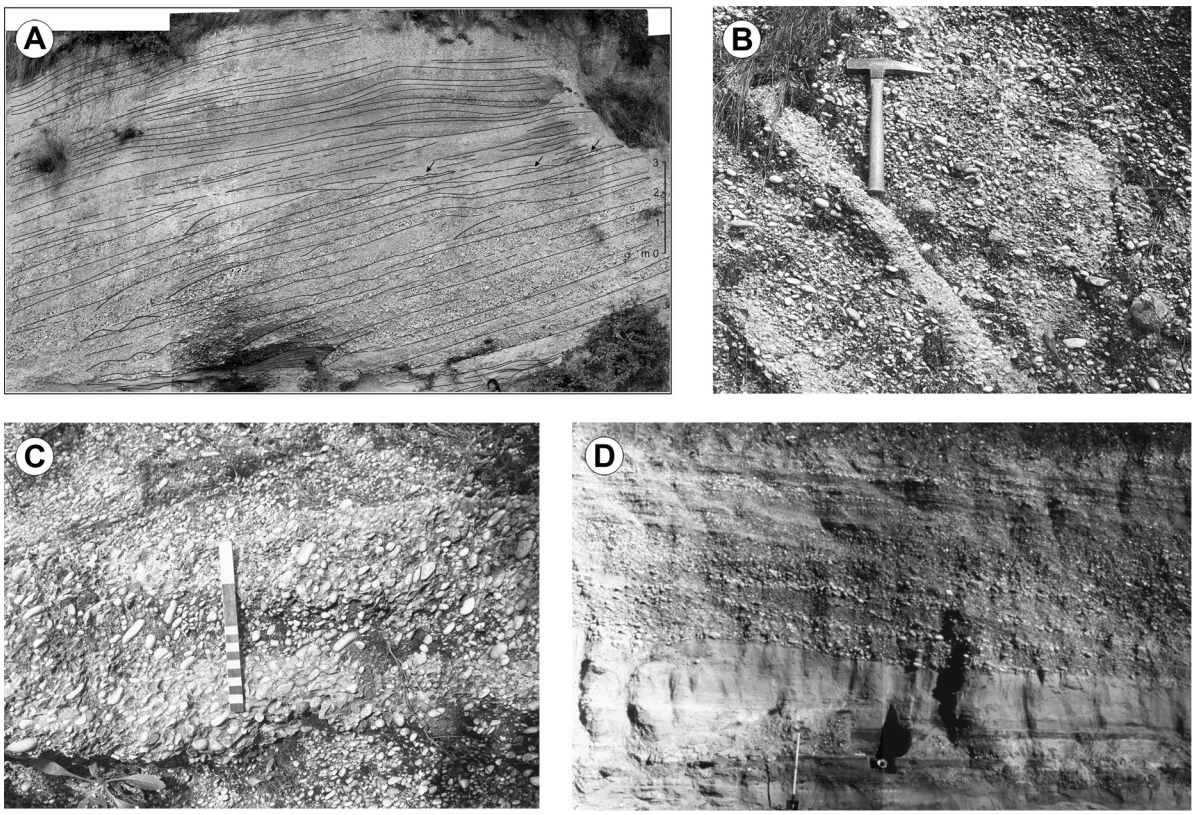

Fig. 15 - General features and details of the FA4 gravels. A) View of an Apenninic beach lithosome slightly tilted leftwards, in a nearly dip-oriented section (land to right). A clear difference in inclination can be appreciated between the upper beachface (FA5) thin- and regularly bedded gravels and lower beachface (FA4) crudely stratified gravel layers, with a break in slope at the transition between them. FA4 clinobeds commonly wedge out near the contact with the FA5 gravels, where they locally leave some erosional remnants (arrows). The continuity of some FA4 beds is interrupted by steps marked by coarser grain sizes. Some trains of megaripples are present in the lower part of the FA4 subunit. Light blue: gravel clinobeds; yellow: sand; purple lines: steps; green lines: backset bedding; blue lines: profiles of megaripples. Middle Pleistocene unit, near the village of Pedaso, SE of the town of Ancona (1:50,000 topographic sheet 315 "Fermo"); B) FA4 beds in a South-Alpine beach lithosome (affected by tectonic tilting) showing landward-dipping well-developed clast imbrication (flow to lower right). Scale bar 20 cm long; C) Detail of a FA4 bed showing upward-steepening imbrication angles. Flow to right. Photos B and C: abandoned quarry on the SW side of the hill 329 m high located E of the town of Vittorio Veneto (1:25.000 topographic map "Vittorio Veneto"); D) Apenninic beach lithosome with gentle dip of clinoforms in a nearly dip-oriented section (land to left) showing FA3 to FA5 facies associations. FA4 gravel clinobeds are characterized by marked lenticularity and predominantly seaward-dipping clast imbrication. MIS 5.1 terrace immediately south of the village of Scanzano Jonico (1:50,000 topographic sheet "Policoro"). Shovel 120 cm high for scale.

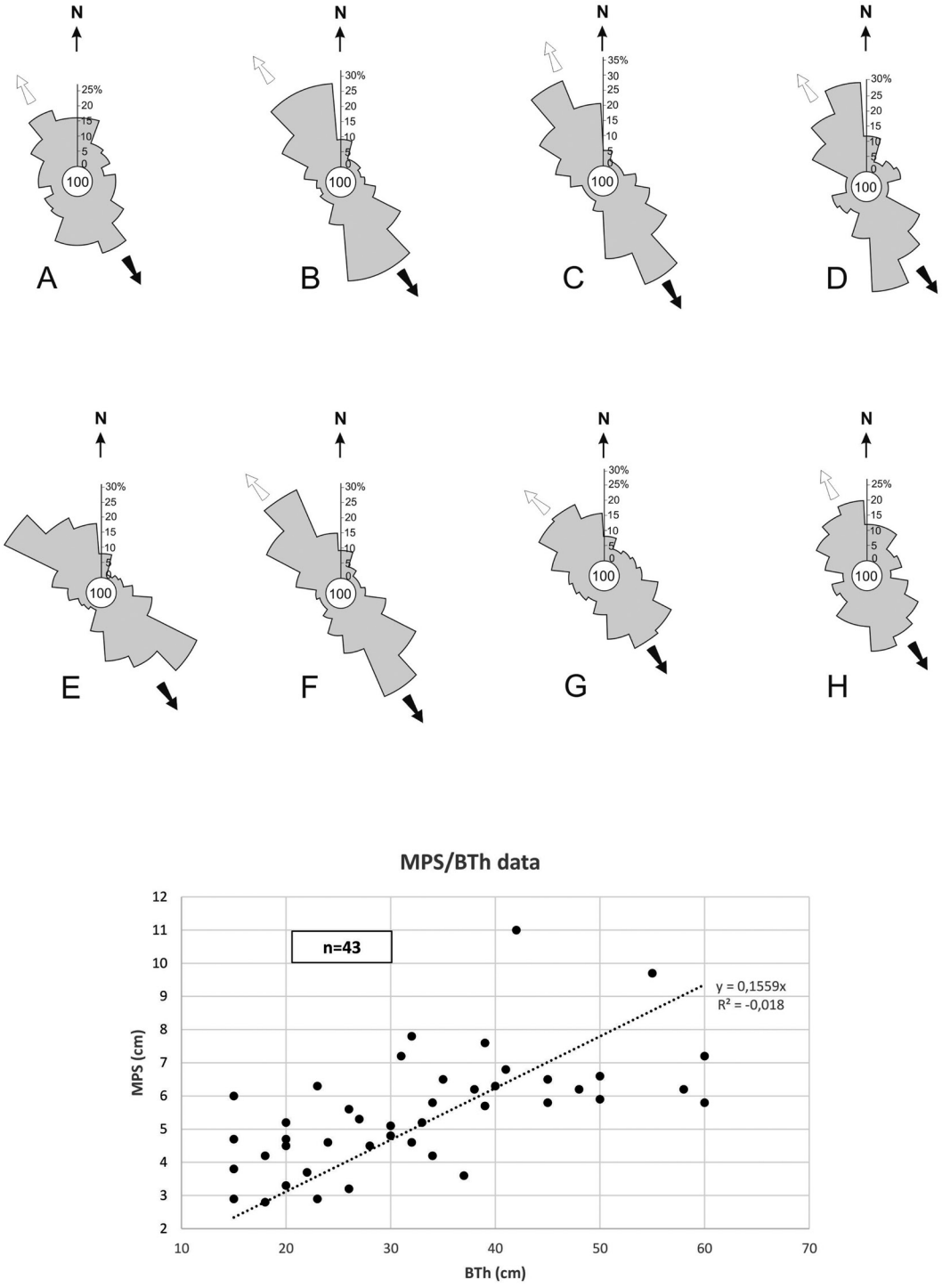

Fig. 16 - Rose diagrams illustrating the fabrics of FA4 gravels in a South-Alpine beach lithosome and diagram showing correlation between maximum particle size (MPS) and bed thickness (BTh). Measures of long-axis orientation of rods showing an a-axis to b-axis ratio over a minimum of 1.70 were made on the upper surfaces of layers occurring in succession upwards. In all roses solid arrows show the direction of progradation; in cases of preferred fabric the approximate dip of imbrication, as inferred from field evidence, is also indicated (open arrow). For each sample some annotations on the textural characteristics are added. A) sample 593: bimodal in size, with large pebbles and rare cobbles in a matrix of small pebbles and granules; B) sample 598: clast-supported and bimodal in size, with large pebbles and rare cobbles in a matrix of small pebbles; C) sample 601: poor to moderate sorting, predominant small to medium pebbles, rare cobbles; D) sample 604: moderate sorting, predominant small pebbles, sparse larger pebbles; note the bimodality of clast long axes orientations; E) sample 607: moderately sorted pebble gravel; F) sample 612: moderately sorted pebble gravel, rare outsize pebbles; G) sample 614: poor sorting, sizes ranging from rare cobbles to small pebbles; H) sample 620: transitional facies between FA4 and FA5 gravels; badly to poorly sorted, sizes ranging from large pebbles to granules; I) MPS/BTh diagram. Measures were made on tabular beds lacking evidence of significant basal erosion. South-eastern side of Monte Stella (about 4 km SW of the town of Vittorio Veneto; 1:25,000 topographic map "Vittorio Veneto").

by flattening (sigmoidal pattern) or the inversion of imbrication dip. A-axis imbrications largely predominate, with dip azimuths consistently sub-parallel to the dip of the clinoforms (Figs. 16 B-F), except for the layers transitional to the FA3 and FA5 gravels, which show a more dispersed fabric (Fig. 16A and, respectively, G,H). In the Apenninic units, visual observations of clast orientation allow to ascertain that the gravel fabric is either isotropic or characterized by imbrication dipping either upslope or downslope. The dip direction and dip angles of the clast imbrication depend on the gradient of clinoforms and the size of clasts: on average, the percentage of downslope- and low-angle-dipping imbrications increases with the lowering of the clinoform gradient and with the increase of clast sizes; indeed, thinner lithosomes with a gentler dip of clinoforms show dominant downslope-dipping clast imbrications with angles of 10°-20°, especially in the case of coarser-grained layers (Fig. 15D); conversely, upslope dipping clast imbrications in these units are locally shown by layers consisting of minute pebbles. On the other hand, lithosomes with steep-gradient and generally higher clinoforms show a higher percentage of upslope-dipping clast imbrications and commonly high angles of imbrication dip. In general, the fabric is more preferred in the layers composed of small pebbles than in coarser-grained beds.

A characteristic feature visible in dip-oriented sections, particularly in units characterized by higher and steeper clinoforms, is represented by local outward-inclined steps interrupting at variable levels the continuity of clinobeds and consisting of second-rank surfaces 35 to 55 cm high, showing dip angles ranging from 25° to 34° with respect to the clinoforms and commonly a slight convexity in the downdip direction (Fig. 15A). Gravels at the steps show coarser than average grain sizes commonly arranged with an updip fining trend and locally with high imbrication angles. Some clinobeds show more than one step.

In Apenninic lithosomes, sandy backset laminasets, locally overlying gravel-filled scours, are sometimes interstratified with FA4 gravel layers in the lower part of the clinoform-stratified FA4 subunit; they are akin in geometry and internal structure to those occurring in FA3, but showing progressive updip decrease in thickness and persistence.

Gravel megaripples are locally present in the lower part of the subunit (Figs. 3, 5, 15A, 17). Exposures of stratal surfaces in South-Alpine lithosomes locally provide three-dimensional views of the megaripples: the crests are straight and sub-parallel (Fig. 17A) or slightly sinuous, in places bifurcating, rarely linguoid, and their average orientation ranges from slightly oblique with respect to the strike of the clinoforms to nearly parallel to it (Fig. 12C). The wavelengths (25-80 cm) are shorter than those of toeset megaripples (Fig. 17A), and wavelength/height ratios range from 5.5 to 7.5. These bedforms are either symmetrical or, more commonly, asymmetrical with steeper sides facing downslope (Fig. 17B); concentrations of larger clasts are seen either on the steeper sides (Fig. 17B) or in the troughs between the crests. The rare linguoid megaripples show steeper sides facing downslope and bearing a pebble concentration.

As in the case of toeset megaripples, co-existing opposite clast imbrications may be present, as well as the draping of the surface of some bedforms by a one-clast-thick row of spherical clasts. Locally, trains of smaller megaripples with wavelengths of 15-20 cm and heights of 3-4 cm are superimposed on larger megaripples.

5.4.2. Interpretation

The FA4 gravel layers represent the clinobeds laid down on the lower beachface. Their common updip and downdip wedging out suggest that generally their emplacement on the lower beachface is not simultaneous with sediment accretion on the upper beachface and toeset area. It is suggested that FA4 gravels are laid down in concert with the erosion of the upper-beachface profile and do not overtake the foot of the lower beachface, except in a minority of cases. Their emplacement

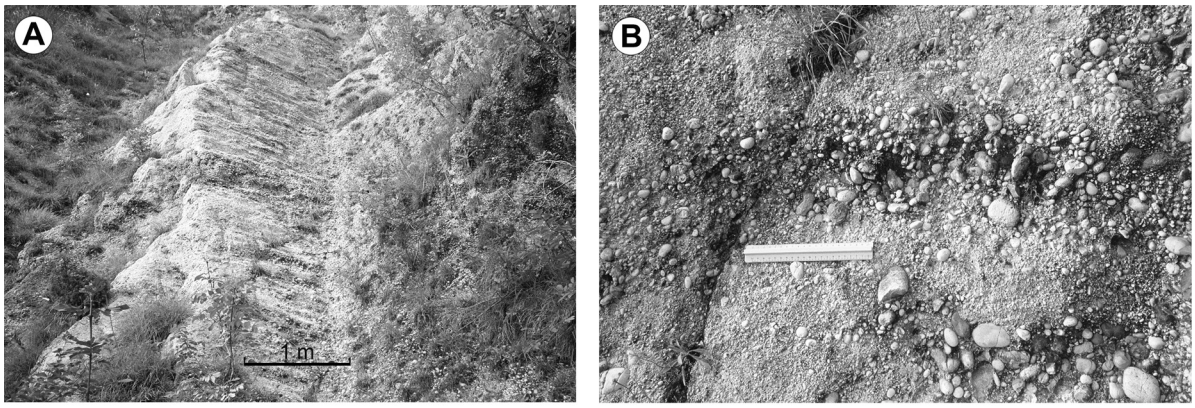

Fig. 17 - Examples of gravel wave megaripples preserved in the lower part of FA4, on a stratal surface of a South-Alpine beach lithosome. A) Straight-crested megaripples. B) Detail of the same surface showing asymmetry of the bedforms with steeper seaward-facing sides on which pebbles are concentrated. Ruler 21.5 cm long for scale. Both photos: abandoned quarry on the SW side of the hill 329 m high located E of the town of Vittorio Veneto (1:25,000 topographic map "Vittorio Veneto").

probably takes place during the waxing stage of storms. Masselink and Puleo (2006) pointed out that during storms, the gradient of the upper part of the beach is in disequilibrium with the new water level, elevated due to wave set-up. As a result, surf zone processes start eroding the upper beachface; the removed gravel is shed offshore under strong cross-shore pressure gradients, accelerating the strength of backwash flows (Masselink and Puleo, 2006), and is laid down on the lower beachface slope. Backwash flows during storms are characterized by large excess shear stress (Wilson, 1987) and can transport great volumes of sediment seaward as bed load.

The physical process of gravel emplacement onto the lower beachface of nearly swash-aligned South-Alpine palaeo-shorelines is thought to be significantly different from that occurring on drift-aligned Apenninic palaeo-shorelines. In the former the characteristic fabric of the lower-beachface gravels reflects an important role of gravity in accelerating the strength of backwash flows. The landward-dipping long-axis imbrication of clasts (Figs. 15B, 16), and common inverse grading point to a mode of transport as gravel carpets dominated by interparticle impacts within Bagnoldian dispersions. Moreover, a fairly good correlation between maximum particle size and bed thickness shown by FA4 beds of South-Alpine lithosomes suggests a well-established equilibrium between the competence and thickness of the depositing flows, which is typical for gravity-driven flows with a high component of dispersive pressure (Nemec and Steel, 1984). The influence of gravity in promoting a preferred fabric is indirectly supported by the common upward steepening of upslope-dipping clast imbrication angles (Fig. 15C). As suggested by Nemec (1990), this may be produced in the last stage of motion, as a result of the internal shearing of gravels prior to the frictional freezing of highly concentrated dispersions. This would lead to an upward steepening of the clast long axes above the base of the bed, implying rotation of the a-axes of clasts toward the vertical. The locally observed inversion of imbrication dip at the layer top may indicate the shear exerted by the run-up flow following the gravity-driven downdip emplacement.

On the other hand, the more variable fabric of lower-beachfaces gravels of Apenninic units, and particularly the predominance of seaward-dipping clast imbrication in units characterized by a gentler dip of clinoforms (Fig. 15D), suggests that the clast orientation was more influenced by strong shear stress on the bed exerted by the onshore-directed and accelerating incident wave-coherent flow in a widened surf zone. This is consistent with the behaviour of predominantly drift-aligned Apenninic systems, inferred to have had a more pronounced tendency to change to an intermediate morphodynamic state during storms.

The downdip grading of FA4 beds into the low-amplitude wavy/lenticular structures observed in some South-Alpine units is inferred to indicate a tendency of the flow to enter supercritical conditions with the development of antidunes at the transition to the beachface toe. In the Apenninic lithosomes, the uncommon thin, impersistent sandy backset laminasets, sometimes overlying gravel-filled scours, occurring interstratified with FA4 gravel layers in the lower part of the FA4 subunit, indicates that flows descending the underwater slope may sometimes be subject to minor, updip migrating hydraulic jumps.

The asymptotic or angular basal contact of FA4 gravel layers may reflect the different energies of waves impacting the shore. Reactivation surfaces locally truncating at generally low angle groups of lower-beachface gravel layers are thought to result from the impact of severe storms, or an abrupt change in the storm direction leading to beach rotation, or a morphologic modification affecting nearby fluvial mouth(s) feeding the beach.The outward-inclined steps interrupting at variable levels the continuity of some clinobeds, mostly observed in units characterized by higher and steeper clinoforms (Fig. 15A), are interpreted to represent the record of the seaward shift of beach step as a response to the changing energy of incident waves during the waxing stages of storms. The beach step is a morphological feature known to be commonly associated with steep, coarse-grained beaches, particularly those composed of gravel. It forms an acute discontinuity in the beach profile at the transition between the breaker and swash regions (e.g., Bauer and Allen, 1995; Ivamy and Kench, 2006; Austin and Buscombe, 2008). The sediment convergence leading to a high concentration of coarser sediment at the beach steps is consistent with the current observation of what occurs at the point where the backwash meets the next incoming wave and generates strong turbulence (see also Dupré et al., 1980; Kirk, 1980; Short, 1984), a process inferred by some authors to coincide with the formation of a hydraulic jump (Buscombe and Masselink, 2006; Austin and Buscombe, 2008). Hughes and Cowell (1987) suggest that the migration and vertical growth of the beach step tend to maintain the steep reflective nature of the beach under rising energy levels. The observed structures resemble the planar cross-bedded conglomerates described by Hart and Plint (1989, 1995, 2003) in the beach toe deposits of the Cardium Formation, interpreted to record the seaward progradation of beach step following a storm surge (see also Forbes and Taylor, 1987; Larson and Sunamura, 1993; Sanders, 2000; Mäkinen and Räsänen, 2003). Specifically, Sanders (2000) reported on the present-day gravelly Dimitra beach of Kos Island (Aegean Sea) the presence of a "storm/swell plunge step" developed at the foot of the beachface near the point of the breakers during storm to swell conditions (his Figs. 3B, 4C, 5, 6). A step at the base of the beachface, inactive under fair-weather conditions, is currently observed in present-day gravel beaches and may represent the record of previous storm events.

Shape sorting processes are not particularly effective on most parts of the lower beachface. Indeed, they are most efficient in the lowermost and uppermost parts of the gravel beach lithosomes, with respectively spherical, more rollable clasts displaced into the toe area, and

discoidal clasts thrown in suspension by large runup excursions onto the uppermost beachface and storm berm, from where they can be hardly removed.

The gravel wave megaripples locally observed in the lowermost part of the lower beachface point to vigorous oscillatory motion at the sea-bed; this would occur during storms characterized by wave fields including a long-period component and/or during the storm-decay stage, when the locally derived sea is replaced by longer-period waves, efficiently stirring the sea bed. The common concentration of pebbles on the steeper seaward-facing sides of megaripples is thought to result from the tendency to seaward migration of these bedforms. This reflects the predominance of the offshore component in the oscillatory flow at the sea bed in the lowermost part of the lower beachface, and it fits the model of Clifton et al. (1971). On the other hand, the local concentration of coarser clasts in the megaripple troughs may indicate that this material is a lag deposit, created by the sweeping – via turbulence in the lee vortex - of the finer-grained and thus more mobile material from the troughs into the crests (Hay et al., 2014). As in toeset gravels, the local involvement of spherical clasts probably implies a selective concentration related to the stress induced by shoaling, storm-decay long-period waves.

5.5. FACIES ASSOCIATION 5 (FA5)

5.5.1. Description

The bulk of this subunit is represented by even, regularly bedded, mostly thin gravel layers with generally high lateral persistence forming the upper parts of the studied clinoform lithosomes (Fig. 18A). Moreover, the uppermost parts include peculiar features, i.e., planoconvex ridges, planar cross-bedded gravel sets (e.g., Fig. 3), and low-relief scour-filling gravel lenses. These uppermost features, however, may be incompletely preserved or lack preservation due to the frequent top-truncation of the lithosomes by erosion, in most cases due to a subsequent transgressive event accompanied by shoreface retreat.

The overall thickness of this subunit is directly proportional to the relief of the clinoform units. The overall stratal geometry is gently convex, due to the gradual downdip increase in bed inclination from a subhorizontal attitude to a maximum dip angle of 4°-5° near the transition to the more inclined FA4 gravels, which corresponds to a distinct break in slope (Figs. 3, 8, 15A). In completely developed lithosomes, the subunit shows an overall bed thickening and coarsening upwards (Fig. 18A), accompanied by a gradual average increase in the size and percentage of discs and worsening of sorting.

In the following description the even-bedded dominant part of the subunit is treated first, and then the peculiar features of the upper to uppermost part are described.

5.5.1.1. The even-bedded succession

The even, regularly bedded gravel layers (Fig. 18A) wedge out updip at a very low angle, and most beds, particularly coarser-grained ones, wedge out downdip, interfingering with the underlying FA4 layers; a minority of beds, generally finer-grained, grade downdip into FA4 gravel beds with physical continuity (Fig. 8). Remnants of FA4 gravels are locally present in the uppermost part of the FA4 subunit, near the contact with the FA5 subunit (arrows in figure 15A).

Most beds are bounded at the base by conformable surfaces, although with local evidence of low-relief-erosion. The general bed parallelism inside the subunit is locally interrupted by low-angle wedging out of single layers or bedsets and low-angle, generally planar truncation surfaces, upon which the gravels have conformable or low-angle relationships. This results in local low-angle discordances between beds or bedsets with erosional or non-erosional contacts. Rare low-amplitude plano-convex quasi-symmetrical thin lenses with wavelengths of 0.4 to 1.5 m, consisting of granules and small pebbles and locally showing upslope dipping low-angle lamination, are visible in dip-oriented sections interspersed through the even-bedded facies.

The FA5 layers range in thickness from 1-2 cm to 35 cm, exceptionally 40 cm. They generally show good to excellent segregation of clasts of different sizes into separate beds, commonly expressed by distinct coarse/fine, well sorted layers (Fig. 18B). Actually, successive layers may vary remarkably in grain size. The gravels are on average significantly finer-grained than FA4 gravels, with a predominance of clast-supported small pebbles, and both openwork and closed-work (mixed sand-gravel) textures (Fig. 18B); however, a minority of layers consist of larger pebbles and also rarely cobbles, sometimes supported by a matrix of small pebbles or granules; this may result in a size bimodality or polymodality, which, although uncommon, is locally present. A lack of grading is predominant; inverse grading is locally present, particularly in finer-grained beds, and normal grading is rare.

The effects of shape sorting are poorly distinct in the lower part of the subunit, where, especially in layers composed of small pebbles, a wide range of forms co-exist. In particular, as observed by Nemec and Steel (1984), the vertical shape variation between adjacent beds is commonly marked, for example by the interbedding of assemblages dominated by disc/blade and sphere/rod shapes, respectively. Conversely, the shape sorting improves in the upper part of the subunit, where the discs progressively increase upwards in size and proportion.

The fabric is dominantly preferred, with well-developed clast imbrication (Fig. 18B), and less commonly it is moderately to poorly preferred or disorderly. Roses of orientation data were obtained in a South-Alpine lithosome (Fig. 19). The pebbles show a preponderance of upslope dipping imbrication in the lower part of the subunit (Fig. 19 A-F); in the middle part, they show either downslope or upslope dipping imbrications, and sometimes reversals of imbrication dip even in adjacent pebble clusters within the same layer (Fig. 19 G,H). On

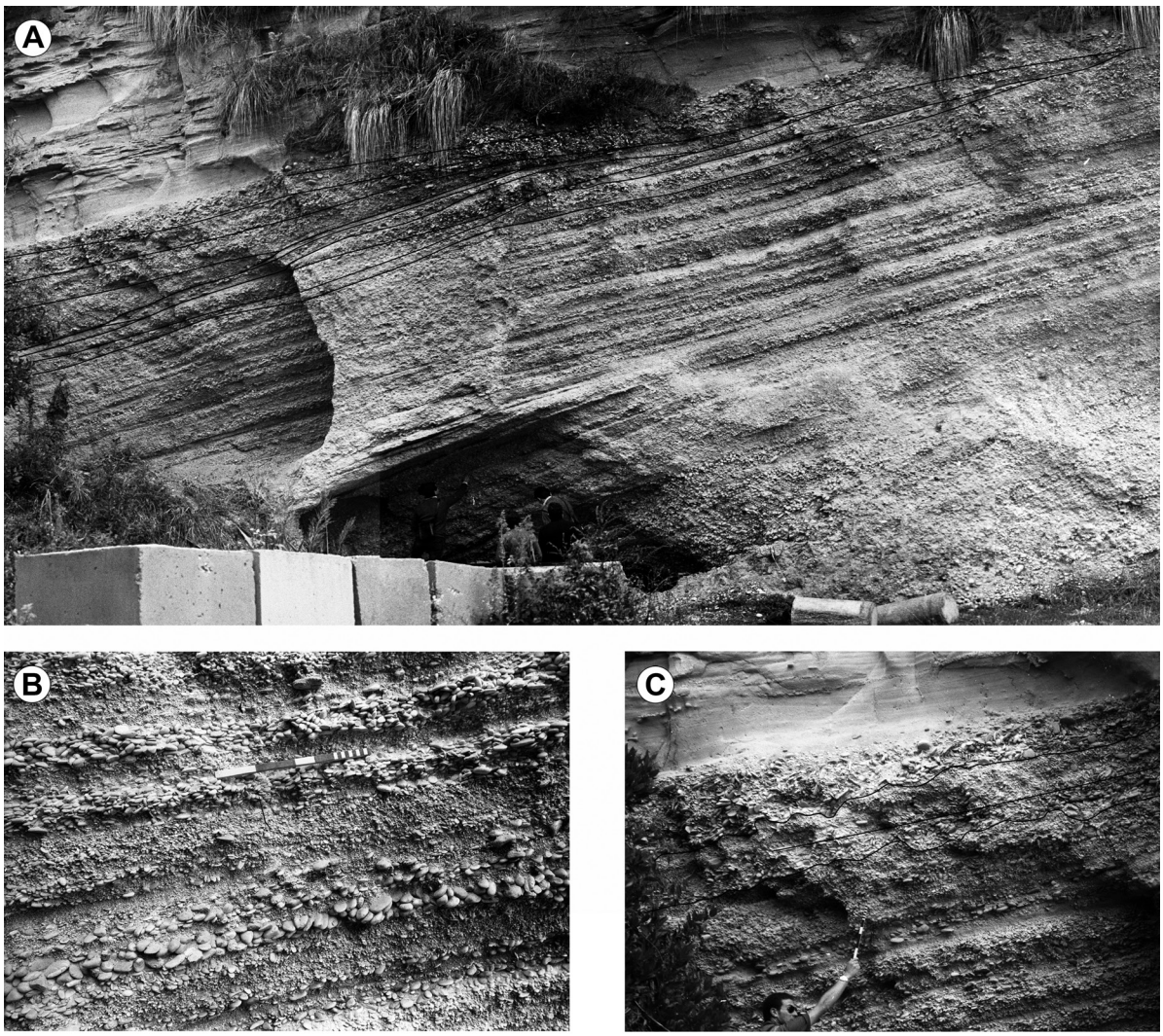

Fig. 18 - Details of FA5 facies association. A) Nearly dip-oriented section of an Apenninic beach lithosome (land to right) slightly tilted leftwards, showing the record of FA5 and the upper part of FA4. The former shows a distinct trend coarsening upwards and an even and regular stratification pattern except for the uppermost part, which is more composite and consists of a bundle of layers dipping gently landwards; this part, characterized by a dominantly chaotic fabric and abundant large discs, is interpreted as a washover unit developed landward of a storm berm. Note also the planoconvex features immediately beneath, interpreted as partly eroded storm berms in a slightly lower position. Persons at the cliff base for scale. Middle Pleistocene, near the village of Pedaso, SE of the town of Ancona (1:50,000 topographic sheet 315 "Fermo"); B) Well-stratified, moderately- to well-sorted granule to pebble gravels of the upper, even-bedded part of the same lithosome, showing a predominance of discoidal clasts. Lower layers show seaward-dipping, runup-controlled pebble imbrication; conversely, some layers consisting of very small pebbles and granules (e.g., in the centre of the photo) show backwash-related landward-dipping imbrication. Note also the tight clast-supported openwork texture, good sorting, and excellent segregation of clasts of different sizes into separate beds; C) Upper part of the same lithosome, showing, above an even and regularly stratified bed package, details of the washover complex showing an abundance of large discs and alternation of layers with an irregular base and disorderly fabric, with more organized beds showing moderately preferred fabric.

the other hand, clasts in the upper part of the zone tend to be oriented with downslope-dipping imbrication (Fig. 19 I,K), except for very small pebbles and/or granules, which may show upslope dipping imbrication. Moreover, as a general feature, smaller, rod-shaped pebbles show mainly a-axis imbrication (Fig. 19), while sparse larger blades or discs tend to show b-axis imbrication. The dip angles of imbrication are generally in the 15°-30° range, but some layers show upward increases in dip angles of imbrication up to the vertical, sometimes with flattening at the top (sigmoidal pattern) or inversion of the imbrication dip in the uppermost part of the layer. In the least inclined layers of the upper part of the even-bedded succession, imbrication dip is more erratic, with the long axes of rods sometimes showing a certain divergence leftwards or rightwards with respect to the dip direction of clinoforms. The Apenninic lithosomes (only visual observations) show an overall predominance of downslope dipping clast imbrications in thinner units with low-gradient clinoforms; conversely thicker units with steeper and

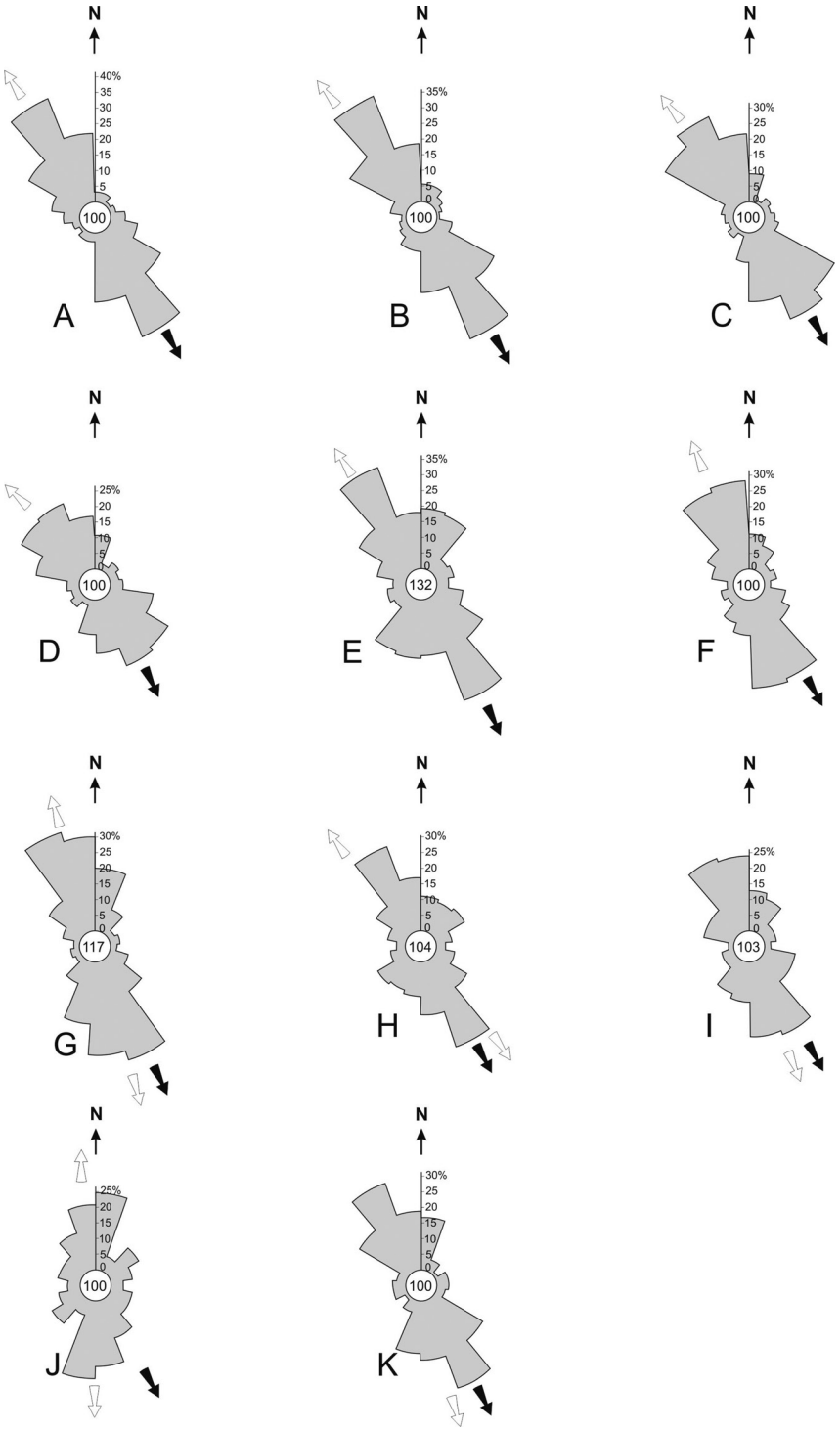

Fig. 19 - Rose diagrams illustrating the fabrics of FA5 even-bedded gravels in a South-Alpine beach lithosome. Measures of the long-axis orientation of rods showing an a-axis to b-axis ratio over a minimum of 1.70 were made on the upper surfaces of layers occurring in succession upwards. In all roses the solid arrows show the direction of progradation; in cases of preferred fabric the approximate dip of imbrication, as inferred from field evidence, is also indicated (open arrows). For each sample some annotations on the textural characteristics are added. A) sample 621: moderate sorting, predominant small pebbles and granules, rare large pebbles and cobbles; B) sample 625: moderate sorting, predominant small pebbles, rare large pebbles; C) sample 628: pronounced size bimodality, with large pebbles in a matrix of granules; D) sample 631: moderate sorting, small pebbles predominant, sparse large pebbles and rare cobbles; E) sample 635: moderate to good sorting, predominant small pebbles, sparse larger pebbles; F) sample 640: moderate sorting, predominant small pebbles, subordinate larger pebbles; G) sample 650: good sorting, predominant small pebbles, rare larger pebbles; H) sample 659: size bimodality, predominant small pebbles, subordinate larger pebbles; I) sample 667: moderate to good sorting, predominant small pebbles, rare larger pebbles and cobbles; J) sample 676: moderate sorting, predominant small pebbles, interstitial granules; K) sample 683: poor sorting, predominant small pebbles, rare larger pebbles, matrix of granules and sand. South-eastern side of Monte Stella (about 4 km SW of the town of Vittorio Veneto; 1:25,000 topographic map "Vittorio Veneto").

higher clinoforms show a pattern of clast imbrications comparable to that shown by South-Alpine lithosomes.

A rare feature observed in strike-oriented sections is represented by a scarcely persistent series of scoop-shaped, low-relief depressions passing laterally to broadly convex-up coarser-grained ridges containing a concentration of large pebbles, with wavelengths ranging from 1 to 9 m.

Loading and "quick bed" injection structures highlighted by convolutions with decimetric lobate synforms and antiforms emphasized by clast orientations are locally present.

5.5.1.2. The upper to uppermost part of the subunit

In wholly preserved lithosomes, peculiar features are present in the upper to uppermost parts of the subunit. These features generally show the maximum grain sizes of the FA5.

Dip-oriented sections may show in the uppermost part of the lithosomes characteristic planoconvex features (Figs. 3, 8, 18A, 20); these are represented by one or more broadly planoconvex ridges with planar, commonly low-angle erosional, or in places conformable, bases. Their internal structure appears to consist of a planoconvex core overlain by a convex-up bundle of strata (Fig. 20). The former is several metres in length and decimetres in height and is coarser-grained than the adjacent beds; layers accreted on it enhance its convex-up shape and show a low-angle downlapping pattern beyond the core crest in the direction opposite to the dip of the clinoforms of the prograding body (Fig. 20). The ridges are usually preserved with their complete characteristic geometry only at the lithosome top; conversely, those occurring at lower levels, interbedded with even, regularly bedded gravel, are generally incomplete, being truncated at the top by planar erosional surfaces (Fig. 20).

The gravel layers involved in the structure typically consist of a mix of clasts of variable size, commonly with a chaotic fabric. Large discs are abundant, 7 to 13 cm in diameter, exceptionally up to 18 cm ("large disc Zone" of Bluck, 1967, 2011) (Fig. 18C), and they are commonly accompanied by a minor number of blades and even equant pebbles and cobbles; commonly larger clasts float in a matrix consisting of sand, granules, or very small pebbles, and gravel beds may be interbedded with sand or granule layers. The chaotic facies locally alternates with better organized gravel beds showing fabric and textural features comparable to the even-bedded FA5 gravels.

Other characteristic units locally occurring in the upper to uppermost part of the subunit are planar cross-bedded gravel sets up to 140 cm thick accreted in the direction opposite to the dip of the clinoforms of the prograding body (Figs. 3, 21). The sets are composed of avalanche foresets with the slip face generally dipping at angles ranging from 18° to 35°, planar in geometry or concave with an asymptotic basal contact; the sets are either bounded at the top by an erosional surface or overlain by a bundle of sub-horizontal topset layers feeding the foreset laminae. The accretion of the set occurs on a substrate either consisting of a channel partially infilled with trough cross-bedded gravels (Figs. 3, 21) or represented by a broadly concave-up erosional depression carved in even-bedded FA5 gravels (e.g., Fig. 3, smaller set on the left).

The gravels composing the sets are of two types: i) in most cases they are well organized, consisting of well sorted pebbles commonly of small size, made up of discs and subordinate blades with fair imbrication, and they are comparable in textural features to the even and regularly bedded FA5 gravels (Figs. 21 A,B); ii) less commonly they are chaotic, badly sorted (Fig. 21C), and irregularly stratified, including large pebbles and also cobbles of variable shapes. In dip-oriented sections, some lithosomes show cross-bedded tabular sets at different levels in the upper part of the subunit, interbedded with FA5 even-bedded gravels (Figs. 3, 21A).

Strike-oriented sections rarely show low-relief gravel lenses with a gently concave-up erosional base and planar top, ranging in width from 2.4 to 4 m, up to 25 cm thick, and generally coarser-grained than the surrounding FA5 gravels.

5.5.2. Interpretation

The FA5 deposits are considered the record of the upper beachface. The high persistence and evenness of beds which make up most part of the subunit significantly contrast with the fair-weather characteristics of the subaerial part of the beach, constructed during the usually long-term, low-energetic recovery stage. The characteristics of the upper-beachface gravels, including texture, size and shape sorting, fabric, and stratal organization, are inferred to require a fast recovery under relatively high-energy conditions, occurring in the immediate waning stage of the storm (e.g., Ivamy and Kench, 2006; Bramato et al., 2012; Grottoli et al., 2017). This assumption is in agreement with the conclusion of Scott et al. (2016) that the post-storm recovery of sand/gravel beaches does not necessarily occur during calm periods and that in many cases high-energy swell events appear to be essential for the recovery of sediment and a vital ingredient in the restoration of pre-storm beach volumes. Due to low steepness, long-period "constructive" waves arrive at the swash zone unbroken with enhanced heights (due to shoaling), thus resulting in large runup excursions (Almeida et al., 2017). The return to a reflective profile may lead to the amplification of the sub-harmonic component of the long-period swell forming part of the storm decay spectra (Wright and Short, 1984; Carter and Orford, 1984), thus providing a mechanism for the accentuation of runup excursions; this in turn results in the activation of the overtopping of the highest berm and the landward accretion of washover gravels. The assumption of a fast recovery in the immediate waning stage of the storm is in agreement with the observation that coarse-sediment beaches tend to respond faster than beaches consisting of fine sand (e.g. Ivamy and Kench, 2006; Bramato et al., 2012). Long-period waves are inferred to actively

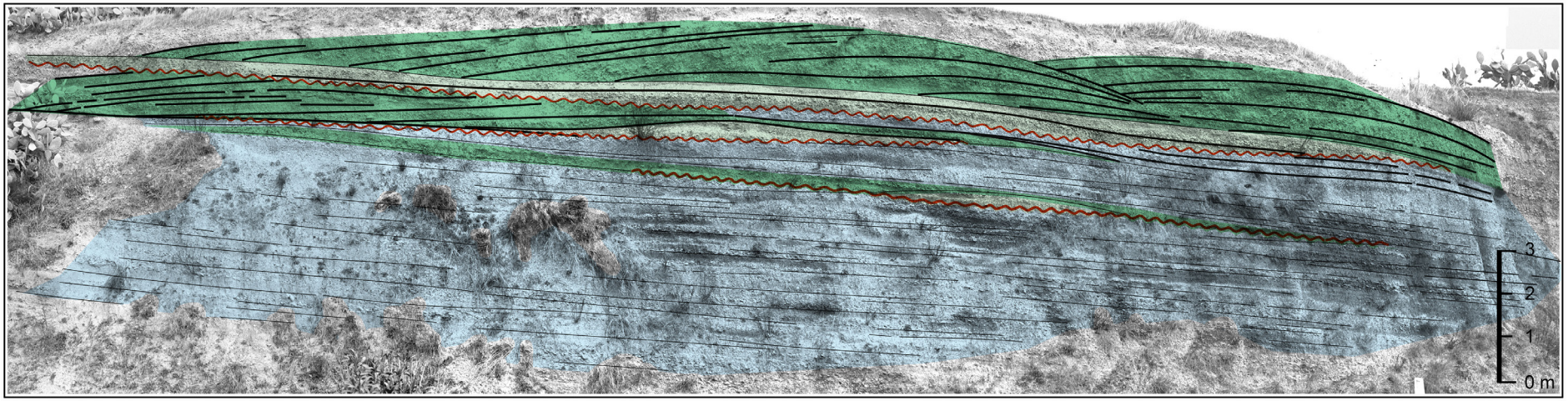

Fig. 20 - View of upper-beachface gravels of an Apenninic lithosome in an oblique section, slightly angled with respect to the dip direction of clinoforms (land to oblique-left). The line drawing documents details of the facies architecture and stratal geometry. The convex-up bundles of strata at the top are interpreted as the record of storm berms with vertical and landward accretion; the cores of these features are low-relief planoconvex gravel ridges, coarser-grained than adjacent beds, bounded at the base by erosion surfaces; the berm remnants at lower levels are truncated at the top by erosional planation surfaces, in contrast with fully preserved topmost bedsets. Light blue: gravel clinobeds of the prograding body; pale green: planoconvex cores of the storm berms; dark green: convex-up stratal bundles recording the accretion of the storm berm; red lines: erosion surfaces. Scale bar in metres. MIS 5.5 terrace, road Metaponto-Matera, between Masseria San Salvatore and Serra Marina (1:50,000 topographic sheet "Ginosa").

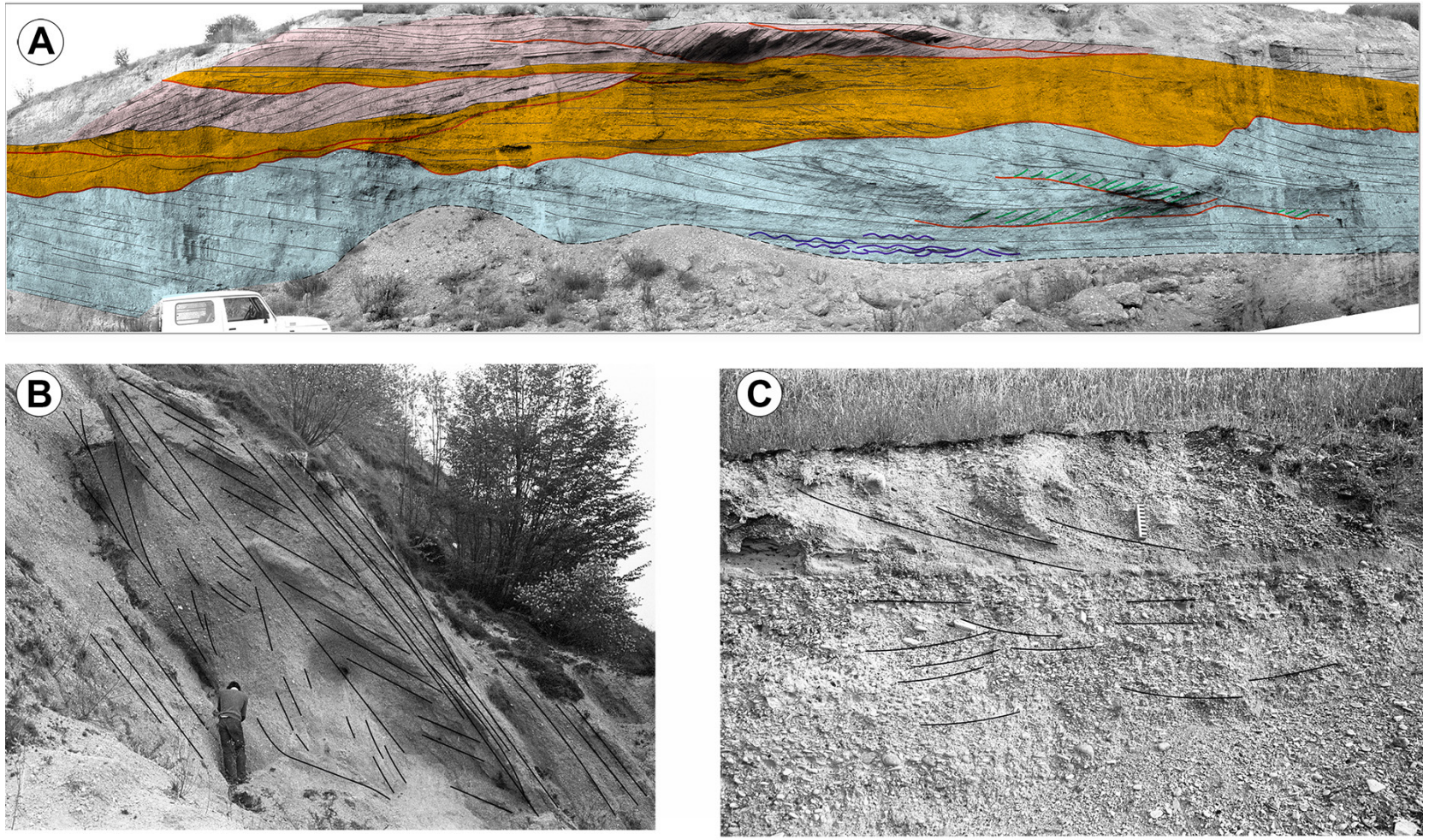

Fig. 21 - Planar cross-bedded sets of inferred washover gravels. A) View of a river-influenced Apenninic beach lithosome in a nearly dip-oriented section. Planar cross-bedded sets of washover gravels are present at four levels, in the upper and uppermost parts of the section; the two lower sets (left) partly infill river channels which accommodate trough cross-bedded gravels in the lower part. Note also, in the prograding wedge at the base of the backshore complex, the sets of gravelly backset laminae and wave megaripples. The line drawing documents details of the facies architecture and stratal geometry. Light blue: prograding gravel wedge; orange: trough cross-bedded fluvial deposits; pink: sets of planar cross-bedded washover gravels; green lines: backset bedding; blue lines: megaripples. Car at lower left for scale. MIS 7.5 terrace, cartroad 350 m ENE of Fontana Lapillo, NNW of Serra Marina (1:50,000 topographic sheet "Ginosa"); B) Upper part of a tectonically tilted South-Alpine beach lithosome. Inferred backshore complex consists of trough cross-bedded channelized fluvial deposits overlain by a set of planar cross-bedded washover gravels, in turn capped by a planoconvex layer bundle interpreted as a storm berm. Person for scale. Track between C.se Val Torond and S. Antonio, about 2.5 km SW of the town of Vittorio Veneto (1: 25,000 topographic map "Vittorio Veneto"); C) Top of an Apenninic beach lithosome showing a set of planar cross-bedded washover gravels with variable textural features at the top of inferred fluvial deposits. Scale bar 16 cm long. Middle Pleistocene, abandoned quarry near Villa Gigli, WSW of Porto Recanati, SE of Ancona (1:25,000 topographic map "Recanati").

promote landward advection of sediment previously lost seaward during storm conditions, as supported by the presence of the erosional remnants of lower-beachface gravels near the upslope end of FA4 layers (arrows in figure 15A). However, the minority of FA5 beds, generally finer-grained than average, that show physical continuity with the lower beachface gravels indicates that also minor accretion of the whole profile of the beachface may occur during this stage.

Masselink and Puleo (2006) stressed the important principle that a feedback between morphology and hydrodynamics is an essential component of the swash zone/beachface morphodynamic system. An example of this principle is the tendency of the foreshore gradient to adjust to the incident wave period, with a flattening of the profile in the case of swash excursions of shorter duration and, conversely, steepening as a response to swash excursions of longer duration than the incident wave period (Holland and Puleo, 2001). The adjustment of the upper-beachface gradient as a result of accretion in the new hydrodynamic equilibrium leads to a convex and steepened profile (Sonu and van Beek, 1971; Masselink and Puleo, 2006).

The beach step during this stage was probably subdued or absent. Step "elimination" takes place by step-crest erosion when wave conditions are not conducive to step maintenance (Bauer and Allen, 1995). The flattening of the beach step is believed by Buscombe and Masselink (2006) to result from the activity of surging breakers, which are held responsible for the high runup leading to the active advection of sediment on the upper beachface. The waves break directly on the steep beachface, and sediment entrained by the wave breaking process is directly advected into the wave uprush, enhancing onshore sediment transport and promoting accretion in the swash zone (Masselink et al., 2010).

Low-angle truncation surfaces in the even-bedded facies may reflect short periods of enhanced erosion, possibly due to impact of severe storms, or changes in the direction of wave incidence or in the beach orientation (e.g., beach rotation). Rare low-amplitude plano-convex quasi-symmetrical thin lenses locally interspersed through the even-bedded facies are regarded as antidunes (e.g., Barwis and Hayes, 1985; Yagishita, 1995).

Fabric patterns in different parts of the upper beachface give significant information on the hydrodynamics of swash processes. Masselink and Puleo (2006) pointed out that the flow acceleration during the runup results in strong shear stress on the seabed, with peak uprush shear stress being currently regarded as nearly twice that of the peak backwash. They noted that the uprush is dominated by bore turbulence and high friction coefficients, especially on steep beachfaces, with much of the sediment supported by turbulent fluctuations. Due to the relatively large hydraulic conductivity of coarse sediments, infiltration/exfiltration can become significantly important processes on gravel beaches (e.g., Almeida et al., 2017). Water infiltration into the bed during the uprush event contributes both to thinning the bottom boundary layer with an increase in shear stress and removing the water available for the subsequent backwash, thus significantly reducing the backwash efficiency. Consequently, seepage forces significantly increase onshore sediment transport in the swash zone (Elfrink and Baldock, 2002). Around flow reversal, the flow velocity is so weak that much of the suspended sediment settles, so that during the backwash the flow is less turbulent and most of the sediment transport occurs as a granular layer dominated by shear derived at the bed (Buscombe and Masselink, 2006; Masselink and Puleo, 2006). Accordingly, the granular moving layer during the backflow probably experiences the effects of the dispersive pressure due to grain collisions (e.g., Bagnold, 1954) and of hindered settling.

An analysis of the long-axis orientation and type of imbrication of upper-beachface gravels, performed in the South-Alpine succession (Fig. 19), provides useful information on the processes of sediment mobilization and transport. Flow efficiency during uprush was probably not significantly reduced by water loss for infiltration: the latter is thought to have been at least partly contrasted by the common presence of sand infiltrated in the interstices of clast-supported gravel and by the internal structure characterized by distinct coarse/fine unit stratification with differential permeability (e.g., Carter and Orford, 1984, 1993). The landward dipping clast imbrication predominant in the lower part of the upper beachface (Fig. 19 A-F) implies that the accelerated backwash maintains sufficient efficiency to orient the clasts in that area; the a-axis orientation of rod-shaped small pebbles parallel to the flow indicates a type of transport dominated by the interparticle impact within Bagnoldian dispersions during the backwash. The local coexistence of seaward and shoreward dipping imbrications in the middle part of the upper beachface (Fig. 19 G,H) is thought to reflect the approximately equivalent roles of uprush and backwash in the clast orientation in that area. Only in the uppermost part of the subunit do the predominant seaward-dipping clast imbrications (Fig. 19 I,K) indicate the prevailing action of wave runup and the inefficiency of backwash flow in re-orienting the clasts, except for the very small pebbles; this probably implies low flow velocity in the initial stage of flow reversal, inadequate to re-orient most part of the clasts. What is worthy to note is that clast a-axis orientation parallel to flow is dominant not only in the backwash-dominated lower part of the upper beachface, as expected due to the currently recognized importance of interparticle impact during the backwash (Buscombe and Masselink, 2006), but even in the run-up-dominated uppermost beachface (Fig. 19), pointing again to the primary role of clast interaction, probably due in this case to high concentration and bedload transport rates accompanied by the reduction of turbulence.

The upward increases in dip angles of imbrication observed in some beds may be an effect of infiltration/exfiltration or fluid, which exerts loading/unloading on

the bed surface, therefore inducing a lift force due to vertical flow/pressure gradient (Baldock et al., 2001). Alternatively, this particular fabric may result from the internal shearing of gravels prior to the frictional freezing of highly concentrated dispersions, an effect already suggested to be common in the process of emplacement of lower-beachface gravel layers.

The local presence of a certain range of directions of clast imbrication in the upper part of the zone may reflect an oblique sawtoothed swash motion.

The predominance of seaward dipping clast imbrications in the whole upper beachface of Apenninic units characterized by lower gradients of the upper beachface is thought to reflect the primary role of the wave runup in the clast orientation, probably due to the inability of the backwash to reach sufficient gravity-driven acceleration.

The high average sorting of the even-bedded upper-beachface gravels is the proof that the hydrodynamic and sediment transport processes have a strong sorting effect on the sediment particles in the swash zone (Holmes et al., 1996). Bluck (1967) and Orford (1975) concluded that most efficient shape- and size-sorting processes are linked to the action of long-period waves. As noted above, good sorting, as well as the striking regularity of upper-beachface stratal organization, are thought to reflect large runup excursions promoted by long-period "constructive" waves characteristic of the early, fast stage of post-storm recovery. The local bimodality or polymodality of clast sizes/shapes may result from the mixing of different clast populations due to the advection of coarser gravels from the lower beachface into the swash zone (Sonu, 1972).

The lack of evidence of beach cusps, except for rare examples of the partial, eroded remnants of small-scale horn-and-bay patterns, may indicate that these features have poor to null preservation potential; however, it cannot be excluded that the record of cusps with dimensions exceeding the extent of the available strike sections escaped identification.

The more or less preserved planoconvex gravel ridges observed in the upper to uppermost part of the subunit (Figs. 3, 8, 18A, 20) are inferred to represent storm berms, i.e. linear mounds of coarser sediment built-up under the strongest run-up activity during high water periods (Maejima, 1983; Carter and Orford, 1984, 1993; McCall et al., 2014). In these conditions, the gravel is transported and stranded around the maximum run-up limit, resulting in sediment accumulation and the vertical accretion of low ridges built up at the seaward margin of the backshore. Orford and Carter (1984) show that steep gravel beachfaces reinforce storm wave run-up, facilitating beach crest accretion during storms. Dip-oriented sections of studied lithosomes show that these planoconvex features are preserved with their complete structure only at the beachface top, whereas they are partially or wholly erased by the emplacement of younger deposits if located in lower positions on the beachface (Fig. 20). The build-up and landward accretion of the ridges are thought to occur both under the action of storm-peak surges and during the storm decay stage, when enhanced runup can be generated by swell waves. The first occurrence is supported by the common evidence of erosion at the base of the ridges (Figs. 8, 20) and a prevalent chaotic fabric, pointing to the violent heaping up of unsorted gravels, including even larger clasts (Fig. 18C); conversely, the second occurrence is supported by the supplementary contribution of better sorted and better organized gravels, inferred to preferentially result from the sorting effect of long-period waves. Actually, the chaotic clast orientations commonly present in the storm berms (Fig. 18C) are thought to reflect a number of possible causes, in addition to the violent heaping up of clasts during storm surges: i) fabric disruption resulting from the burial and subsequent decay of the flotsam stored up-beach, such as logs and wood debris, uprooted sea grass, or seaweed communities torn from the sea bottom; ii) the growth and decay of plant roots (e.g., Maejima, 1982; Hunter et al., 1984); iii) the loading exerted by the walking of large vertebrates.

The abundance of the disc-shaped clasts, commonly of large size, in the composition of storm-berm gravels is attributed to their lower settling velocity with respect to other clast shapes when transported in suspension; this type of transport prevails under the action of maximum-runup storm waves (Bluck, 1967, 2011), which promotes the throw of the discs up high on the beach together with other morphometric classes. Unlike other classes, such as spheres or rods which can be selectively re-mobilized by the backwash, the discs are trapped high on the beach due to limited sliding during the backwash on a smooth substrate formed by sand or granules. The large discs may therefore be regarded as a lag concentration. The local association of the beds containing large discs with sand layers in the uppermost part of the zone, and specifically in the storm berms, is regarded as the evidence that shoreface sand put in suspension under the breakers during the storm peak may be transported by strong runup to the top of the beach and deposited together with large discs.

The tabular sets of landward accreted avalanche foresets (Figs. 3, 21) are believed to represent washover gravels infilling either shallow backshore depressions (e.g., Fig. 3, smaller set on the left) or terminal reaches of fluvial channels (e.g., Fig. 3, thicker set on the right; Fig. 21), with foreset accretion starting from a step corresponding to the channel bank (see also Spaggiari et al., 2006). The dip of the trough cross-bedded gravels of the partial channel fill suggests that terminal fluvial reaches were mostly sub-parallel to the shoreline, as often observed in modern settings; less common is the evidence of palaeoflow direction sub-perpendicular to the inferred trend of the shoreline (e.g., the major channelized unit in Fig. 21A). As in the case of the storm berms, the textures of the gravels involved in the washover sets, alternatively chaotic, badly sorted and irregularly bedded (Fig. 21C) or well sorted and distinctly stratified (Fig. 21 A,B), suggest that overtopping and overwashing may have occurred

during storm-related surges and the storm decay stage, the latter characterized by the action of long-period waves with large runup excursions, more effective as shape- and size-sorting process (*e.g.*, Orford and Carter, 1982; Forbes et al., 1991; Bluck, 1999).

Shallow gravel-filled scours locally observed in strike sections to cross the upper-beachface gravels are inferred to indicate that overtopping and washover processes under strong run-up activity were locally accompanied by the scouring of small rills normal to the shoreline.

The preservation of more than one planar cross-stratified set interbedded with FA5 gravels at different heights of the clinoform body (Figs. 3, 21A) suggests "climbing" progradation as a response to rising relative sea level, concomitantly with a high rate of sediment influx preventing beach retreat.

6. SHAPE AND SIZE SORTING

The distribution of clast shapes and sizes on gravel beaches is predominantly determined by beach hydrodynamic processes (e.g., Bluck, 1967; Kirk, 1980; Bourgeois and Leithold, 1984), with the effectiveness of shape- and size-sorting processes being higher on beaches characterized by a more vigorous wave climate. The textural characteristics of gravel beaches confirm Bluck's (1967) observation that where efficient size sorting occurs, strong shape sorting also occurs. In the 2011 paper Bluck used an approach to processes involved in clast shape and size sorting and in the construction of the lithosome architecture mainly focused on the role of fair-weather hydrodynamics. The work by Orford (1975) and later studies by Williams and Caldwell (1988) proposed a model of clast shape and size sorting linked to storm-driven and gradual lower-energy processes.

This study focuses on the critical role of high-energy processes. Specifically, effective cross-shore size and shape sorting processes (the selective concentration of large discs in the highest part of the beach profile and of spherical large pebbles and cobbles in the toeset zone) are thought to occur both during storm conditions and in the subsequent, highly energetic early recovery of the storm decay stage inferred to be dominated by longer-period waves. It is believed that under the latter conditions, shape- and size-sorting processes are significantly more efficient. This is supported by the conclusions reached by Bluck (1967) and Orford (1975), who established through a quantitative analysis that the degree of textural zonation is a function of the manner in which energy is expended in terms of the wave phase and breaker type, with maximum sorting effects appearing as a product of swell wave action.

A significantly higher sensitivity to the shape sorting process is shown by larger clasts (Fig. 22), whereas small pebbles fail to show a significant shape differentiation between the various subunits (Massari and Parea, 1988a).

The shape spectrum and the relative proportion of different shapes is also currently known to be significantly influenced by the isotropy or anisotropy of the lithologies present in the clast source area (e.g., Bluck, 1967). For instance, the abundance of discoidal clasts in the upper-beachface deposits of the Apenninic lithosomes of the Marche region is certainly correlated with the widespread presence in the nearby Apennines of stratigraphic units consisting of limestones and marly limestones with a tendency to easily split into flat fragments, such as the thin-bedded pelagic Cretaceous formations; remarkably different is the case of the South-Alpine lithosomes of the eastern Southern Alps, where the prevailing clast shapes with a significantly lower average flatness index reflect the predominance in the source area of more isotropic lithologies, such as Triassic massive dolostones.

7. THE PALAEOCLIMATE

Paleobotanical data from lower Messinian pre-evaporitic deposits revealed strong climate gradients within the Mediterranean, with the northern sub-basins characterized by moist climate and a positive hydrological budget and precipitation sufficiently high for the persistence of a "subtropical humid forest" (Bertini and Martinetto, 2011; Sabino et al., 2020). The latter authors showed that strong climate gradients across the Mediterranean Basin occurred in coincidence with a restriction of the Atlantic-Mediterranean gateways, an event that would have made the Mediterranean more vulnerable to high-frequency climatic changes. It is important to note that during the Messinian pre-evaporitic times, as well as during the middle and late Pleistocene, the deposition is currently known to have been strongly influenced by precession-driven climate fluctuations. During precession minima, characterized by maximum seasonality (winter insolation minima and summer insolation maxima), a greater influence of Atlantic-born depressions in the Mediterranean could have increased the activity of cyclonic storms and the river discharge from the northern borderlands of the Mediterranean (Rohling and Hilgen, 1991). Toucanne et al. (2015) pointed out that the close relationship between the ITCZ (Intertropical Convergence Zone) northward motion, the North Africa summer monsoon and the rainfall activity over the northern Mediterranean borderlands, indicates a positive correlation between the intensity of the North African summer monsoon and the cyclogenesis activity on the Mediterranean in concomitance with the aphelion-related increase in rainfall during precession minima. The extreme seasonality could have led to increase of the air-sea temperature contrast and, correspondingly, the necessary heat and moisture fluxes required for the development and strengthening of cyclonic circulations over the Mediterranean (Trigo et al., 1999, 2002; Meijer and Tuenter, 2007; Kutzbach et al., 2014). This assumption finds a support in the observations of Soria et al. (2014), who described a precession-controlled cyclical shallow-marine terrigenous succession on the Betic margin of the western Mediterranean deposited during a high sea level phase prior to the onset of the Messinian salinity

crisis, showing evidence of combined effect of river supply nourishing coastal zones and storm-influenced sedimentation.

The late Miocene precession-driven climatic conditions, characterized by increase of fresh-water input, and also held to be responsible for the occurrence of the sapropel cycle patterns, are akin to those recorded in Pleistocene marine successions located throughout the Mediterranean (e.g. Turco et al., 2001). In a study of the GDEC-4-2 borehole located on the East Corsica margin (northern Tyrrhenian Sea), Toucanne et al. (2015) provided precisely dated evidence for enhanced rainfall in the Mediterranean during warm precession-ruled isotope substages of interglacial periods, probably in response to the intensification of the Mediterranean storm track in autumn/winter, and in coincidence with the timing of the North African monsoon and sapropel deposition. These 'pluvial' events probably originated from the cyclogenesis mechanisms in the Mediterranean (Trigo et al., 1999, 2002).

8. DISCUSSION

A comparison with the present-day wave climate of the Mediterranean is regarded as suitable, considering that the present interglacial climate is akin from several aspects to that existing at the time of deposition of the examined beach lithosomes, and observing that the palaeogeography of the Italian seas, even in early Messinian times (Fig. 1), was not substantially different from the present-day one, particularly concerning the palaeo-Adriatic Sea. It has been already observed that the present Mediterranean Sea is subject, despite its relatively limited dimensions, to extratropical severe storms, mainly forming and growing via baroclinic instability (Casas-Prat and Sierra, 2013, with references).

Although the longer-term "memory" typical of the oceanic sites is lacking in the landlocked Mediterranean Sea, and relatively short fetch results in a dominant wind sea, present-day beaches during storm events commonly experience a wave-spectrum bimodality (Inghilesi et al.,

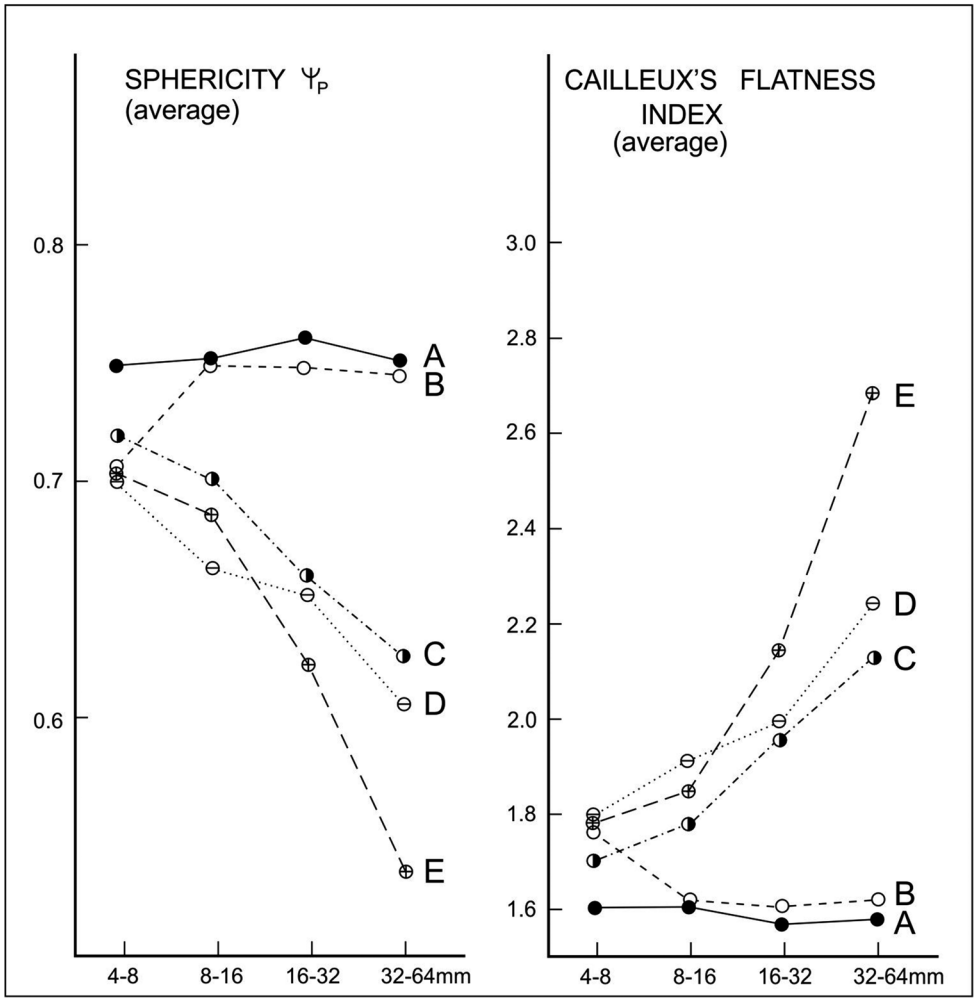

Fig. 22 - Folk's sphericity index and Cailleux flatness index plotted against size for 38 gravel samples from South-Alpine beach lithosomes of the Vittorio Veneto area. A: toeset zone; B: lower beachface (lower part); C: lower beachface (upper part); D: upper beachface (lower part); E: upper beachface (upper part). Much higher sensitivity to shape-sorting processes is clearly shown by larger-sized clasts. (from Massari and Parea, 1988a).

2012; Casas-Prat and Sierra, 2013; Ruju et al., 2019). The wave climate does not display the complexity of the energy distribution among the various frequencies and directions of wave systems typical of the ocean: a 2D spectrum predominates, namely wind sea and swell (Inghilesi et al., 2012; Cavaleri et al., 2018). Almeida et al. (2017, with references) stressed the importance of the bimodality of the storm wave climate as an important factor potentially increasing wave runup and enhancing the occurrence of overwash on gravel beaches. Although reconstructing the wave characteristics from the record of palaeo-beaches is a task with a high level of uncertainty, it is suggested that the wave spectrum during storm events recorded in the studied lithosomes had, likewise, a bimodal shape in most cases, with high-energy wind waves of local origin associated with a swell component. Palaeocurrent data (Fig. 12) are consistent with the predominant influence of a south-easterly wind, suggested to represent the ancestor of the present-day Sirocco; during winter aphelion of precession minima this wind was probably active, blowing from the Saharan region of northern Africa to the Mediterranean stormy depressional area. As above noted, the present-day Sirocco wind blows along the main axis of the Adriatic, channelled between the Apennines and Dinaric Alps, and is characterized by long, moderate-intensity fetches (Archetti and Romagnoli, 2011) of up to 700 km, causing long waves. Therefore, a swell component is particularly important for waves traveling along the main basin axis (Lionello et al., 2003). This component is regarded as having a critical role in fast beach recovery during the storm decay stage, when local storm winds and downwelling abate and wave steepness significantly decreases.

Present-day storms generated by Sirocco impact the northern Adriatic coast almost perpendicularly to the shoreline, with fully developed sea states, and long and regular waves, and they are associated with high storm surges (Cavaleri et al., 2018); on the other hand, this wind impacts obliquely the Apenninic coast of both central Adriatic and Gulf of Taranto (see above), thus favouring the longshore drift. As a result, the former beaches are predominantly swash-aligned, whereas the latter are drift-aligned. The stratal organization, palaeocurrent pattern, and overall architecture of the studied lithosomes suggest similar differences in behaviour linked to the beach orientation with respect with the wave approach and prevailing winds. The Apenninic palaeo-beaches, located on the NW-oriented western coast of the palaeo-Adriatic, behaved as *drift-aligned* systems (Davies 1980; Orford et al., 1991) characterized by a nearshore circulation that was generally asymmetric during high-energy events. Palaeoflows also suggest that a skewed bar/interbar system, with bars and rip channels oriented obliquely to the shore, may have been a common feature. The sparse to common seaward-dipping clast imbrication observed in the beachface gravel beds indicates the strong shear stress of onshore-directed incident wave-coherent flow and the enhanced sensitivity to incident wave energy, inferred to lead to significant storm-driven widening of the surf zone. All of these features indicate that Apenninic palaeo-beaches underwent a change to a morphodynamic intermediate state (in the sense of Wright and Short, 1984) during high-energy events, with the development of a nearshore bar/rip morphology. As stressed by Aagaard et al. (2013), in this beach state strong morphodynamic feedbacks between hydrodynamic processes and morphology create large cross-shore and alongshore transport gradients, ensuring high morphological variability, dynamic beach states and high sediment transport rates.

Conversely, evidence from stratal organization of the South-Alpine palaeo-shorelines shows that, during high-energy events, rip cells and the associated inshore topography were only sporadically activated, effectiveness of longshore drift was remarkably scarce, and surf zones were very narrow. In these steeper-gradient beaches, accelerated backwash and cross-shore pressure gradients were significantly aided by gravity; the role of the interparticle impacts in the flows moving on the lower-beachface slope is highlighted by the predominance of landward-dipping a-axis clast imbrication in the deposits. Moreover, storm-driven return flow compensating the onshore wave mass transport was weaker compared to the Apenninic palaeo-beaches, as reflected by a more limited spectrum of structures linked to supercritical flows and a lack of those implying higher-energy conditions. On the other hand, wave megaripples are apparently more common in the upper shoreface and lowermost beachface of South-Alpine shorelines, possibly due to the maximum fetch of the inferred predominant south-easterly wind. The related beaches behaved therefore as almost *swash-aligned* systems, dominated by cross-shore motions (Davies et al., 1980; Orford et al., 1991), a setting most probably linked to their location on the landlocked embayment of the northern end of the Palaeo-Adriatic Sea resulting in an almost perpendicular exposure to the inferred predominant south-easterly wind.

The distinctive characteristics allowing a differentiation between the South-Alpine and Apenninic systems are presented in table 1 and figure 23.

The internal organization of the studied beach lithosomes must be regarded as composite in nature: the overall architecture results from the interfingering of subunits mostly lacking mutual physical continuity and pointing to formation under different hydrodynamic stages. The evolution of the beach-nearshore profile during a storm cycle may be tentatively summarized as follows (Fig. 24).

The *waxing stage of storms* is characterized by the powerful erosion of the upper-beachface by high-steepness waves and surf zone processes, and the discharge of large volumes of gravel into the lower beachface by accelerated backwash and cross-shore pressure gradients. The beach step is subject to shifting in position downdip as a response to changing wave conditions during this stage. At the *storm peak*, the breaking of large storm

Table 1 - Comparison of main characteristics of the South-Alpine and Apenninic beach lithosomes.

	SOUTH-ALPINE LOWER MESSINIAN BEACHES	APENNINIC PLEISTOCENE BEACHES
Morphodynamic behaviour	Nearly swash-aligned systems, dominated by cross-shore motions; changing only sporadically to an intermediate state during storms	Drift-aligned systems changing to intermediate state during storms, with development of nearshore bar/rip morphology
Fabric of upper-beachface gravels	Clast imbrication mostly dipping landwards (backwash-controlled) in the lower part of the zone and seawards (runup -controlled) in the upper part	Similar fabric, except in thinner parasequences with lower-gradient clinoforms, where clast imbrication dips seawards
Surf zone during storm events	Narrow	Wide
Lower-beachface gravel beds in dip-oriented sections	More regular, generally high-gradient beds, with a tendency to tabular geometry	More irregular; lenticular (locally sigmoidal), with strongly erosional bases in parasequences with lower-gradient beds
Fabric of lower-beachface gravels	Dominant a-axis imbrication with landward dip. Local upward steepening of imbrication angles. Fabric indicative of important role of gravity-driven dispersive pressure in the flows	Common weak fabric; dip of clast imbrication depending on clast size and gradient of clinoforms: seaward-dipping imbrications are shown by larger clasts in gentler-dipping clinobeds
Wave megaripples	Common	Moderately common
Structures recording supercritical flows at the beachface toe	Sandy and gravelly antidunes	Tendency to develop a greater variety of structures: sandy and gravelly antidunes; sharp-based gravel layers, locally as infill of steep-walled scours (hydraulic jump facies), overlain by sandy sets of backset laminae; rare chute-and-pool structures
Sandy trough cross-laminated sets related to longshore drift	Uncommon	Common in both upper shoreface and toeset areas, locally interstratified with sandy backset-laminated sets in the latter area
Components of the Facies Association 2	Predominant amalgamated hummocky or swaley cross-stratified sets and sandy megaripples; others components unusual	All components of the FA well expressed

waves and high cross-shore pressure gradients drive a strong offshore-directed return flow (undertow) that can quickly reach a supercritical state and be potentially subject to hydraulic jumps at the beachface-shoreface transition. The effects, mostly conspicuous in Apenninic lithosomes, include: i) scours paved/infilled by coarse gravel, recording the impact of hydraulic jumps, whose upstream migration generates sandy backset laminasets; ii) low-amplitude wavy to lenticular structures that are inferred to result from the migration and aggradation of antidunes; iii) local chute-and-pool structures. In the uppermost part of the beach strong runup leads to the build-up of a storm berm and overwashing. In the toeset area of the Apenninic lithosomes a mutual transition can occur between supercritical flows subject to hydraulic jumps and the longshore migration of three-dimensional dunes. Deposition is partitioned in this stage between nearshore and backshore areas. During the *waning stage of the storm* long-period waves lead to the fast recovery of upper-beachface gravels and renewed overtopping and overwashing; moreover, strong oscillatory motion at the seabed results in the generation or accretion of wave megaripples in the upper shoreface and toe of the beachface, with a selective concentration of spherical

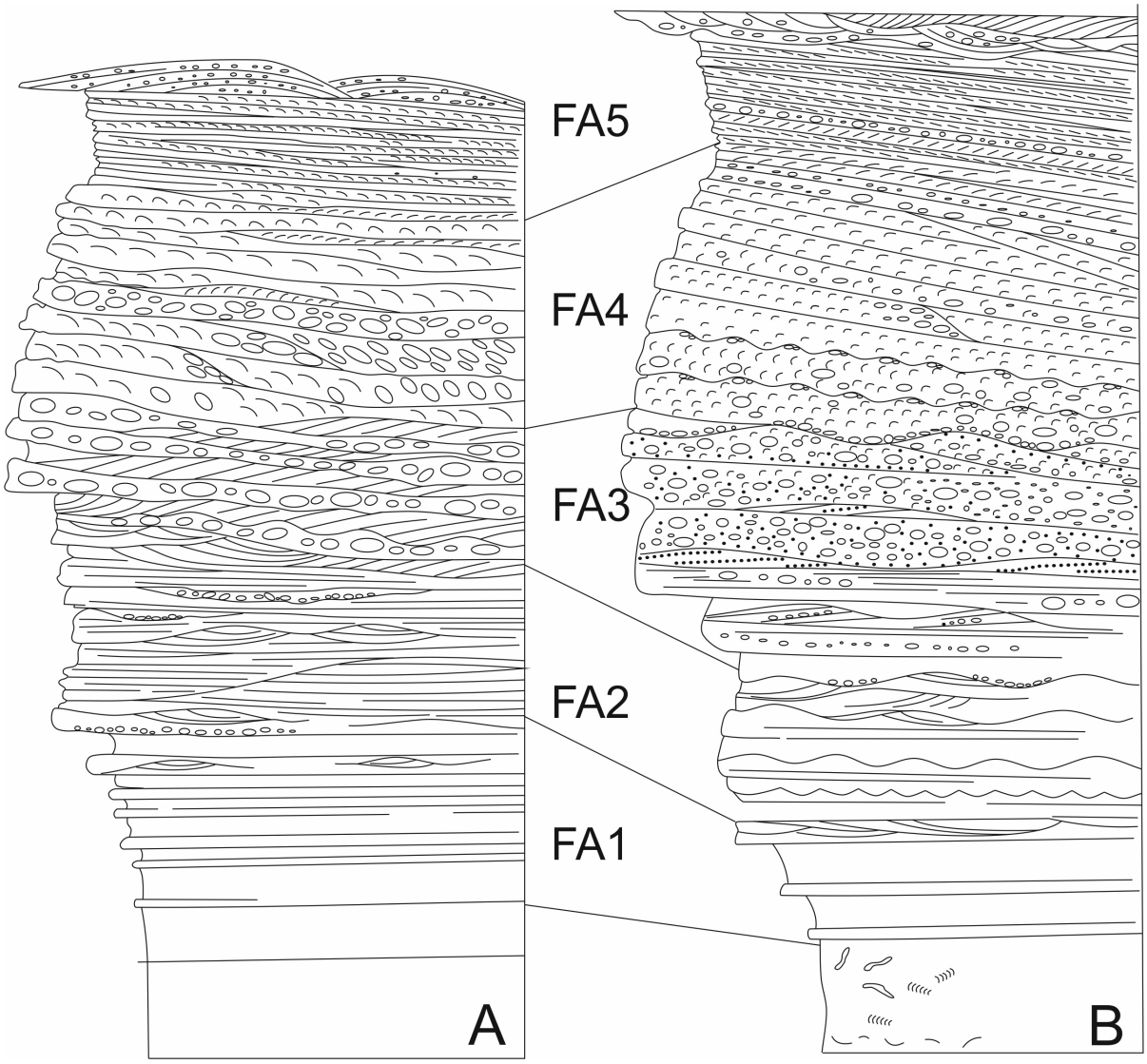

Fig. 23 - Compared idealized logs of the Apenninic (left) and South-Alpine (right) beach lithosomes (not to scale).

clasts. Most effective shape-and size-sorting processes are achieved in this stage.

Classic descriptions of beach cycles link beach states to seasonal changes, such as a summer berm profile and a depleted winter profile (e.g., Komar, 1998). However, cyclic changes largely driven by the frequency and intensity of storm impacts and inter-storm recovery have been commonly observed and increasingly documented on pure gravel beaches (e.g., Sherman, 1991; Sanders, 2000; Roberts et al., 2013, among others). The stratal organization and general architecture of the studied beach lithosomes support the point that the predominant signature is that left by processes linked to storm impacts and immediate storm-decay recovery, whereas fair-weather features have virtually null preservation potential, being mostly vulnerable to erosion during high-energy events (Vos and Hobday, 1977; Reading, 1996; Massari and Parea, 1988a).

It is believed that the storm signature, although inferred to represent and intrinsic feature of the stratigraphic record of gravel beaches, was emphasized in the studied lower Messinian and middle to upper Pleistocene lithosomes, due to the climatic context characterized by intensification of the Mediterranean storm track during precession minima. Moreover, an improvement of the preservation potential of the stratigraphic record was promoted in this climatic context by the significant increase in the fluvial input allowing nourishment and active progradation of the shorelines.

9. CONCLUSIONS

The main conclusions are:

1) The processes linked to the storm impact and immediate storm-decay recovery left the predominant signature to the stratal organization and general

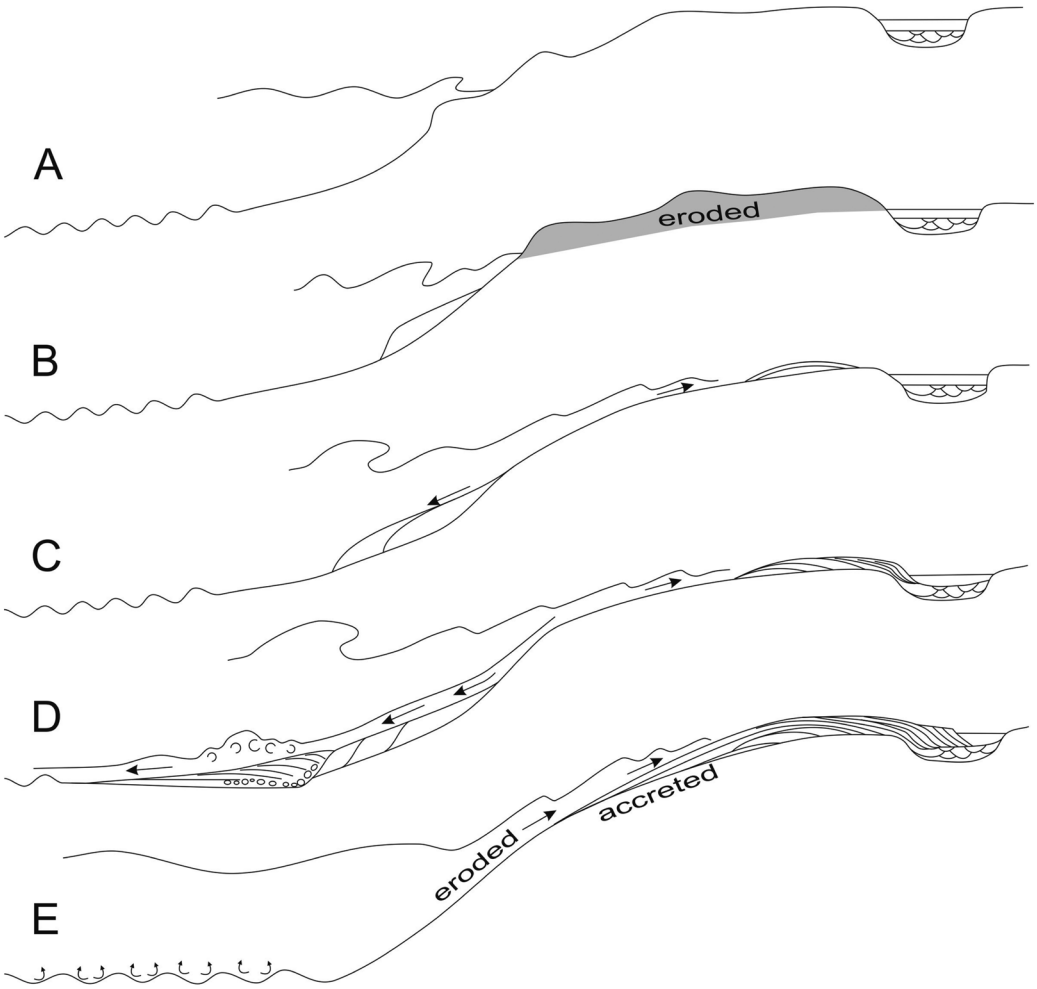

Fig. 24 - Schematic interpretative profiles of gravel beach and nearshore zone on Mediterranean coasts during a severe storm, implying a large temporal variation in wave energy. A) Fair-weather profile; B) Waxing stage of a storm: the upper beachface is eroded and the removed material is discharged onto the lower beachface; C) Energy conditions approaching the peak of the storm: the lower beachface is further acccreted downdip, concurrently with the offshore shift of the beach step; a storm berm starts to be built in the uppermost part of the beach profile. D) Peak of the storm: highly energetic undertow during high-magnitude events enters supercritical conditions; in the more energetic setting of Apenninic palaeo-beaches the undertow is subject to hydraulic jumps at the beachface-shoreface transition, resulting in scour-based gravel layers overlain by sandy backset laminasets. Storm berm and washover deposits are landward accreted in the backshore area. E) During the waning storm stage, long-period waves with large runup excursions restore a steeper beach profile by depositing thin-bedded foreshore gravels advected updip from the lower beachface, and lead to the further accretion of washover deposits. Strong oscillatory motion on the nearshore sea bed produces (or accretes) trains of wave megaripples.

architecture of the studied beach lithosomes: the fossil record is therefore biased towards high-energy deposits and sedimentary structures, and the characteristics of the preserved deposits cannot be predicted on the basis of the knowledge of normal processes influencing modern beach sediments.

2) Observations on the fossil record provide a unique opportunity for insight into facies associations and the reconstruction of the involved genetic processes, particularly those active at the toe of the beachface and upper shoreface under the impact of high-energy events, hardly accessible in present-day beaches due the logistical challenge of making *in situ* measurements under these conditions. A significant part of this study illustrates in detail the range of sedimentary structures generated in the lower-beachface and toeset areas during storm events. Specifically, at the *storm peak*, the breaking of large storm waves and high cross-shore pressure gradients drove a strong offshore-directed return flow (undertow) that could quickly reach a supercritical state and be potentially subject to hydraulic jumps at the beachface-shoreface transition.

3) The studied Lower Messinian and middle to upper Pleistocene lithosomes show significant differences in general architecture. Due to the oblique approach of storm waves, the former palaeo-beaches, located on Apenninic palaeo-coasts, can be defined as *drift-aligned* systems during high-energy events, with the development of very dynamic intermediate states characterized by a prominent bar/rip topography, an energetic undertow,

and large cross-shore and alongshore transport gradients. Conversely, evidence from stratal organization of the South-Alpine palaeo-shorelines shows that, during high-energy events, rip cells and the associated inshore topography were only sporadically activated, effectiveness of longshore drift was remarkably scarce, and surf zones were very narrow. In these steeper-gradient beaches, accelerated backwash and cross-shore pressure gradients were significantly aided by gravity; the role of the interparticle impacts in the flows moving on the lower-beachface slope is highlighted by the predominance of landward-dipping a-axis clast imbrication in the deposits. Moreover, storm-driven return flow compensating the onshore wave mass transport was weaker compared to the Apenninic palaeo-beaches, as reflected by a more limited spectrum of structures linked to supercritical flows and a lack of those implying higher-energy conditions. Therefore, stratal organization and overall architecture indicate an almost *swash-aligned* beahaviour of these palaeobeaches, dominated by cross-shore motion, a setting most probably linked to their location on the landlocked embayment of the northern end of the Palaeo-Adriatic Sea (Fig. 1) resulting in an almost perpendicular exposure to an inferred predominant south-easterly wind.

4) during the early Messinian times, as well as during the middle and late Pleistocene, the deposition was strongly influenced by precession-driven climate fluctuations. During precession minima, characterized by maximum seasonality (winter insolation minima and summer insolation maxima) a greater influence of Atlantic-born depressions in the Mediterranean could have increased the activity of cyclonic storms and the river discharge. It is believed that the storm signature, although inferred to represent and intrinsic feature of the stratigraphic record of gravel beaches, was emphasized in the studied lithosomes due to this climatic context. Moreover, an improvement of the preservation potential of the stratigraphic record was promoted by the significant increase in the fluvial input allowing nourishment and active progradation of the shorelines.

ACKNOWLEDGEMENTS - The author would like to thank C. Di Celma and S. Milli whose constructive insights greatly improved the manuscript. N. Michelon is acknowledged for technical support. The field work was financially supported by Centro di Studio per i Problemi dell'Orogeno delle Alpi Orientali (C.N.R., Padova, Italy) and by C.N.R. grant CT. No. 83.02203.05.

REFERENCES

Aagaard T., Greenwood B., Hughes M.G., 2013. Sediment transport on dissipative, intermediate and reflective beaches. Earth-Science Reviews 124, 32-50.

Aagaard T., Vinther N., 2008. Cross-shore currents in the surf zone: rips or undertow? Journal of Coastal Research 24, 561-570.

Alexander J., Bridge J.S., Cheel R.J., Leclair S.F., 2001. Bedforms and associated sedimentary structures formed under supercritical water flows over aggrading sand beds. Sedimentology 48, 133-152.

Almeida L.P., Masselink G., McCall R., Russell P., 2017. Storm overwash of a gravel barrier: Field measurements and XBeach-G modelling. Coastal Engineering 120, 22-35.

Amorosi A., Caporale L., Cibin U., Colalongo M.L., Pasini G., Ricci Lucchi F., Severi P., Vaiani S.C., 1998. The Pleistocene littoral deposits (Imola sands) of the northern Apennines foothills. Giornale di Geologia 60, 83-118.

Archetti R., Romagnoli C., 2011. Analysis of the effects of different storm events on shoreline dynamics of an artificially embayed beach. Earth Surface Processes and Landforms 36, 1449-1463.

Artoni A., 2013. The Pliocene-Pleistocene stratigraphic and tectonic evolution of the central sector of the Western Periadriatic Basin of Italy. Marine and Petroleum Geology 42, 82-106.

Austin M.J., Buscombe D., 2008. Morphological change and sediment dynamics of the beach step on a macrotidal gravel beach. Marine Geology 249, 167-183.

Austin M.J., Masselink G., 2006. Observations of morphological change and sediment transport on a steep gravel beach. Marine Geology 229, 59-77.

Bagnold R.A., 1954. Experiments on a gravity-free dispersion of large solid spheres in a Newtonian fluid under shear. Proceedings of the Royal Society of London. Series A, Mathematical and Physical Sciences 225, 49-63.

Baldock T.E., Baird A.J., Horn D.P., Mason T.E., 2001. Measurements and modelling of swash induced pressure gradients in the surface layers of a sand beach. Journal of Geophysical Research 106 (C2), 2653-2666.

Bartholomä A., Ibbeken H., Schleyer R., 1998. Modification of gravel during longshore transport (Bianco Beach, Calabria, southern Italy). Journal of Sedimentary Research 68, 138-147.

Barwis J.H., Hayes M.O., 1985. Antidunes on modern and ancient washover fans. Journal of Sedimentary Petrology 55, 907-916.

Bauer B.O., Allen J.R., 1995. Beach steps: An evolutionary perspective. Marine Geology 123, 143-166.

Bergillos R., Ortega-Sánchez M., Masselink G., Losada M., 2016. Morpho-sedimentary dynamics of a micro-tidal mixed sand and gravel beach, Playa Granada, southern Spain. Marine Geology 379, 28-38.

Bertini A., Martinetto E., 2011. Reconstruction of vegetation transects for the Messinian-Piacenzian of Italy by means of comparative analysis of pollen, leaf and carpological records. Palaeogeography Palaeoclimatology Palaeoecology 304, 230-246.

Bertoni D., Sarti G., Benelli G., Pozzebon A., Raguseo G., 2010. Radio Frequency Identification (RFID) technology applied to the definition of underwater and subaerial coarse sediment movement. Sedimentary Geology 228, 140-150.

Bitencourt V.J.B., Dillenburg S.R., 2020. Application of multivariate statistical techniques in alongshore differentiation of coastal barriers. Marine Geology 419, 106077.

Bluck B.J., 1967. Sedimentation of beach gravels: examples from South Wales. Journal of Sedimentary Petrology 37, 128-156.

Bluck B.J., 1999. Clast assembling, bed forms and structure in gravel beaches. Transactions of the Royal Society of Edinburgh Earth Sciences 89, 291-323.

Bluck B.J., 2011. Structure of gravel beaches and their relationship to tidal range. Sedimentology 58, 994-1006.

Bourgeois J., Leithold E.L., 1984. Wave-worked conglomerates-depositional processes and criteria for recognition. In: Koster E.H., Steel R.J. (Eds.), Sedimentology of Gravels and Conglomerates. Canadian Society of Petroleum Geologists, Memoir 10, 331-343.

Bramato S., Ortega-Sánchez M., Mans C., Losada M.A., 2012. Natural recovery of a mixed sand and gravel beach after a sequence of a short duration storm and moderate sea states. Journal of Coastal Research 28, 89-101.

Brückner H., 1980. Marine Terrassen in Süditalien. Eine quartärmorphologische Studie über das Kustentiefland von Metapont. Düsseldorfer Geographische Schriften 14, pp. 222.

Buscombe D., Masselink G., 2006. Concepts in gravel beach dynamics. Earth-Science Reviews 79, 33-52.

Cantalamessa G., Di Celma C., 2004. Sequence response to syndepositional regional uplift: insights from high-resolution sequence stratigraphy of late Early Pleistocene strata, Periadriatic Basin, central Italy. Sedimentary Geology 164, 283-309.

Carter R.W.G., Orford J.D., 1984. Coarse-clastic barrier beaches: a discussion of the distinctive dynamic and morphosedimentary characteristics. Marine Geology 60, 377-384.

Carter R.G.W., Orford J.D., 1993. The morphodynamics of coarse clastic beaches and barriers: a short-and long-term perspective. Journal of Coastal Research, Special Issue 15, 158-179.

Cartigny M.J.B., 2012. Morphodynamics of supercritical high-density turbidity currents. PhD Thesis, Utrecht Studies in Earth Sciences 10, pp. 153.

Cartigny M.J.B., Ventra D., Postma G., van Den Berg J.H., 2014. Morphodynamics and sedimentary structures of bedforms under supercritical-flow conditions: new insights from flume experiments Sedimentology 61, 712-748. doi: 10.1111/sed.12076.

Casas-Prat M., Sierra J.P., 2013. Projected future wave climate in the NW Mediterranean Sea. Journal of Geophysical Research 118, 3548-3568.

Castellarin A., Cantelli L., 2000. Neo-Alpine evolution of the Southern Eastern Alps. Journal of Geodynamics 30, 251-274.

Cavaleri L., Abdalla S., Benetazzo A., Bertotti L., Bidlot J.-R., Breivik Ø., Carniel S., Jensen R. E., Portilla-Yandun J., Rogers W. E., Roland A., Sanchez-Arcilla A., Smith J.-M., Staneva J., Toledo Y., van Vledder G. P., van der Westhuysen A. J., 2018. Wave modelling in coastal and inner seas. Progress in Oceanography 167, 164-233.

Cavaleri L., Bertotti L., 2004. Accuracy of the modelled wind and wave fields in enclosed seas. Tellus 56A, 167-175.

Ciaranfi N., Ghisetti F., Guida M., Iaccarino G., Lambiase S., Pieri P., Rapisardi L., Ricchetti G., Torre M., Tortorici L., Vezzani L., 1983. Carta neotettonica dell'Italia meridionale. Pubblicazione n. 515 del Progetto Finalizzato Geodinamica, Unità Operativa Regionale 6.2.3. Consiglio Nazionale delle Ricerche, Bari.

Clifton H.E., Hunter R.E., Phillips R.L., 1971. Depositional structures and processes in the non-barred high-energy nearshore. Journal of Sedimentary Petrology 41, 651-670.

Clifton H.E., 1981. Progradational sequences in Miocene shoreline deposits, southeastern Caliente Range. Journal of Sedimentary Petrology 51, 165-184.

Clifton H.E., 2003. Supply, segregation, successions, and significance of shallow marine conglomeratic deposits. Bulletin of Canadian Petroleum Geology 51, 370-388.

Cotter E., 1985. Gravel-topped offshore bar sequences in the Lower Carboniferous of southern Ireland. Sedimentology 32, 195-213.

Conley D.C., Beach R.A., 2003. Cross-shore sediment transport partitioning in the nearshore during a storm event. Journal of Geophysical Research 108, C3, 3065. doi: 10.1029/2001jc001230.

Davidson-Arnott R.G.D., Greenwood B., 1976. Facies relationships on a barred coast, Kouchibouguac Bay, New Brunswick, Canada. In: Davis R.A. Jr., Ethington R.L. (Eds.), Beach and Nearshore Sedimentation. SEPM (Society for Sedimentary Geology), Special Publication 24, 149-168.

Davies J.L., 1980. Geographical Variation in Coastal Development. Longman, London, pp. 212.

Davis R.A. Jr, Clifton H.E., 1987. Sea-level change and the preservation potential of wave dominated and tide dominated coastal sequences. In: Nummedal D., Pilkey O.H., Howard J.D. (Eds.), Sea Level Fluctuation and Coastal Evolution. SEPM (Society for Sedimentary Geology), Special Publication 41, pp. 167-178.

De Celles P.G., 1987. Variable preservation of Middle Tertiary, coarse-grained, nearshore to outer-shelf storm deposits in southern California. Journal of Sedimentary Petrology 57, 250-264.

De Raaf J.F.M., Boersma J.R., Van Gelder A., 1977. Wave-generated structures and sequences from a shallow marine succession, Lower Carboniferous, County Cork, Ireland. Sedimentology 24, 451-483.

Di Celma C., Pitts A., Jablonská D., Haynes J.T., 2020. Backset lamination produced by supercritical backwash flows at the beachface-shoreface transition of a storm-dominated gravelly beach (middle Pleistocene, central Italy. Marine and Petroleum Geology 112, 103987.

Di Celma C., Ragaini L., Caffau M., 2016. Marine and nonmarine deposition in a long-term low-accommodation setting: an example from the Middle Pleistocene Qm2 Unit, eastern Central Italy. Marine and Petroleum Geology 72, 234-253.

Dott R.H., Bourgeois J., 1982. Hummocky stratification: significance of its variable bedding sequences. Geological Society of America Bulletin 93, 663-680.

Duller R.A., Mountney N.P., Russell A.J., Cassidy N.J., 2008. Architectural analysis of a volcaniclastic jökulhlaup deposit, southern Iceland: sedimentary evidence for supercritical flow. Sedimentology 55, 939-964.

Duo E., Trembanis A.C., Doher S., Grottoli E., Ciavola P., 2018. Local-scale post-event assessments with GPS and UAV-based quick response surveys: a pilot case from the Emilia-Romagna (Italy) coast. Natural Hazards and Earth System Sciences 18, 2969-2989.

Dupré W.R., 1984. Reconstruction of palaeo-wave conditions during the Late Pleistocene from marine terrace deposits, Monterey Bay, California. Marine Geology 60, 435-454.

Dupré W.R., Clifton H.E., Hunter R.A., 1980. Modern sedimentary facies of the open Pacific Coast and Pleistocene analogs from Monterey Bay, California. In: Field, M.E., Bouma A.H., Coburn I.P., Douglas R.G., Ingle J.C. (Eds.), Quaternary Depositional Environments of the Pacific Coast. SEPM (Society for Sedimentary Geology), Pacific Section, Pacific Coast Paleogeography Symposium 4, 105-120.

Elfrink B., Baldock T.E., 2002. Hydrodynamics and sediment transport in the swash zone: a review and perspectives. Coastal Engineering 45, 149-167.

Forbes D.L., Taylor R.B., 1987. Coarse-grained beach sedimentation under paraglacial conditions. Canadian Atlantic Coast. In: Fitzgerald D.M., Rosen P.S. (Eds.), Glaciated Coasts. Academic Press, San Diego, 52-86.

Forbes D.L., Taylor R.B., Orford J.D., Carter R.W.G., Shaw J., 1991. Gravel-barrier migration and overstepping. Marine Geology 97, 305-313.

Ghielmi M., Minervini M., Nini C., Rogledi S., Rossi M., 2013. Late Miocene-Middle Pleistocene sequences in the Po Plain e Northern Adriatic Sea (Italy): the stratigraphic record of modification phases affecting a complex foreland basin. Marine and Petroleum Geology 42, 50-81.

Ghielmi M., Serafini G., Artoni A., Di Celma C., Pitts A., 2019. From Messinian to Pleistocene: tectonic evolution and stratigraphic architecture of the Central Adriatic Foredeep (Abruzzo and Marche, Central Italy). In: Vigliotti M., Tropeano M., Pascucci V., Ruberti D., Sabato L., (Eds.) Field Trips - Guide-book, 34th IAS Meeting of Sedimentology, Rome (Italy) September 10-13, Pre-Meeting Field Trip A4, 53-91 (A4 1-39).

Gorrell G., Shaw J., 1991. Deposition in an esker, bead and fan complex, Lanark, Ontario, Canada. Sedimentary Geology 72, 285-314.

Greenwood B., Osborne Ph.D., 1990. Vertical and horizontal structure in cross-shore flows: an example of undertow and wave set-up on a barred beach. Coastal Engineering 14, 543-580.

Grottoli E., Bertoni D., Ciavola P., 2017. Short- and medium-term response to storms on three Mediterranean coarse-grained beaches. Geomorphology 295, 738-748.

Hampson G.J., Storms J.E.A., 2003. Geomorphological and sequence stratigraphic variability in wave-dominated, shoreface-shelf parasequences. Sedimentology 50, 667-701.

Harley M.D., Andriolo U., Armaroli C., Ciavola P., 2014. Shoreline rotation and response to nourishment of a gravel embayed beach using a low-cost video monitoring technique: San Michele-Sassi Neri, Central Italy. Journal of Coastal Conservation 18, 551-565.

Hart B.S., Plint A.G., 1989. Gravelly shoreface deposits: a comparison of modern and ancient facies sequences. Sedimentology 36, 551-557.

Hart B.S., Plint A.G., 1995. Gravelly shoreface and beachface deposits. In: Plint, A.G. (Ed.), Sedimentary Facies Analysis: A Tribute to the Research and Teaching of Harold G. Reading. International Association of Sedimentologists Special Publication 22, 75-99.

Hart B.S., Plint A.G., 2003. Stratigraphy and sedimentology of shoreface and fluvial conglomerates: insights from the Cardium Formation in NW Alberta and adjacent British Columbia. Bulletin of Canadian Petroleum Geology 51, 437-464.

Hay A.E., Zedel L., Stark N., 2014. Sediment dynamics on a steep, megatidal, mixed sand-gravel-cobble beach. Earth Surface Dynamics 2, 443-453.

Héquette A., Desrosiers M., Hill P.R., Forbes D.L., 2001. The influence of coastal shoreface sediment transport under storm-combined flows. Journal of Coastal Research 17, 507-516.

Holland K.T., Puleo J.A., 2001. Variable swash motions associated with foreshore profile change. Journal of Geophysical Research 106, 4613-4623.

Holmes P., Baldock T.E., Chan R.T.C., Neshaei M.A.L., 1996. Beach evolution under random waves. Proceedings of the 25th International Conference on Coastal Engineering, Orlando, Florida, 3006-3018.

Hughes M.G., Cowell P.J., 1987. Adjustment of reflective beaches to waves. Journal of Coastal Research 3, 153-167.

Hunter R.E., Clifton H.E., Phillips R.L., 1979. Depositional processes, sedimentary structures, and predicted vertical sequences in barred nearshore systems, southern Oregon coast. Journal of Sedimentary Research 49, 711-726.

Hunter R.E., Clifton H.E., Hall N.T., Csaszar G., Richmond B.M., Chin J.L., 1984. Pliocene and Pleistocene coastal and shelf deposits of the Merced Formation and associated beds, northwestern San Francisco peninsula, California. SEPM (Society for Sedimentary Geology), Midyear Meeting, San José, California, Field trip guidebook 3, pp. 1-29.

Inghilesi R., Catini F., Bellotti G., Franco L., Orasi A., Corsini S., 2012. Implementation and validation of a coastal forecasting system for wind waves in the Mediterranean Sea. Natural Hazards and Earth System Sciences 12, 485-494.

Ivamy M.C., Kench P.S., 2006. Hydrodynamics and morphological adjustment of a mixed sand and gravel beach, Torere, Bay of Plenty, New Zealand. Marine Geology 228, 137-152.

Jennings J., Shulmeister J., 2002. A field based classification scheme for gravel beaches. Marine Geology 186, 211-228.

Katsura Y., Masuda F., Obata I., 1984. Storm-dominated shelf sea from the Lower Cretaceous Choshi Group, Japan. Annual Report of Institute of Geoscience, the University of Tsukuba 10, 92-95.

Kirk R.M., 1980. Mixed sand and gravel beaches: morphology, processes and sediments. Progress in Physical Geography 4, 189-210.

Komar P.D., 1998. Beach Processes and Sedimentation, second edition. Prentice Hall, New Jersey.

Kutzbach J.E., Chen G., Cheng H., Edwards R.L., Liu Z., 2014.

Potential role of winter rainfall in explaining increased moisture in the Mediterranean and Middle East during periods of maximum orbitally-forced insolation seasonality. Climate Dynamics 42, 1079-1095.

Larson M., Sunamura T., 1993. Laboratory experiment on flow characteristics at a beach step. Journal of Sedimentary Petrology 63, 495-500.

Leckie D.A., Walker R.G., 1982. Storm- and tide-dominated shorelines in Cretaceous Moosebar - lower Gates interval - outcrop equivalents of deep-basin gas trap in western Canada. American Association of Petroleum Geologists Bulletin 66, 138-157.

Leithold E.L., Bourgeois J., 1984. Characteristics of coarse-grained sequences deposited in nearshore, wave-dominated environments - examples from the Miocene of south-west Oregon. Sedimentology 31, 749-775.

Lionello P., Nizzero A., Elvini E., 2003. A procedure for estimating wind waves and storm-surge climate scenarios in a regional basin: the Adriatic Sea case. Climate Research 23, 217-231.

Longuet-Higgins M.S., 1983. Wave set-up, percolation and undertow in the surf zone. Proceedings of the Royal Society of London. Series A, Mathematical and Physical Sciences 390, 283-291.

Maejima W., 1982. Texture and stratification of gravelly beach sediments, Enju beach, Kii Peninsula, Japan. Journal of Geosciences, Osaka City University 25, 35-51.

Maejima W., 1983. Prograding gravelly shoreline deposits in the Early Cretaceous Yuasa Fomation, western Kii Peninsula, southwestern Japan. Journal of the Geological Society of Japan 89, 645-660.

Maejima W., Nakanishi T., Nakajo T., 2001. Storm and recovery stage sedimentation records in the shoreline deposits of the Miocene Tôgane Formation, Southwestern Japan. Journal of Geosciences, Osaka City University 44, 163-171.

Mäkinen J., Räsänen M., 2003. Early Holocene regressive spit-platform and nearshore sedimentation on a glaciofluvial complex during the Yoldia Sea and the Ancylus Lake phases of the Baltic Basin, SW Finland. Sedimentary Geology 158, 25-56.

Mancin N., Barbieri C., Di Giulio A., Fantoni R., Marchesini A., Toscani G., Zanferrari A., 2016. The Friulian-Venetian Basin II: paleogeographic evolution and subsidence analysis from micropaleontological constraints. Italian Journal of Geosciences 135, 460-473.

Mancin N., Di Giulio A., Cobianchi M., 2009. Tectonic vs. climate forcing in the Cenozoic sedimentary evolution of a foreland basin (Eastern Southalpine system, Italy). Basin Research 21, 799-823.

Mason T., Coates T.T., 2001. Sediment transport processes on mixed beaches: a review for shoreline management. Journal of Coastal Research 17, 645-657.

Massari F., 1975. Sedimentazione ciclica e stratigrafia del Tortoniano superiore-Messiniano fra Bassano e Vittorio Veneto. Memorie degli Istituti di Geologia e Mineralogia dell'Università di Padova 31, pp. 57.

Massari F., 1997. High-frequency cycles within Pleistocene forced-regressive conglomerate wedges (Bradanic area, southern Italy) filling collapse scars. Sedimentology 44, 939-958.

Massari F., 2017. Supercritical-flow structures (backset-bedded sets and sediment waves) on high-gradient clinoform systems influenced by shallow-marine hydrodynamics. Sedimentary Geology 360, 73-95.

Massari F., Grandesso P., Stefani C., Jobstraibizer P.G., 1986. A small polyhistory foreland basin evolving in a context of oblique convergence: the Venetian basin (Chattian to Recent, Southern Alps, Italy), In: Allen P., Homewood P., (Eds.), Foreland Basins. IAS (International Association of Sedimentologists), Special Publication 8, 141-168.

Massari F., Iaccarino S., Medizza F., 1976. Depositional cycles in the Tortonian-Messinian of the Southern Alps (Italy): transition from fn-delta to alluvial fan sedimentation. C.N.R. Programma Geodinamica. Messinian Seminar N. 2, Gargnano, September 5-12, 1976, Field trip guidebook, pp.17-37.

Massari F., Mellere D., 1993. Cyclicity in non-marine foreland-basin sedimentary fill: the Messinian conglomerate-bearing succession of the Venetian Alps (Italy). In: Marzo M., Puigdefábregas C., (Eds.), Alluvial Sedimentation. IAS (International Association of Sedimentologists), Special Publication 17, 501-520.

Massari F., Parea G.C., 1988a. Progradational gravel beach sequeces in a moderate to high-energy, microtidal marine environment. Sedimentology 35, 881-913.

Massari F., Parea G.C., 1988b. Progradational gravel beach sequences in the hinterland of the Gulf of Taranto. In: Colella, A. (Ed.) Fan Deltas, Calabria, Italy 1988. Excursion Guidebook. Cosenza, 99-138.

Massari F., Parea G.C., 1990. Wave-dominated Gilbert-type gravel deltas in the hinterland of the Gulf of Taranto (Pleistocene, southern Italy). In: Colella A., Prior D.B. (Eds.), Coarse-Grained Deltas. IAS (International Association of Sedimentologists), Special Publication 10, 311-331.

Masselink G., Black K.P., 1995. Magnitude and cross-shore distribution of bed return flow measured on natural beaches. Coastal Engineering 25, 165-190.

Masselink G., Puleo J.A., 2006. Swash-zone morphodynamics. Continental Shelf Research 26, 661-680.

Masselink G., Russell P., Blenkinsopp C., Turner I., 2010. Swash zone sediment transport, step dynamics and morphological response on a gravel beach. Marine Geology 274, 50-68.

Masselink G., van Heteren S., 2014. Response of wave-dominated and mixed-energy barriers to storms. Marine Geology 352, 321-347.

McCall R., Masselink G., Poate T., Roelvink J., Almeida L., Woodroffe M., Russell P., 2014. Modelling storm hydrodynamics on gravel beaches with XBeach-G. Coastal Engineering 91, 231-250.

McCall R.T., Masselink G., Poate T.G., Roelvink J.A., Almeida L.P., 2015. Modelling the morphodynamics of gravel beaches during storms with XBeach-G. Coastal Engineering 103, 52-66.

Meijer P.T., Tuenter E., 2007. The effect of precession-induced changes in the Mediterranean freshwater budget on circulation at shallow and intermediate depth. Journal of

Marine Systems 68, 349-365.

Neal A., Pontee N.I., Pye K., Richards J., 2002. Internal structure of mixed-sand-and-gravel beach deposits revealed using ground-penetrating radar. Sedimentology 49, 789-804.

Neboit R., 1981-1982. Instabilité et morphogenèse au Quaternaire en Lucanie orientale. Revue de géographie physique et de géologie dynamique 23, 15-26.

Nemec W., 1990. Aspects of sediment movement on steep delta slopes. In: Colella A., Prior B.D. (Eds.), Coarse-Grained Deltas. IAS (International Association of Sedimentologists), Special Publication 10, 29-73.

Nemec W., Steel R.J., 1984. Alluvial and coastal conglomerates: their significant features and some comments on gravelly mass-flow deposits. In: Koster E.H., Steel R.J. (Eds.), Sedimentology of Gravels and Conglomerates. Canadian Society of Petroleum Geologists, Memoir 10, 1-31.

Nielsen L.H., Johannessen P.N., Surlyk F., 1988. A Late Pleistocene coarse-grained spit-platform sequence in northern Jylland, Denmark. Sedimentology 35, 915-937.

Oliveira C.M.M., Hodgson D.M., Flint S.S., 2009. Aseismic controls on in situ soft-sediment deformation processes and products in submarine slope deposits of the Karoo Basin, South Africa. Sedimentology 56, 1201-1589.

Orford J.D., 1975. Discrimination of particle zonation on a pebble beach. Sedimentology 22, 441-463.

Orford J., 1987. Coastal processes: the coastal response to sea-level variation. In: Devoy R.J.N. (Ed.), Sea Surface Studies. Springer, Berlin, Heidelberg. Sea Surface Studies, 415-463.

Orford J.D., Carter R.W.G., 1982. Crestal overtop and washover sedimentation on a fringing sandy barrier coast, Carnsore Point, southeast Ireland. Journal of Sedimentary Petrology 52, 265-278.

Orford J.D., Carter R.W.G., 1984. Mechanisms to account for the longshore spacing of overwash throats on a coarse clastic barrier in southeast Ireland. Marine Geology 56, 207-226.

Orford J.D., Carter R.W.G., Jennings J.C., 1991. Coarse clastic barrier environments: evolution and implications for Quaternary sea-level interpretation. Quaternary International 9, 87-104.

Parea G.C., Fontana D., Valloni R., Vinci A., 1980. Sediment dispersion and coast evolution between Capo Spulico and Taranto during the Quaternary. Geografia Fisica e Dinamica Quaternaria 3, 3-15.

Postma G., Kleverlaan K., Cartigny M.J.B., 2014. Recognition of cyclic steps in sandy and gravelly turbidite sequences, and consequences for the Bouma facies model. Sedimentology 61, 2268-2290.

Postma G., Nemec W., 1990. Regressive and transgressive sequences in a raised Holocene gravelly beach, southwestern Crete. Sedimentology 37, 907-920.

Poulain P.-M., 2001. Adriatic Sea surface circulation as derived from drifter data between 1990 and 1999. Journal of Marine Systems 29, 3-32.

Ragaini L., Cantalamessa G., Di Celma C., Didaskalou P., Impiccini R., Lori P., Marino M., Potetti M., Ragazzini S., 2006. First Emilian record of the boreal affinity bivalve Portlandia impressa Perri, 1975 from Montefiore dell'Aso (Marche, Italy). Bollettino della Società Paleontologica Italiana, 45, 227-234.

Reading H.G., 1996. Sedimentary Environments: Processes, Facies and Stratigraphy.Third edition, Blackwell Science, Oxford, pp. 688

Ricci Lucchi F., 1986. The Oligocene to Recent foreland basins in the northern Apennines. In: Allen P.A., Homewood P., (Eds.), Foreland Basins. IAS (International Association of Sedimentologists), Special Publication 8, 105-139.

Roberts T.M., Wang P., Puleo J.A., 2013. Storm-driven cyclic beach morphodynamics of a mixed sand and gravel beach along the Mid-Atlantic Coast, USA. Marine Geology 346, 403-421.

Rohling E.J., Hilgen F.J., 1991. The eastern Mediterranean climate at times of sapropel formation: a review. Geologie en Mijnbouw 70, 253-264.

Ruju A., Passarella M., Trogu D., Buosi C., Ibba A., De Muro S., 2019. An operational wave system within the monitoring program of a Mediterranean beach. Journal of Marine Science and Engineering 7, 32.

Russell H.A.J., Arnott R.W.C., 2003. Hydraulic jump and hyperconcentrated-flow deposits of a glacigenic subaqueous fan: Oak Ridges Moraine, Southern Ontario, Canada. Journal of Sedimentary Research 73, 887-905.

Sabino M., Schefuß E., Natalicchio M., Dela Pierre F., Birgela D., Bortels D., Schnetger B., Peckmann J., 2020. Climatic and hydrologic variability in the northern Mediterranean across the onset of the Messinian salinity crisis. Palaeogeography, Palaeoclimatology, Palaeoecology 545, 109632.

Sanders D., 1997. Upper Cretaceous transgressive shore zone deposits ("Untersperger Marmor" Auct.) in the eastern part of the Tyrol (Austria): an overview. Geologisch-Paläontologische Mitteilungen Innsbruck 22, 101-121.

Sanders D., 2000. Rocky shore-gravelly beach transition, and storm/post-storm changes of a Holocene gravelly beach (Kos Island, Aegean Sea): stratigraphic significance. Facies 42, 227-244.

Santoro E., Ferranti L., Burrato P., Mazzella M.E., Monaco C., 2013. Deformed Pleistocene marine terraces along the Ionian Sea margin of southern Italy: Unveiling blind fault-related folds contribution to coastal uplift. Tectonics 32, 737-762.

Scott T., Masselink G., O Hare T., Saulter A., Poate T., Russell P., Davidson M., Conley D., 2016. The extreme 2013/2014 winter storms: Beach recovery along the southwest coast of England. Marine Geology 382, 224-241.

Sherman D.J., 1991. Gravel braches. National Geographic Research and Exploration 7, 442-452.

Short A.D., 1984. Beach and nearshore facies: southeast Australia. Marine Geology 60, 261-282.

Slootman A., Simpson G., Castelltort S., De Boer P.L., 2018. Geological record of marine tsunami-backwash: the role of the hydraulic jump. The Depositional Record 4, 59-77.

Slootman A., Vellinga A.J., Cartigny M.J.B., 2019. Build-up-and-fill structure: The depositional signature of strongly aggradational chute-and-pool bedforms. Marine and River Dune Dynamics - MARID VI - 1-3 April 2019 - Bremen, Germany, 213-218.

Sonu C.J., 1972. Bimodal composition and cyclic characteristics

of beach sediments in continuously changing profiles. Journal of Sedimentary Petrology 42, 852-857.

Sonu C.J., Van Beek J.L., 1971. Systematic beach changes on the outer banks, North Carolina. The Journal of Geology 79, 416-425.

Soria J.M., Giannetti A, Monaco P., Corbí H., García-Ramos D., Viseras C., 2014. Cyclically-arranged, storm-controlled, prograding lithosomes in Messinian terrigenous shelves (Bajo Segura Basin, western Mediterranean). Sedimentary Geology 310, 1-15.

Spaggiari R. I., Bluck B.J., Ward J.D., 2006. Characteristics of diamondiferous Plio-Pleistocene littoral deposits within the palaeo-Orange River mouth, Namibia. Ore Geology Reviews, 28, 475-492.

Stefani C., 1987. Composition and provenance of arenites from the Chattian to Messinian clastic wedges of the Venetian foreland basin (Southern Alps, Italy). Giornale di Geologia 49, 155-166.

Stefani C., Fellin M.G., Zattin M., Zuffa G.G., Dalmonte C., Mancin N., Zanferrari, A., 2007. Provenance and palaeogeographic evolution in a multi-source foreland: the Cenozoic Venetian-Friulian basin (NE Italy) Journal of Sedimentary Research 77, 867-887.

Sturani C., Sampò M., 1973. Il Messiniano inferiore in facies diatomitica nel bacino terziario piemontese. Memorie della Società Geologica Italiana 12, 334-358.

Svendsen I.A., 1984. Mass flux and undertow in a surf zone. Coastal Engineering 8, 347-365.

Swift D.J.P., Figueiredo A.G., Freeland G.L., Oertel G.F., 1983. Hummocky cross-stratification and megaripples: a geological double standard? Journal of Sedimentary Petrology 53, 1295-1317.

Toscani G., Marchesini A., Barbieri C., Di Giulio A., Fantoni R., Mancin N., Zanferrari A., 2016. The Friulian-Venetian Basin I: architecture and sediment flux into a shared foreland basin. Italian Journal of Geosciences 135, 444-459.

Toucanne S., Angue Mintoʾo C.M., Fontanier C., Bassetti M.A., Jorry S.J., Jouet G., 2015. Tracking rainfall in the northern Mediterranean borderlands during sapropel deposition. Quaternary Science Reviews 129, 178-195.

Trigo I.F., Bigg G.R., Davies T.D., 2002. Climatology of cyclogenesis mechanisms in the Mediterranean. Monthly Weather Review 130, 549-569.

Trigo I.F., Davies T.D., Bigg G.R., 1999. Objective climatology in the Mediterranean region. Journal of Climate 12, 1685-1696.

Turco E., Hilgen F.J., Lourens L.J., 2001. Punctuated evolution of global climate cooling during the late Middle to early Late Miocene: High-resolution planktonic foraminiferal and oxygen isotope records from the Mediterranean. Paleoceanography, 16, 405-423.

Vaucher R., Pittet B., Humbert T., Ferry S., 2018. Large-scale bedforms induced by supercritical flows and wave-wave interference in the intertidal zone (Cap Ferret, France). Geo-Marine Letters 38, 287-305.

Vos R.G., Hobday D.K., 1977. Storm beach deposits in the late Palaeozoic Ecca Group of South Africa. Sedimentary Geology 19, 217-232.

Walker R.G., Plint A.G., 1992. Wave and storm-dominated shallow marine systems. In: Walker R.G. James N.P. (Eds.), Facies Models: Response to Sea-Level Change. Geological Association of Canada, St John's, Newfoundland, pp. 219-238.

Wenz W. 1942. Zur Kenntnis des Fossilen Land- und Süsswasser mollusken Venetiens. Memorie dell'Istituto Geologico della Regia Università di Padova 14, pp. 51.

Williams A.C., Caldwell N.E., 1988. Particle size and shape in pebble beach sedimentation. Marine Geology 82, 199-215.

Wilson K.C., 1987. Analysis of bed-load motion at high shear stress. Journal of the Hydraulics Division 113, 97-103.

Wright L.D., Chappell J., Thom B.G., Bradshaw M.P., Cowell P., 1979. Morphodynamics of reflective and dissipative beach and inshore systems: southeastern Australia. Marine Geology 32, 105-140.

Wright L.D., Short A.D., 1984. Morphodynamic variability of surf zones and beaches: a synthesis. Marine Geology 56, 93-118.

Wright M.E., Walker R.G., 1981. Cardium Formation (U. Cretaceous) at Seebe, Alberta - storm-transported sandstones and conglomerates in shallow marine depositional environments below fair-weather wave base. Canadian Journal of Earth Sciences 18, 795-809.

Yagishita K., 1995. Antidunes in a small gorge on the beach sand, the Sanriku Coast, northeast Japan. Journal of Sedimentological Society of Japan 42, 21-28.

Yorath C.J., Bornhold B.D., Thompson R.E., 1979. Oscillation ripples on the northern Pacific continental shelf. Marine Geology 31, 45-58.

Zattin M., Stefani C., Martin S., 2003. Detrital fission-track analysis and sedimentary petrofacies as keys of alpine exhumation: the example of the Venetian Foreland (European Southern Alps, Italy). Journal of Sedimentary Research, 73, 1051-1061.

Zhang W., Cui Y., Santos A.J., Hanebuth T.J.J., 2016. Storm-driven bottom sediment transport on a high-energy narrow shelf (NW Iberia) and development of mud depocenters. Journal of Geophysical Research (Oceans) 121, 5751-5772.